EXPERIMENTAL INVESTIGATIONS OF SAD TO SCISSION DYNAMICS IN LOW ENERGY FISSION

A Thesis Submitted
in Partial Fulfilment of the Requirements
for the Degree of

DOCTOR OF PHILOSOPHY

by

RAGHAVA VARMA

to the

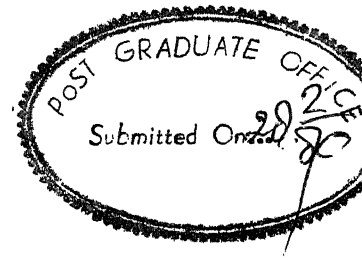

CERTIFICATE

Certified that the work presented in this thesis entitled "**Experimental Investigations of Saddle to Scission Dynamics in Low Energy Fission**" by Mr. Raghava Varma, has been done under our supervision and that it has not been submitted elsewhere for a degree.

G. K. Mehta
(Supervisor)
Professor Of Physics
Indian Institute of Technology
Kanpur

V. S. Ramamurthy
(Co-Supervisor)
Nuclear Physics Divis
Bhabha Atomic Research
Bombay

ACKNOWLEDGEMENTS

In reverence and with great pleasure, I acknowledge guidance, help and knowledge imparted by my supervisors G. K. Mehta and Dr. V. S. Ramamurthy. I must also thank S. S. Kapoor who though officially, was not my supervisor bu taken a keen interest in the planning execution and analysis work mentioned herein. I thank Dr. Kapoor for being a co source of encouragement and inspiration. I thank Prof. Mehta for his sincerity towards the completion of this work which provided the extra push which took it through the various necks encountered. Dr. Ramamurthy has been a friend, philsophe guide for the last four years and I thank him for that. It was enjoyable being introduced to the methodology of research by I am concious of my own failing to live up to their trus honour many a times. I do not have words to thank them for generosity in overlooking my shortcomings.

I acknowledge the generous help and the hospitality e by all the members of the Fission Physics Section, B.A.R.C. B I am thankful to Dr R K Choudhury for helping me in setting u smooth running of the experiments. In this connection I must thank my friends Mohanty Aruna Alok Nayak and Surya for smiling help without which none of the experiments would have successful. I have benefitted enormously from the nu discussions with Dr. S K Kataria and Dr D M Nadkarni. thankful to them. I cherish very sweet memories of the hospitality extended by Mrs Ramamurthy and Mrs Kataria duri stay at Bombay.

to join the four corners at Delhi Bombay Calcutta and Kanpu
am also thankful to Prof Waghmare for going over the manuscri
this thesis

I must also thank Masood and Biplab who have spent ma
sleepless nights at VECC unhesitatingly in the initial stage
this work.

I would also like to thank

——— The staff of the Variable Energy Cyclotron C
Calcutta who have inconvenienced themselves consid
many times to give us the beam.

——— Prof. P.N. Mukherjee and his group for lending u
orlec modules sometimes despite their own needs.

——— Prof. P.G. Dhande for allowing me to use the CAD
Computer at I.I.T. Kanpur and Siddhartho for helpi
to use it.

——— Prof. R.M. Singru and the staff of the Van de
laboratory I. I. T. Kanpur for their help.

——— My friends - Vinay, KK, Srini, Alok, Raje, Manu,
Ghantu, Dada, Ravi and Godre and other hall fourites
have made my stay at I.I.T. Kanpur somewhat memorable.

——— My friends at Bombay - Vineet, Rajiv, M.N. Rao, A
and Rout for their hospitality during my visits there.

——— Finally all my teachers, friends and family members
I have not been able to acknowledge explicitly but I
it to them for what I am

February 23, 1989

Raghavavarma.
(Raghava Varma)

LIST OF CONTENTS

LIST OF TABLES

LIST OF FIGURES

SYNOPSIS

EXPERIMENTAL INVESTIGATIONS OF SADDLE TO SCISSION DYNAMICS IN LOW ENERGY FISSION

RAGHAVA VARMA
Ph. D.
Department of Physics
Indian Institute Of Technology, Kanpur
January, 1989.

Nuclear fission is a process in which a heavy nucleus divides in two or more nuclei either spontaneously or induced by an energetic projectile. Discovered in 1939, the early interest in the process was mainly to put the largest known energy release in a reaction (approximately 200 MeV) to commercial and military use. The interest in the physics of the process arose mainly because, apart from giant resonance, fission was the only known nuclear reaction involving rather drastic rearrangement of nuclear matter. While the development of heavy-ion accelerators in the last two decades, has brought out other new phenomena such as the deep inelastic collisions involving nuclear collective motion to the forefront, the importance of fission studies has not diminished. This is primarily because the nuclear fission can be considered as an elementary collective process without the uncertainities of reaction dynamics as in the case of heavy ion reactions. Further, in the case of low energy fission, the nuclear matter is much

SYNOPSIS

EXPERIMENTAL INVESTIGATIONS OF SADDLE TO SCISSION DYNAMICS IN LOW ENERGY FISSION

RAGHAVA VARMA
Ph. D.
Department of Physics
Indian Institute Of Technology, Kanpur
January, 1989.

Nuclear fission is a process in which a heavy nucleus divides in two or more nuclei either spontaneously or induced by an energetic projectile. Discovered in 1939, the early interest in the process was mainly to put the largest known energy release in a reaction (approximately 200 MeV) to commercial and military use. The interest in the physics of the process arose mainly because, apart from giant resonance, fission was the only known nuclear reaction involving rather drastic rearrangement of nuclear matter. While the development of heavy-ion accelerators in the last two decades, has brought out other new phenomena such as the deep inelastic collisions involving nuclear collective motion to the forefront, the importance of fission studies has not diminished. This is primarily because the nuclear fission can be considered as an elementary collective process without the uncertainities of reaction dynamics as in the case of heavy ion reactions. Further, in the case of low energy fission, the nuclear matter is much

cooler thermodynamically and therefore the dynamics is strongly influenced by nuclear shell structure effects and the superfluid nature of nuclear matter. Therefore, fission studies, often serve as a test bed of models developed in heavy ion induced reaction studies.

It is known that for all nuclei having mass number greater than about 100, fission has a positive Q value. However, only the heaviest actinides are known to have measurable spontaneous fission rates. This is due to the existence of an energy barrier for fission. It is known that this energy barrier can be understood in terms of shape evolution of the nucleus and the associated deformation potential energy surface. In this model, fission is a continuous evolution of the nuclear shapes starting from the nearly spherical compound nucleus to two well separated fragments at infinity. In the deformation space, two distinct milestone configurations along the fission path can be identified. The first one is the fission saddle point. This is the point of maximum deformation potential energy which the nucleus must pass to undergo fission. In this sense, it is a point of no return from where the separation into two fragments becomes imminent. The second milestone configuration is the scission point at which the nuclear interaction between the two fragments vanishes. The fragment mass and charge are uniquely determined at this point. How are these affected by the saddle point shapes is still an open question. The separation of the two fragments, then takes place purely as result of coulomb repulsion. While to the first order, the coulomb interaction energy at scission point gets converted

into fragment kinetic energy, as they separate, there is also shape relaxation of the nascent fragments. The deformation energy of the fragments is then converted into their excitation energy. The excited fragments then cool by the emission of neutrons and gamma rays. In a typical experiment it is the asymptotic fragments at infinity which reach the detector. The experimental observables in fission studies are the relative probability of fission, the fragment mass, charge, energy and angular distribution and the nature of the secondary radiations emitted by the fragments. The nature of the collective motion between the formation of the compound nucleus to the saddle point, from saddle point to the scission point and the separation dynamics beyond the scission point, have important consequences on the final observables. Conversely, one can learn about the nature of collective dynamics along the fission path from these measurements.

It is now known that the motion upto the saddle point is highly dissipative and in the case of low energy fission it takes place in time scales of the order of 10^{-16} seconds. On the other hand, the nature of collective dynamics between the saddle and the scission points is not fully understood. During this phase, the nuclear shape changes from a deformed mono-nucleus to a higly necked di-nucleus. The nature of the dissipative force also expected to change correspondingly. While it is estimated that the time scale involved is of the order of 10^{-20} seconds or less, the precise nature of the dynamics is not known.

Detailed studies of the secondary radiations such as the neutrons and the gamma rays, including the light charge particles

emitted close to scission have given very important information on the scission dynamics. For example, it is now well known that the nascent fragments at scission are highly deformed and scission takes place off axially, resulting in appreciable angular momentum of the fragments from spontaneous fission of even-even nuclei with zero spin. However, the effect of pairing, deformation and the shell structure are not fully understood.

The measurement of total kinetic energy of the fission fragments as a function of the excitation energy of the target, yields information on the degree and the nature of dissipation present in collective nuclear dynamics. If the system is viscous then the excitation energy of the compound nucleus will not appear in the kinetic energy of the fragments, whereas if it is in a superfluid state all the excitation energy will go in as kinetic energy of the fragments. The degree of excitation energy appearing in the total kinetic energy can give a good measure of the viscosity of the system.

In the present work we have studied :

(a) the gamma ray multiplicity distribution as a function of fragment charge ratio.

(b) anisotropy of the gamma rays with repect to fragment direction of motion as a function of gamma ray energy.

(c) the correlations of the total kinetic energy of the fragments and the excitation energy of the fissioning nucleus.

in an effort to obtain further information on the nature of the motion between the saddle point and the scission point, and about

the scission process itself.

PROMPT GAMMA RAY MULTIPLICITY DISTRIBUTION AND GAMMA RAY ANISOTROPY WITH RESPECT TO FRAGMENT MOTION IN THE SPONTANEOUS FISSION OF ^{252}Cf

In the first experiment, we studied the multiplicity distribution of the prompt gamma rays emitted from the fission fragments in the spontaneous fission of ^{252}Cf as a function of fragment charge ratio. The average number of prompt gamma rays and the width of the multiplicity distribution are measured. The fission fragments were detected by a solid state surface barrier detector kept at a distance of 3 cm from a ^{252}Cf source in a vacuum chamber. A high purity germanium detector (HPGe), kept at 90° to the direction of fragment motion, was used to detect the K X-rays emitted by the fission fragments. The K X-ray energy is a signature of the charge of the emitting fragment. Two sodium iodide detectors were placed in a plane perpendicular to the HPGe detector. Coincidence was demanded between the pulses from the fission fragment detector, X-ray detector and one or both of the gamma ray detectors. The K X-ray spectrum was recorded in a multichannel analyzer first in coincidence with the fission fragments, then in coincidence with the fission fragments and either of the gamma rays and finally in coincidence with the fission fragments and both the gamma rays. After suitable unfolding of the spectra, the data was analysed to get the mean multiplicity and the width of the gamma ray multiplicity

distribution as a function of the charge ratio of the heavy and the light fragments. The mean multiplicity indicated some odd-even dependence. The width of the distribution exhibited strong signatures of shell structure, deformation and odd-even nature of the fragments. It showed odd-even effects for nuclei having closed shell structure i.e. for Z=51 to 55. In the deformed region i.e. Z=56-60 the odd-even effects were absent. Further, the width is much lower for nuclei in the region Z=56-59.

These results can be qualitatively understood as follows: angular momentum in a deformed nucleus is carried as collective rotation, whereas in the spherical nucleus it is carried as aligned single-particle spins. Consequently, the deformed nucleus deexcite by the E2 rotational cascades. These being transitions from fixed energy states, do not contribute to the width in the multiplicity distribution. On the other hand, in a spherical nucleus the deexcitation has to be statistical in nature. The width of the distribution arises either due to the width in statistical emission or due to the initial spin distribution of the fragments. As observed in this work, this gives rise to a smaller width for deformed fragments as compared to the spherical fragments.

In the second experiment, we studied the anisotropy of the prompt gamma rays with respect to the direction of fragment motion as a function of gamma ray energy. For this purpose, the ^{252}Cf source was mounted in a vacuum chamber and the fission fragments were detected by two solid state surface barrier detectors kept at a distance of 3 cm and at 90° to each other. The gamma rays were

detected by a large sodium iodide detector (5 inch X 5 inch) kept 60 cm away from the source and along the direction of motion of one of the fission fragments. Fission fragment energy, gamma ray energy and the time interval between the fission pulse and the gamma ray pulse were recorded event by event in list mode on a magnetic tape using a computer based data acquisition system. Time of flight technique was used to eliminate neutrons since they are strongly correlated with the direction of fragment motion and any contamination by them will thereby result in positive anisotropy.

It was found that in the region of gamma ray energy $300<E_\gamma<700$ keV, gamma anisotropy is positive with a maximum of 1.26 ± 0.01 at around 520 keV. For higher energies anisotropy decreases but remains positive. For energies less than around 300 keV the anisotropy is slightly negative. Qualitaively, the result can be understood in terms of the Strutinsky's prescription that the E2 transitions are expected to enhance the anisotropy, whereas E1 statistical gamma rays are expected to decrease the anisotropy.

A Monte Carlo program which simulates the statistical neutron and gamma ray emission from nuclei carrying appreciable angular momentum and energy has been developed to calculate the initial spin distribution of the fission fragments. The code explicitly includes nuclear shell effects on the level densities. It is assumed that the nucleus dissipates angular momentum only after reaching the yrast line by the emission of rotational cascade. The program uses the known expressions for the decay widths for neutrons and statistical gamma ray emission to calculate the average multiplicity and the width of the multiplicity

distribution due to statistical gamma rays. We have calculated the spin distribution of fragments by subtracting the width due to E1 transitions from the experimentally measured widths.

MEASUREMENT OF THE VARIATION OF TOTAL KINETIC ENERGY (TKE) OF THE FISSION FRAGMENTS AS A FUNCTION OF EXCITATION ENERGY OF THE FISSIONING NUCLEUS IN THE REACTION $^{238}U(\alpha,\alpha'f)$

We have studied the kinetic energy distribution of the fission fragments in the fission of ^{238}U induced by inelastic scattering of 60 MeV alpha particles from the Variable Energy Cyclotron in Calcutta. Correlated fission fragments were detected by two surface barrier detectors placed at approximately 4 cm from the target in a typical back to back arrangement. Scattered alpha particles were detected and identified by a E-ΔE detector telescope kept at an angle of 30° to the beam axis. Coincidence between the ΔE detector and the fission detector formed the master pulse for a five parameter recording, in list mode on a magnetic tape, of the pulses from the two fission detectors, the two detectors of the telescope and the time difference between the fission and the ΔE detector. The energies of the two correlated fission fragments yield the masses of the fragments and the energy of the scattered alpha particles gives the excitation energy of the fissioning nucleus. Suitable corrections for the energy loss suffered by the fragments due to the finite thickness of the target and the backing material, neutron evaporation and the recoil of the fissioning nucleus were applied.

We have measured the total kinetic energy in the excitation energy range of 8.5 MeV to 28.5 MeV. In the region 6.5 MeV to 8.5 MeV, the data is not reliable due to the contamination of the elastic peak from the Carbon in the backing. It was found that in the excitation energy range of 8.5 to 12.5 MeV, the total kinetic energy decreases with the excitation energy and above 22.5 MeV, it shows a slow increase with the excitation energy. In between, the TKE remains constant with the increase in excitation energy. We have also measured the variation of TKE as a function of excitation energies for mass separated fragments. We find that the slope of the curve $\overline{TKE}$ versus E_x increases as a function of excitation energy for asymmetric masses but it does not show any significant variation.

While the experiment allowed us to study the effect of excitation energy on the total kinetic energy of the mass separated fragments, the analysis has brought out a serious limitation of not only the present results, but also of the earlier results. The correction in the single fragment kinetic energy due to neutron evaporation was made on the basis of previous experimental results which give neutron yield as a function of excitation energy of the fissioning nucleus and the fragment mass assuming that all the neutrons are emitted from the fully acclerated fragments. This assumption may be incorrect because of multichance fission i.e. fission following the emission of neutrons from the fissioning nucleus at higher excitation energy. The emission of these neutrons does not change the kinetic energy of the fragments as opposed to those neutrons which are

emitted from the fragments in motion. Another new dimension has been added by a series of recent measurements of neutrons emitted in fission following fusion in heavy ion reactions. It has been established by the presence of enhanced number of pre-scission neutrons that a substantial excitation energy of the compound nucleus is dissipated by the emission of these neutrons before the scission takes place. Correction for the neutrons evaporated from compound nucleus was made on the basis of standard statistical model with the known expression for the escape widths for the neutrons and fission. It was found that this correction changes the slope of the $\overline{TKE}$ versus E_x curve appreciably. Since the experimental information on the dependence of the number of scission neutrons as a function of excitation energy of the compound nucleus and the mass of the fragments is not available, we could not correct our results for their presence. However, we have demonstrated that it is of crucial importance to know this quantity in the determination of nature of the behaviour of total kinetic energy as a function of excitation energy.

The thesis contains the details of the measurement, analysis and the conclusions drawn from them in four chapters. Chapter I gives general information about the subject of fission dynamics and its relevance as a unique probe of nuclear macrophysics. Chapter II contains the gamma ray measurements. Chapter III discusses the total kinetic energy measurements. In Chapter IV, we discuss our results and how they have contributed towards a better understanding of the process and where they have fallen short.

The appendices give details of the analysis procedure used for the total kinetic energy measurements and the listing of the statistical model code and the other programs developed by us in the analysis of our data.

CHAPTER 1

FISSION - THE UNIQUE PROBE OF NUCLEAR MACROPHYSICS

[1.1] INTRODUCTION

The discovery of nuclear fisson in 1939[1], involving the division of a heavy nucleus into two comparable parts and liberating a large amount of energy[2], opened up a Pandora's box for the nuclear physicists. While the early interest in the process was mainly to put the largest known energy release in a reaction, nearly 200 MeV, to military and commercial uses, the interest in the physics of the process arose mainly because of its unique collective character. In fact, the phenomenon was so different from the other nuclear reactions known at that time that it led to the study of the fission process almost in isolation of rest of the nuclear physics. While the development of heavy ion accelerators, has diluted this uniqueness to some extent by bringing out several other new reaction channels involving nuclear collective motion to the forefront, the importance of fission studies has still not diminished, primarily because fission is an elementary collective process, without the uncertainities of the reaction dynamics which are there in the case of heavy ion reactions. Further, in low energy fission, the nuclear matter is thermodynamically cooler and

therefore, the dynamics is strongly influenced by nuclear shell structure effects and the superfluid nature of nuclear matter. Hence, fission studies often serve as a test bed of models developed in heavy ion induced reaction studies.

On the basis of simple energetics fission is a positive Q-value reaction[3], for nuclei having mass number more than about 100. However, only the heaviest nuclei have measurable spontaneous fission rates. This is due to the existence of an energy barrier for fission which increases rather rapidly with decreasing charge of the fissioning nucleus. The existence of this energy barrier can be understood in terms of a shape evolution of the nucleus and the associated deformation potential energy surface. In this model, developed by Bohr and Wheeler[4] on the basis of an idea provided by Meitner and Frisch[5], fission is a continuous evolution of the nuclear shapes starting from the nearly spherical compound nucleus to two well separated fragments at infinity. Fig[1.1] (taken from Ref. 6) shows the potential energy as a function of deformation. The figure also shows the deformation energy contours as a function of two principal deformation coordinates β_2 and β_4. In the deformation space, two distinct *milestone configurations* along the fission path can be identified - *the fission saddle point* and *the scission point*. Fig.[1.1] shows the saddle point as determined by the liquid drop model. As we see, the fission saddle point is the point of maximum deformation potential energy which the nucleus must pass to undergo fission. It is, in this sense, the point of no return when separation into two fragments becomes imminent. At the

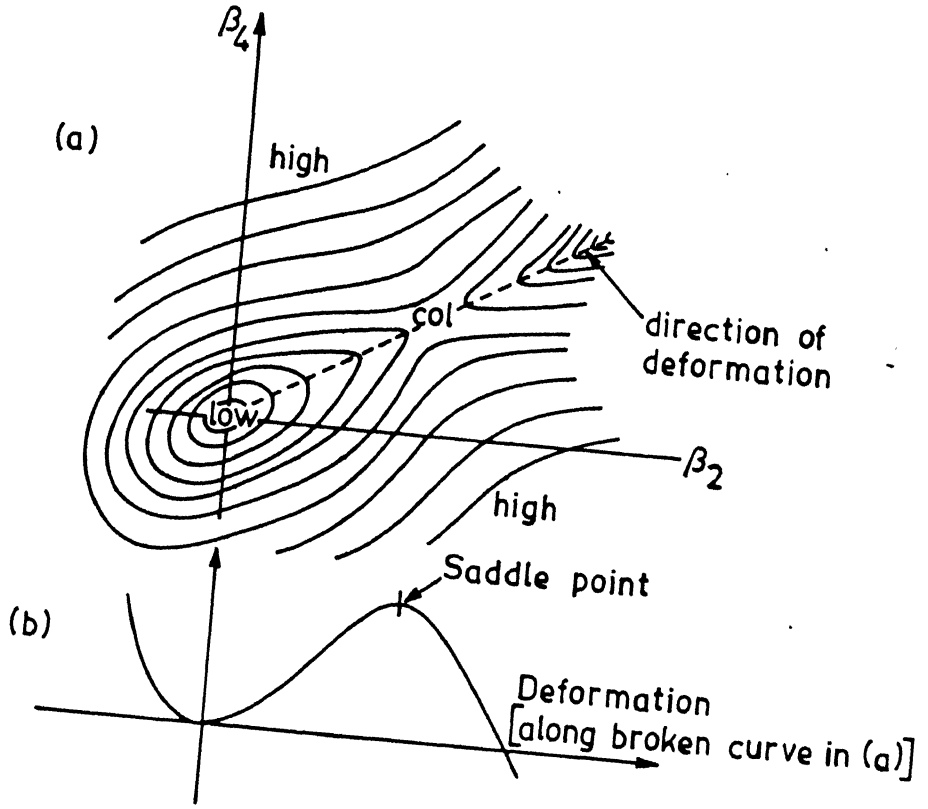

Fig. 1.1. Liquid drop model potential energy contour of a fissioning nucleus as a function of quadrupole and hexadecapole deformation parameters. Potential energy versus deformation along the fission direction is also shown. (Ref. 6).

scission point, the nuclear interaction between the nascent fragments vanishes thereby freezing the fragment mass and charge. The separation of the two fragments beyond the scission point takes place purely as a result of the Coulomb repulsion between them. While to the first order the Coulomb interaction energy at scission gets converted into fragment kinetic energies, there is also a shape relaxation of the highly deformed nascent fragments. This results in the deformation energy of the fragments at scission appearing as their excitation energy. The excited fragments *cool* by the emission of neutrons and gamma rays. It is the cold fragments at infinity which reach the detectors in an experiment. The typical experimental observables are- the probability of fission, the fragment mass, charge, energy and angular distributions, and the nature of secondary radiations emitted during the fission process or by the fragments after scission. The nature of the collective motion between the compound nucleus stage and the saddle point, from the saddle point to the scission point and the separation dynamics beyond the scission point have important consequences on the final observables. Conversely, one can learn about the nature of the multidimensional deformation potential energy surface, and the collective dynamics along the fission path from these measurements.

Fig[1.2] (taken from Ref.7) shows the average time scales involved during the various stages of the fission process. It also shows at what stage the secondary radiations from the fragments come when they deexcite. The idea about the time scales[8] involved

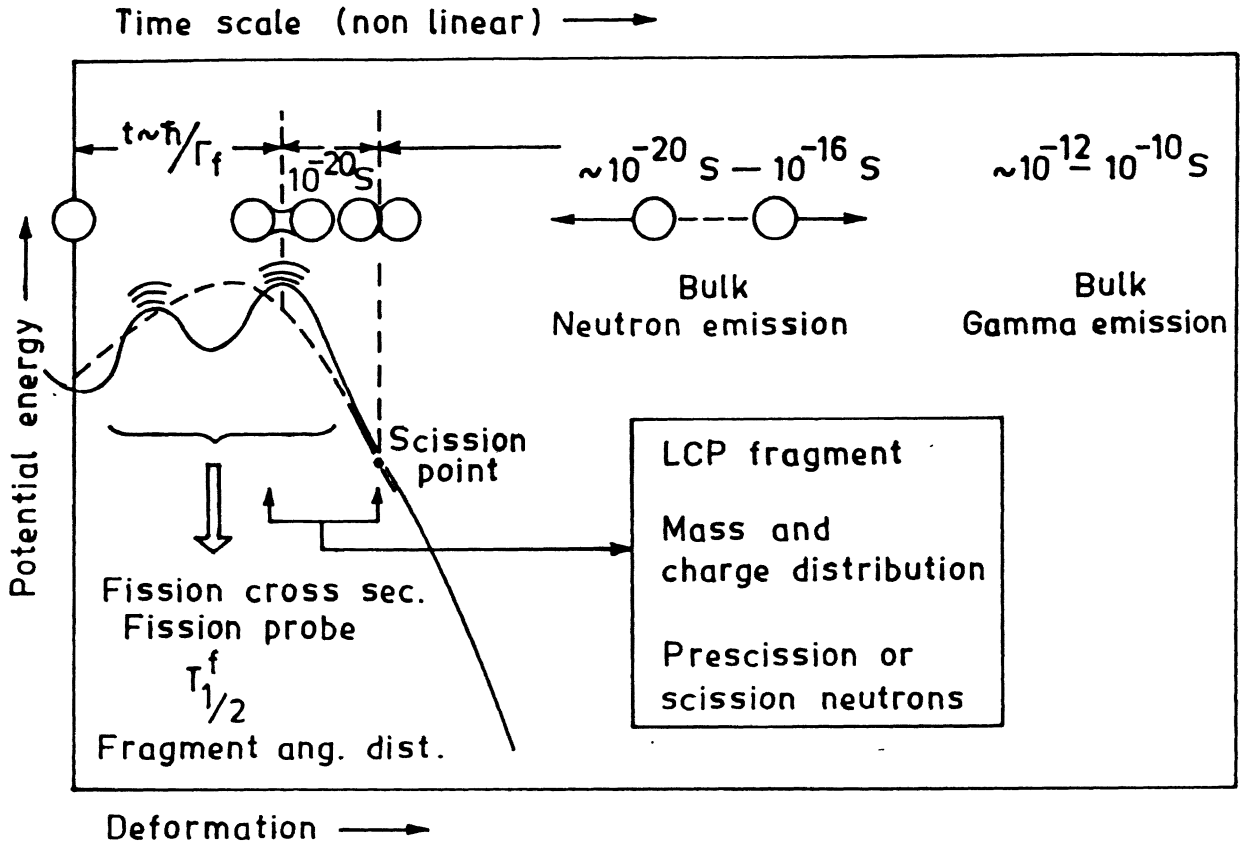

Fig. 1.2. Schematic illustration of different stages of the fission process and corresponding time scale. (Taken from ref. 7)

in the motion of the nucleus from compound nucleus to the saddle point comes from the lifetime studies. The number of neutrons emitted from the fissioning nucleus during its descent from saddle to scission along with some theoretical input gives us the time the nucleus takes in its descent from saddle to scission. The anisotropy in neutron and gamma emission gives us the time scales involved for fragments to attain the maximum velocity.

[1.2] MACROSCOPIC APPROACH TO NUCLEAR COLLECTIVE MOTION IN FISSION

The macroscopic approach of the *liquid drop model* (LDM), with a few cosmetic touches here and there, has been the mainstay in the description of the rich variety of phenomenon unravelled by the fission process with the passage of time. This is primarily because a typical actinide nucleus consisting of about 240 nucleons has about 720 *degrees of freedom*. A formal description of all the dynamical properties of this system starting from a many body Hamiltonian and a solution of the relevant Schrödinger equations of motion is however quite impractical since neither the many body Hamiltonian is known nor is it easy to solve the equations of motion.

In discussing fission, our interest is not in knowing the individual behaviour of the nucleons microscopically but only in their overall collective behaviour. The problem is considerably simplified if one treats the nucleus on its way to fission as two

charged drops. The maximum number of degrees of freedom required to describe the collective motion of two rotating and vibrating nuclei is 17. A workable model of fission, should therefore select only 17 collective degrees of freedom out of the total 3A degrees of freedom and treat them separately from the remaining 3A-17 *internal* degrees of freedom.

In such a treatment, the dynamics is strongly affected by the assumptions regarding the *coupling* between the collective and the internal degrees. The coupling could be *weak*, *strong* or *intermediate between the two*. These weak and the strong coupling give rise to to the two principal branches of nuclear models, the adiabatic[9,10] and the statistical model[11,12]. If further assumptions are introduced in either branch, of which the principal one is the smallness of the surface thickness compared to the nuclear radius (ie an expansion in powers of $A^{-1/3}$), we obtain the non-viscous and the viscous versions of the liquid drop model[13,14]. This classification of nuclear models brings out the fact that the liquid drop model is not to be regarded as opposed to either the adiabatic or the statistical model but on the contrary, it is a particularly simple version of these models and could be used as a starting point for either. It should however be borne in mind that the fundamental question that from first principles whether one would expect the weak or the strong coupling approximation to be more nearly correct is yet to be satisfactorily answered. On the basis of the experimental results we cannot discard either of the two lines of thought. Intutively, one expects that at high

excitation energies the strong coupling statistical model may be valid while at low energies, partly because of the superfluid nature of nuclear matter, the situation may be different.

The precise choice of the collective coordinates is crucial in determinig the nature of motion. The coupling between the internal and the collective degrees of freedom has assumed added significance with the discovery of other modes of large scale collective motion[15,16] and the question of degree of viscosity prevalent in large scale collective motion is now of paramount importance. There have been some early attempts[17] to explain the mass asymmetry in actinide fission on the basis of this coupling but the idea did not receive as much attention as it deserved. It is only in the last two decades that terms like viscosity, friction etc. have come into widespread use. Unfortunately till now our knowledge of this parameter remains sketchy and far from complete.

A complete description of the three stages of the fission process requires knowledge of three physical quantities :

(a) *the deformation potential energy landscape* i.e. the total potential energy of the nuclear system as a function of deformation parameters in a multidimensional space since several deformation coordinates are necessary to describe nuclear shapes along the fission path, especially when the fissioning nucleus is strongly deformed.

(b) *the inertial mass parameter* of the fissioning system at all deformations in order to determine the fission path and the fission barrier penetrability.

(c) *the damping of the fission mode* i.e. its coupling to other degrees of freedom especially during its descent from saddle to scission.

The potential energy as a function of the collective coordinates can be obtained, for example, from the liquid drop idealization of a sum of surface and Coulomb energies. Similarly, the inertia (in general a tensor) can be calculated for irrotational flow of the nuclear fluid. The potential energy surface and the inertial mass term are interdependent. The damping term is needed in the macroscopic treatment of a many body system by a few generalized coordinates where the remaining internal degrees act as a heat sink. This can be visualized as the flow of energy from the collective coordinates to the internal degrees of freedom.

There exist two approximate formulae for the rate of this flow based on simplified nuclear models[18,19]. They are basically based on the fact whether the mean free path is small or large.

(i)If the mean free paths are small compared to the overall size of the system, flow of energy takes place from collective motion into internal degrees due to *two-body collisions* between the nucleons in the nuclei, resulting in a dissipative flow similar to ordinary viscous fluids.

(ii) If the mean path between nucleons is large, then there is the so called *one body dissipation* which results from the collisions of the nucleons with the moving boundary of the nuclear potential well.

Two elemetary dissipation formulae for the one-body dissipation have been derived to describe the rate of energy flow from collective to single particle degrees of freedom - *the wall formula*[20] for a freely communicating shape and *the window formula*[21] for two weakly communicating shapes in relative motion. The wall formula is relevant for convex nuclear shapes without a neck while a window formula is for shapes with a strong constriction as in the late stages of fission or the initial stages of a nucleus-nucleus collision. A generalization of the wall and the window formulae is called for when the two pieces are deformable and weakly communicating as in the last stages of the fission process. There have been some attempts in this direction recently[22].

For cold nuclei with relatively long mean free paths for nucleon-nucleon collisions, the two body viscosity is small and can usually be neglected in comparison to the one body dissipation. The dynamical evolution of the system can then be obtained from the classical equations of motion[23]:

$$\frac{d}{dt}\left(\frac{dL}{dq_i}\right) = \frac{dL}{dq_i} - \frac{d\Phi}{dq_i}$$

$$\Phi = Q/2$$

where q_i are the generalized coordinates and the second term on the R.H.S. of the equation represents the dissipative term.

A qualitative discussion of the fission process does not even require seventeen degrees of freedom. An intelligent choice of

collective coordinates may reduce it further. Swiatecki[24], shape parametrizing the nucleus, postulated that a minimum of three degrees of freedom are essential to estimate the barrier height and also the dynamcal evolution of the process. His three macroscopic coordinates are:

1. the relative separation variable,
2. the neck thickness variable,
3. the mass asymmetric constant.

In this approach, the macroscopic deformation potential energy is calculated as a function of shape parameters. It consists of the sum of an electrostatic energy, nuclear surface energy and shell and pairing correction energies. The potential energy landscape for a typical heavy nucleus exhibits two local minimas separated by a saddle point pass -one of the local minimas correspond to the fused system while the other corresponds to a configuration of separated fragments. The term local minima has been used since, in general, the potential energy is not stationary with respect to the mass asymmetry. The saddle point is, therefore, only a *conditional* saddle point, with the physical meaning of a mountain pass only if the asymmetry is effectively held fixed. For not too large asymmetries (asymmetry less than the Businaro-Gallone[25] critical mass asymmetry) and no shell effects, the potential energy decreases with decreasing mass asymmetry. It therefore drives the system towards symmetry when the asymmetry relaxes and the system becomes symmetric. The energy becomes stationary with respect to the mass asymmetry degree of freedom and the *conditional saddle*

point becomes a *true unconditional saddle point* and the bounded inner region of low energy becomes the compound nucleus region. Another interesting aspect of the potential landscape is the existence of two distinct valleys misaligned with respect to each other[26] - the fission valley of connected shapes and the two fragment valley of disconnected shapes. They are separated by an energy ridge over a narrow range of relative separation around the scission point. The motion in the LDM valley is highly damped and the dissipation is dependent on the collective coordinate. The time scales involved for motion in the three degrees of freedom are also distinctly different - partly because of the differences in the relevant inertial masses and partly because of the differences in the nature of the dissipative forces. In particular, the motion in the neck degree of freedom is the fastest and consequently, the neck rupture takes place almost at constant relative separation.

We will now briefly discuss how the different experimental studies of the fission process lead to detailed information on the structure of the potential energy surface and the nature of nuclear collective dynamics on this surface.

[1.3] THE DEFORMATION POTENTIAL ENERGY SURFACE

One of the earliest and the most extensive pieces of experimental information on the fission process is related to the structure of the deformation potential energy surface upto the fission saddle point. This is obtained by measurement of fission

probabilities, half lives in spontaneous fission and fission cross-sections in particle induced fission. Though the height of the fission barrier is a small fraction of the total energy released in the process, it plays a crucial role in deciding the fission probabilities and the angular distribution of the fragments. The *experimental* fission barrier height exhibits a *strong decrease* with *increasing charge* of the fissioning nuclei. This is in qualitative agreement with the predictions of the liquid drop model. However, the simple liquid drop model fails to explain the near constancy of the fission barrier height and the asymmetric mass distribution in the fission of actinide nuclei. This alongwith the more recent discovery of long lived fission isomers and widely spaced sub-barrier fission resonances has led to the development of the so called macroscopic-microscopic approach[27] for the calculation of nuclear deformation potential energies. With a deformation dependent shell correction energy superimposed on the smooth liquid drop model deformation potential energy, it was shown by Strutinsky[28] that the fission barriers are double-humped for actinide nuclei. In this approach, for all deformations along the fission path the potential energy of the nucleus can be expressed as a sum of two terms $E_M(s)$ and $E_m(s)$. The $E_M(s)$ represents the energy obtained by the LDM, whereas $E_m(s)$ is the shell correction

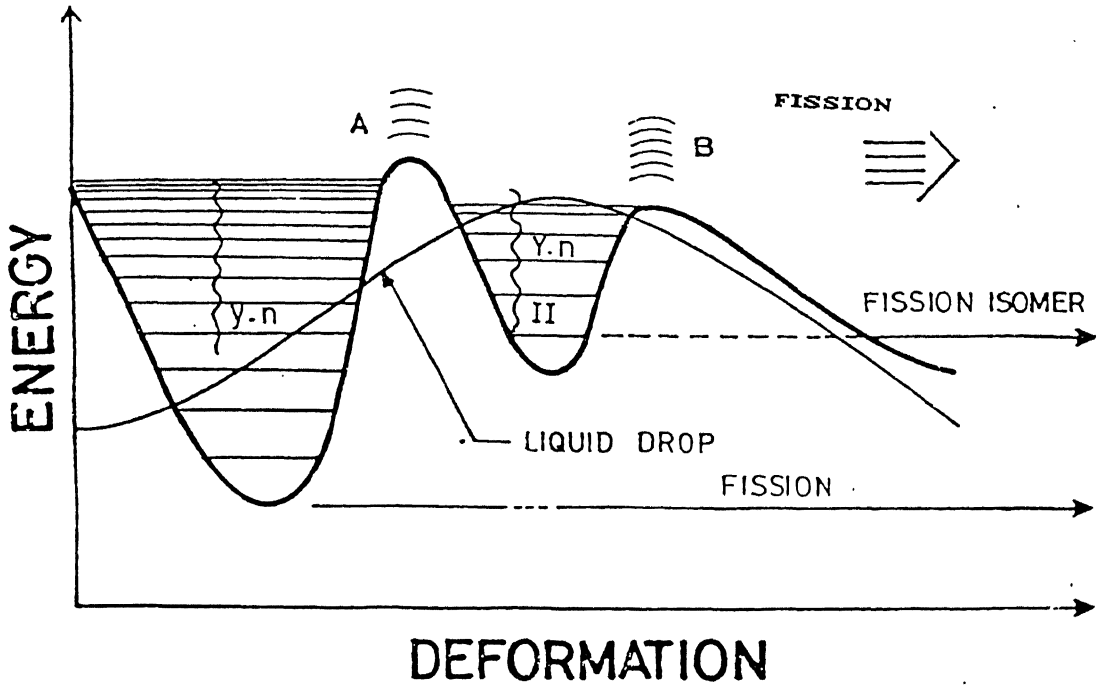

Fig. [1.3] Schematic Illustration of The Double Humped barrier.

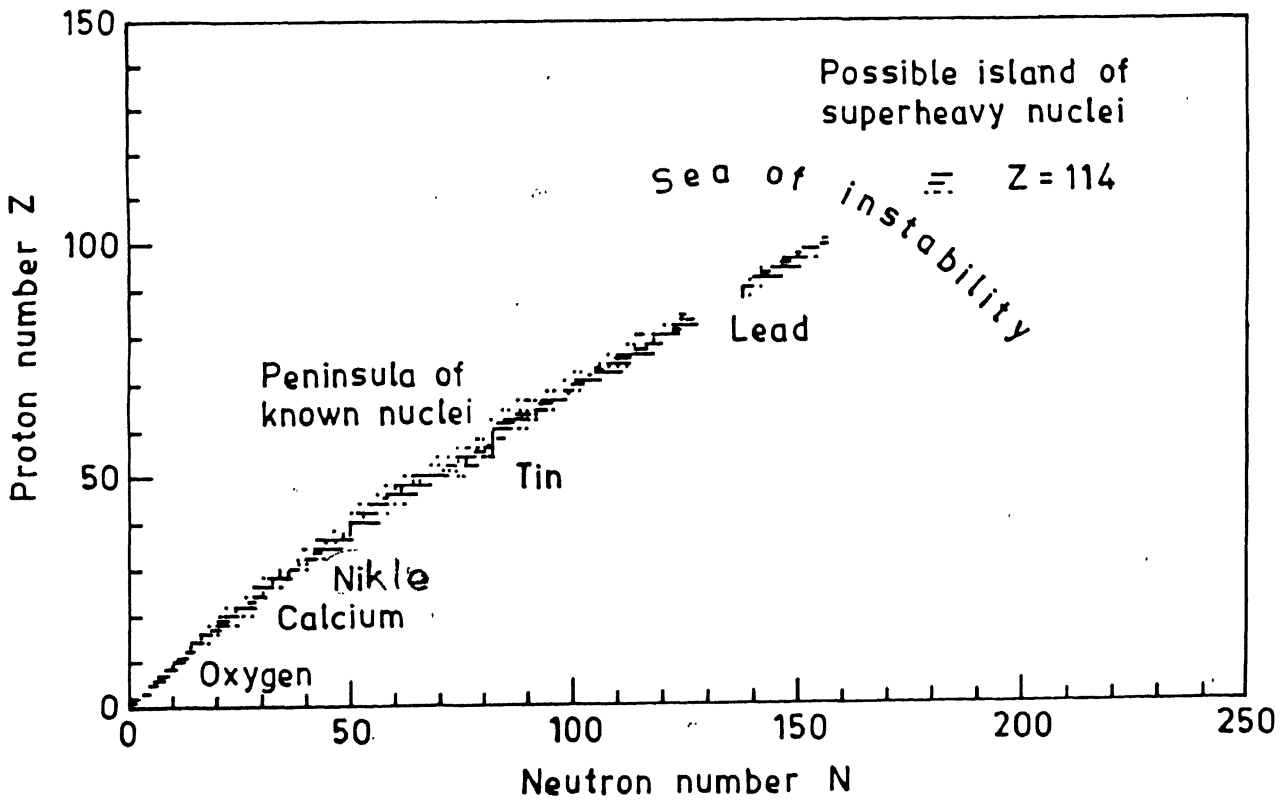

Fig. 1.3(b). Predicted island of superheavy nuclei around the doubly closed shell Z = 114, N = 184.

which is derived from the value of single particle level density at the Fermi surface. Nilsson model[29] with spheroidal shape was used to obtain $E_m(s)$. Fig[1.3a] shows the liquid drop potential as a fuction of deformation now incorporating Strutinsky's microscopic correction to get the double humped barrier. To digress a bit, one of the most important predictions of this approach was the existence of super-heavy elements [see Fig.1.3b]. This was one of the motivations for the development of heavy ion accelerators. Though we have had limited success in the synthesis of transuranium elements, the advent of accelerators has provided other manifestations of large scale collective motion.

It has been shown that while the first barrier is mass symmetric, the second barrier is mass asymmetric[30]. Detection and measurement of the rotational gamma rays in the second minimmum has provided direct experimental support to the picture of the double humped fission barrier[6]. The deformation potential energy surface for actinide nuclei can now be calculated to an accuracy sufficient to yield fission barrier heights within 0.5 MeV. There have also been some recent measurements of the conditional fission barrier heights through studies of highly asymmetric fission which are in general agreement with the predictions of the liquid drop model. Fission barrier heights of medium mass nuclei continue to defy a complete understanding with the liquid drop model over predicting the barrier heights by 5-10 MeV. Second order corrections to the liquid drop model such as finite range effects, compressibility and charge redistribution effects seem to be playing an important role

in deciding the fission barrier heights[31].

Further investigations along these lines are clearly required. There is no direct experimental information on the structure of the deformation potential energy surface beyond the fission saddle point. The calculated slope of the potential energy beyond the saddle point depends rather sensitively on the magnitude of the nuclear curvature tension because of the highly necked in shapes encountered at this stage of the process. The value of the nuclear curvature tension is however not known unambiguously at present because there is a discrepancy between the theoretical estimates of this quantity and the value deduced from nuclear mass fits. The determination of slope is important as it contains information on the nuclear viscosity present during the descent of the nucleus from saddle to scission. Considering that the nature of collective dynamics beyond the fission saddle point will be dependent on the slope of the potential energy, there is an urgent need to resolve this discrepancy. However, there are a number of experimental measurements which can throw some light on this problem.

One of these is the study of the light charged particles emitted in the so called *ternary fission*[32]. The angular distribution of the LCPs is sharply peaked perpendicular to the fission fragment direction. This implies that LCPs are emitted from the vanishing neck region between the two nascent fission fragments when they are fairly close to each other. Its subsequent motion can be understood in terms of the effect of the Coulomb field of the two fragments. Based on this a trajectory calculation can be

performed which alongwith other things gives us the idea of prescission kinetic energy i.e. the energy accumulated by the nucleus before it divides in two. The value of the prescission kinetic energy is an important parameter in the determination of the viscosity.

Recent measurements[33] on the emission of neutrons in coincidence with fission have shown that an appreciable fraction of the neutrons are emitted during the saddle to scission descent of the nucleus. The fraction of excitation energy going into the emission of these scission neutrons as compared to the energy appearing in the prescission kinetic energy can yield information on the nuclear viscosity during this stage of the fission process. However, our present understanding of the reaction dynamics and also the experimental input is still not adequate enough to deduce a reliable value of the viscosity coefficient.

A major fraction of the energy released in fission appears as the total kinetic energy of the fission fragments. As mentioned earlier, this energy first appears as the Coulomb interaction energy at scission and then gradually gets converted into fragment kinetic energies as they separate to infinity. The variation of total kinetic energy as a function of Z is well documented. It has been found that to the first order total kinetic energy varies linearly with $Z^2/A^{1/3}$ [34]. Substantial experimental information on the variation of total kinetic energy with the excitation energy for the actinide nuclei exists in literature[35].The variation seems to depend crucially on the relative height of the two barriers.

However, in light of recent results on increased scission neutron multiplicity in both heavy ion as well as light ion induced reaction[33], the results on the variation of the total kinetic energy with excitation energy of fissioning nuclei have become suspect. We will elaborate more on this in Chapter 3 where we present our result on the measurement of the variation of total kinetic energy with excitation energy for fission fragments from ^{238}U. The nature of this variation determines the magnitude of viscosity. The nature of the collective dynamics between the saddle and the scission points and temperature dependence of the scission act may yield a small dependence of the kinetic energy on the excitation energy of the compound nucleus. Experimental information on this aspect of the process is quite meagre and additional experiments may be most useful.

[1.4] MASS AND CHARGE RELAXATION IN FISSION

The asymmetric fragment mass and charge distributions in low energy fission of actinide nuclei have remained a challenge to nuclear theorists for several decades. While it has been established well that the asymmetry arises mainly due to the shell structure effects of the nascent fragments, the exact mechanism of mass and charge evolution leading to the observed asymmetry is not yet known. While the quasistationary models have had some success, it has been established that simple considerations based on the static deformation potential energy are not adequate to explain the

asymmetry. The collective dynamics in the mass asymmetry degree of freedom seems to be playing a crucial role beyond the fission saddle point. This includes not only the kinetics governed by the inertia and the driving potential but also the nature of the dissipative forces in operation between the saddle point and the scission point. This has given rise to statistical models based on full equilibrium at the scission point, stochastic models of nucleon exchange between the nascent fragments[36] and dynamical models with finite viscosity[37]. The nature of mass evolution is yet to be fully resolved. Recent observations[38] of odd-even effects in the primary mass and charge yields further complicate the problem.

[1.5] ANGULAR DISTRIBUTION OF THE FISSION FRAGMENTS

In fission induced by an energetic projectile, the fragments exhibit an anisotropy with respect to the incident beam direction. Bohr applying the ideas of the collective model to the deforming fissioning nucleus, explained the observed fragment angular distributions on the basis of his *channel theory*[39]. In this theory, the angular distribution of the fission fragments are related to the quantum levels of the fissioning nucleus atthe saddle point. Thus, spectroscopy of highly deformed nuclei comes naturally from the study of fission fragment angular distribution measurements. Extended to the medium excitation energy region with a statistical distribution of levels at the fission saddle point, the measured anisotropies yield direct information on the nuclear moments of

inertia and therefore on the shape of the saddle point. Underlying the Bohr model and its extension to high excitation energies is the assumption that the tilting mode attains equilibrium at the fission saddle point and does not change during the descent to scission. Extensive measurements[40] of fragment anisotropies for a number of systems over a wide range of bombarding energies have clearly demonstrated the smooth transition from the discrete level regime close to the fission barrier to the statistical region, a rapid washing out of nuclear shell effects on the level densities with excitation energy and shape parameters of fission transition state nuclei at high excitation energies consistent with the predictions of the liquid drop model. Fragment angular distribution is one of the well understood features of the fission process at present and it promises to be a senstive probe of angular momentum transfer in heavy ion induced reactions.

A very interesting correlation between the fragment anisotropy and the mass has been seen in a few experiments[41]. While the correlation can be explained in some cases on account of multichance fission, the effect appearing to be genuine in the others. If so, this demands a reevaluation of our present understanding of fragment mass and angular distributions, for, it is generally believed that the angular distributions are frozen at the saddle point while the mass and charge distributions are decided only at the scission point. This may rule out any correlation between the two observables.

[1.6] SECONDARY RADIATIONS FROM FISSION FRAGMENTS

The configurations of the two fragments touching each other at scission determines various distributions in fission. It is beleived that both the bulk properties as well as the microscopic properties are decided during this stage of motion of the nuclei on its way to fission. At the instant of separation, the primary fragments acquire considerable energy from the following sources– the intrinsic excitation energy of the fragments at scission, the deformation energy of the fragments at scission and the coulomb excitation of one of the fragments by the other during separation. The fragments then deexcite through the emission of γ ray, neutrons and sometimes a charged particle. By studying the mass, charge and kinetic energy of the fragment and the properties of the secondary radiation by which fragments deexcite, one can study the nature of the collective motion from saddle to scission. Most of the excitation energy is released in the form of neutron emission and so studies of prompt neutron emission provide information about the deformation and excitation energies of the fragments at scission. The majority of the neutrons are emitted from fission fragments in a very short time (less than 4×10^{-14} seconds after scission). The number of neutrons as a function of fragment mass for thermal neutrons was first observed by Fraser and Milton[42]. The number of neutrons ($\bar{\nu}$) shows a typical saw tooth structure first increasing with mass upto symmetric division, then falling sharply beyond symmetry and after that increasing with mass. It has also been

observed that with the increase in excitation energy of the compound nucleus this saw tooth structure gets washed away[43]. This behaviour has been interpreted on the basis of shell effects and deformation characteristics of fragments. Thus, neutron measurements are expected to yield, apart from the magnitude of the excitation energy that is transferred into internal excitation energy, also the information on the role played by the shell deformation and pairing effects on the deexcitation of the fragments.

Studies of photons were stimulated in the 1950's by the realization that the experimentally observed gamma ray energy from fission is greater than the theoretical estimates based on the assumption that gamma emission takes place after neutron emission. The total energy going towards gamma ray emission is about 8 MeV/ fission[40]. The average binding energy of the neutrons in these neutron rich fission fragments is around 4-5 MeV. Thus, the gamma rays taking away 8 MeV is slightly puzzling as one more neutron can be emitted. One of the reasons could be that the fission fragments carry some angular momentum also and the gamma rays are emitted to dissipate this angular momentum. Calculations including angular momentum effects predict the value closely but they predict that above the neutron binding energy the photon emission approaches zero.

The angular distribution of gamma rays is forward peaked with respect to fragment direction. Strutinsky[44] has interpreted this in terms of aligned scission dynamics resulting in fission fragments,

even from even-even nucleus in its ground state, possessing appreciable angular momentum. The gamma rays from fission fragments exhibit an anisotropy of 12 to 15 % and it is dependent on the energy of gamma ray. The study of anisotropy in gamma emision is also important to investigate if the energy from fission channel is being transferred into the giant resonance. The fission fragments are known to possess 10-15$\hbar$ of angular momentum and 15-20 MeV excitation energy. At this energy most of the angular momentum is taken away by the gamma ray. The number of gamma rays that are emitted in fission depends not only on the excitation energy of the fragments but also on the nature of the excited states of these neutron rich fragments. The multiplicity studies in heavy ion reactions are known to provide the spin distribution of the emitting nucleus. Although there exists a huge data bank with regards to the average number of gamma rays emitted in a variety of nuclei, there are only a few investigations on the average width of the gamma ray multiplicity distribution. The average width is an important parameter in the estimation of the spin distribution of the fission fragments. The width in the angular momentum distribution and even the relative spin that is imparted to the fission fragments arises due to the saddle to scission dynamics. Thus, the study of secondary radiations which occur at time scales orders of magnitude greater than the saddle to scission dynamics throws some light on the nature of dynamics involved.

A detailed study of the multiplicity distribution is called for since the concepts of single particle degree of freedom, the

nuclear shape degrees of freedom, angular momentum and pairing all influence the gamma ray emission process very crucially. All these various shell effects are predicted to decrease and then vanish at sufficiently high excitation energy. Gamma rays from fission fragments with moderate amount of excitation energy and spin therefore provide an excellent tool in this endeavour because a rapidly rotating nucleus is quite sensitive to shell effects, changing rapidly with angular momentum and deformation. Further, all these effects are present in the phenomenon of fission in which the density of levels in a highly deformed and often rapidly rotating system governs the fate of the nucleus. It is in these limits of exciation energy and angular momentum that our experimental knowledge is very limited. We discuss more of this in chapter 2 wherein we have calculated the spin distribution of the fission fragments resulting from scission dynamics. We also present the variation of the width and mean multiplicity as a function of charge ratio of the fission fragments. We also present our results on the prompt gamma ray anisotropy as a function of gamma ray energy. The anisotropy studies are important in the study of the competition between the E1 and the E2 modes of emission. This competition has been seen in the deexcitation of the heavy ion reaction residues and has prompted us to investigate the nature of deexcitation of fission fragments to look for this competition.

[1.7] CONCLUSIONS

The fission phenomenon offer many opportunities for the study of a phenomenon occuring in nuclear matter under extreme conditions with respect to shape, spin and excitation energy. It is thus clear that the fission process probes very nearly all aspects governing these *large scale collective motion*- the structure of the multidimensional deformation potential energy surface, the inertial and the dissipative aspects of the collective dynamics, and the general nuclear behaviour far off the equilibrium configurations. While heavy ion reactions have considerably widened the scope of such studies, the simplicity of the fission process has retained its elementary character. There still remain several aspects of the fission process which continue to defy a full understanding even today. Fifty years after its discovery, the fission process continues to be unique and challenging.

[1.8] REFERENCES

1. O.Hahn and F.Strassman, Naturwissenschaften 27 (1939) 11.
2. O.R.Frisch, Nature 143 (1939) 426.
3. A.E.S.Green, Phys. Rev.95 (1954) 1006.
4. N.Bohr and J.A.Wheeler, Phys. Rev. 56 (1939) 426
5. L.Meitner and O.R.Frisch, Nature 143 (1939) 239.
6. S.Bjornholm and J.E.Lynn,Rev. Mod. Phys. 52 (1980) 725.
7. S.S.Kapoor, *Talk delivered at IAEA School at Trieste, Italy in February 1988.*

8. D.Hilcher, *Proc. International Conf. Nucl. Phys. Calcutta* 1989 (in press).

9. J.R.Nix and A.J.Sierk, Phys. Rev. C21 (1980) 982.

10. J.R.Nix and A.J.Sierk, Nucl. Phys. A428 (1984) 161.

11. P.Fong, Phys. Rev. 135 (1964) 1339.
P.Fong, Phys. Rev. 102 (1956) 434.

12. L.Wilets, "*Theories of Nuclear fission*" Clarendon Press, Oxford (1964).

13. W.D.Myers, Nucl. Phys.A204 (1973) 465.

14. W.D.Myers and W.J.Swiatecki, Nucl. Phys.A336 (1980) 267.

15. G.F.Bertsch, P.F.Bortingnon and R.A.Broglia Rev. Mod. Phys. 55 (1983) 287.

16. J.R.Huizenga and W.U.Schöder, *in Treatise on Heavy Ion Science Vol* 2Plenum Press (1984).

17. H.A.Krammers, Physica VII nr 4 (1940) 284.
D.L.Hill and J.A.Wheeler, Phys. Rev. 89 (1953) 1102.

18. C.F.Tsang, Phys. Scr. 10A (1974) 90.

19. J.Blocki, Ann. Phys. 113 (1978) 330.

20. J.Randrup, Ann. Phys. 112 (1978) 356.

21. J.Randrup and W.J.Swiatecki, Ann. Phys. 125 (1980) 193.

22. S.K.Samaddar, D.Sperber, M. Zielinska-Pfabe, M.I.Sobel and S.I.Garpmen, Phys. Rev. C23 (1981) 760.

23. J.R.Nix and A.J.Sierk, *Proc. International Conf. Nucl. Phys. Bombay* (World Scientific) 1984

24. W.J.Swiatecki, Phys. Scr. 24 (1981) 113.

25. U.L.Businaro and S.Gallone, Nuovo Cim. 1, 629, (1955) 1277.

L.G.Moretto, M.A.McMahan, L.G.Sobotka and W.J.Wozniak, *Proc. International Conf. Nucl. Phys. Bombay* (World Scientific) 1984.

26. W.J.Swiatecki, Phys. Rep. 4 (1981) 113.

27. W.J.Swiatecki, Phys.Rev. 109 (1955) 937.

28. V.M.Strutinsky, Nucl.Phys. A95 (1967), 420.

29. S.G.Nillson, C.Tsang, A.Sobiczewski, Z.Szymanski, S.Wycelb, C.Gustafson, I.L.Lamm, P.Moller and B.Nillson, Nucl.Phys. A131 (1969) 1.

30. E.K.Hyde, *Nucl. Properties of the heavy elements Vol* III *Fission Phenomenon* (Prentice Hall).

31. A.V.Ignatuk, G.N.Smirenkin, M.G.Itkis, S.I.Mul'gin and V.N. Okolvich, Sov.J. Nucl.Phys. 16 (1985) 307.

32. N.Carjan, A.Sandulesch, V.V.Paskerich, Phys. Rev. C11 (1975) 782.

33. S.S.Kapoor, H.Baba and S.G. Thompson, Phys. Rev. 149 (1966) 965.

34. J.R.Nix and A.J.Sierk, *Proc. International Conf. Nucl. Phys. Bombay* (World Scientific) 1984.

35. P.David, J.Debrus, H.Janszen, J.Schulze, M.N.Harakeh, J.Van Der Plicht and A.Vander Woude, Nucl. Phys. A380 (1982) 27.

36. V.S.Ramamurthy, *Ph.D. Thesis* (Bombay University)

37. W.Norenberg, *Proc. Symp. on Phys. and Chem. of Fission* (Vienna 1969)

38. M.N.Rao, R.K.Choudhury and D.C.Biswas, *Proc. International Conf. Nucl. Phys. Calcutta* 1989 (in press).

39. A.Bohr, *Proc. U.N.Int. Conf. Peacful Uses At. Energy* 2 (1956) New York.

40. R.Vandenbosch and J.R.Huizenga, *Nuclear Fission* Academic Press (1971).

41. S.S.Kapoor, *Talk delivered at IAEA Experts on fission data at* MITO Japan.

42. J.S.Fraser and J.C.D.Milton, Phys.Rev. 93 (1954) 818.

43. C.J.Bishop, R.Vandenbosch, R.Alley, R.W.Shaw Jr. and I. Halpern, Nucl. Phys. A150 (1970) 129.

44. V.M.Strutinsky, Sov. J. JETP 10 (1960) 600.

CHAPTER II

GAMMA EMISSION FROM FISSION FRAGMENTS

[2.1] INTRODUCTION

Gamma ray emission by excited nuclei, be it from fission fragments or reaction products formed in nuclear collisions or a product of radioactive decay, has been a rich source of information on nuclear structure and reaction mechanism. In fact, nuclear spectroscopy as a well defined branch of nuclear physics grew largely as a result of measurements of discrete gamma ray transitions close to the ground state. More recently, studies of discrete gamma ray transitions in rapidly rotaing nuclei has led to the discovery of backbending phenomenon[1,2], in particular, and more generally to a detailed information on the structure of nuclei with large spin.

There is also a continuum component to the gamma ray spectrum arisisng from the statistical nature of gamma ray emmision at high excitation energies of the emitting nuclei. Studies of the continuum component, however, are hampered by the unavoidable interference from the compton continuum. Nevertheless, continuum gamma rays have provided valuable information. For example, in fission fragments it is the gamma ray measurements which led to the information on the magnitude of fission fragments spin[3,4]. It is now known[4] that even in the case of spontaneous fission of

even-even nuclei fission fragments carry about 10-15 units of angular momentum arising due to scission dynamics.

In the last few years, there is also an increasing interest in the study of continuum gamma rays from nuclei with large spin produced in heavy ion reactions. These have now become feasible with the development of large volume germanium detectors with anti-compton shields which results in appreciable reduction in the Compton background gamma rays. The study of the continuum gamma rays has opened up new vistas in the study of the mechanism of gamma ray emission from hot rapidly rotating nuclei. In light of some recent results[5-8] from the heavy ion laboratories, we have had to revise a few of our earlier concepts. It is now conjectured[6,7] that the E1 statistical gamma rays and the E2 rotational cascade compete with each other, whereas previously it was believed that the nucleus reaches the yrast state by the emission of statistical gamma rays and then dissipates the angular momentum and rotational energy by the emmission of E2 cascade along the yrast line.

One of the ways to study this possible competition between the E1 and the E2 modes of gamma emission is to investigate the nature of gamma rays emitted from the fission fragments. This study has a distinct advantage as compared to the study of gamma rays from reactions either induced by heavy ions or by light ions. This is because in case of light ion induced reactions, most of the energy brought in goes into heating the system giving it very little angular momentum, thereby populating the system at the extreme left

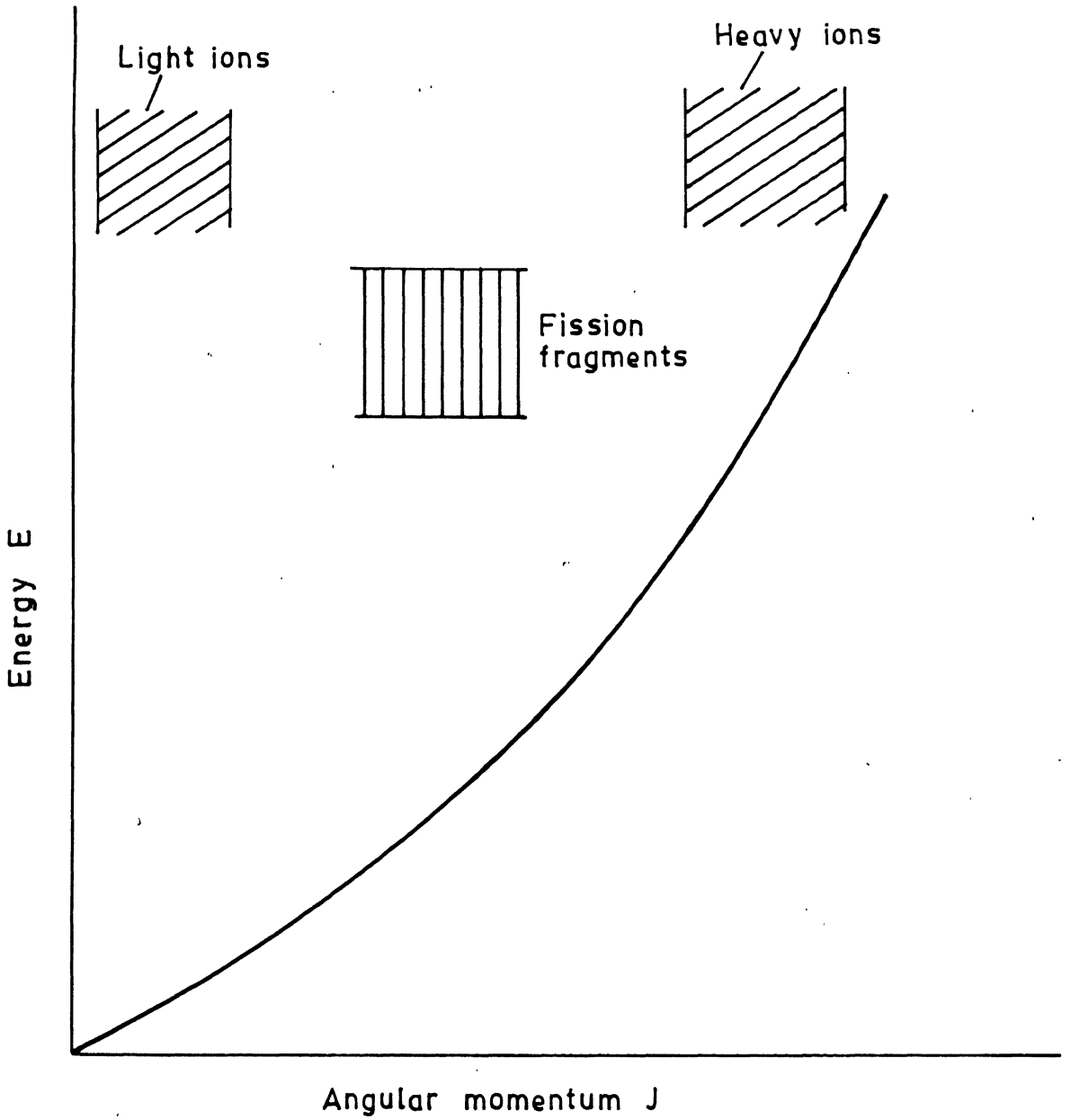

Fig. 2.1. A typical yrast plot showing the region populated by heavy ion and light ion induced reaction as compared to region populated by fission fragments.

of the yrast plot. Fig.[2.1] illustrates the region populated by the light ion induced reaction on a typical yrast plot. The nucleus, in this case, is expected to decay primarily by particle emission and once this is inhibited then by the emission of E1 statistical gamma rays. On the other hand, in reactions induced by heavy ions, alongwith the excitation energy, a lot of spin is also imparted to the nucleus thereby populating it upto the extreme right of the yrast plot as shown in the Fig.[2.1]. The nucleus is spinning rapidly and a substantial amount of the energy brought in is locked up as rotational energy. Though the nucleus is expected to decay both by E2 rotational cascades and E1 statistical gamma rays, there is uncertainity associated with the reaction dynamics and the nuclear matter is thermodynamically hot. The single particle properties and the pairing effect is therefore expected to be considerably diluted.

The fission fragments with spin of 10-15 $\hbar$ and excitation energy of 15-20 MeV are in the middle region of the yrast plot as shown in Fig.[2.1]. The competition between the E2 and E1 gamma rays is expected to be enhanced. The role played by close shell structure, pairing and deformation in gamma emission is better investigated in case of gamma emission by fission fragments. We can study nuclei with Z ranging from 35 to 65 in a single experiment under identical conditions. This spans the region of nuclei which are spherical, deformed and soft. In case of fission fragments, another advantage is the gamma spectroscopy of neutron rich nuclei, which is beyond the realms of heavy ion accelerators but comes naturally in this case.

The fission fragments emit gamma rays in the last stage of their de-excitation process[4]. The fission fragments carry a lot of excitation energy arising due to scission dynamics and de-excite first by neutron emission which takes place within about 10^{-16} to 10^{-14} seconds. Gamma ray emission takes place after that, upto a time as late as 10^{-9} seconds. There are also delayed gamma rays which are mainly due to radioactivity of the neutron rich fission products and isometric transitions. These delayed gamma rays contain very little information about the fission dynamics and we will discuss them no further.

From the study of angular distributions and the multiplicity distributions of prompt gamma rays, it is possible to infer the spin of the fragments. The overall picture, now, is one in which the fragments in spontaneous and thermal neutron induced fission appear to have 10-15 $\hbar$ of angular momentum oriented preferentially about 90° to the fission axis[5]. The electrostatic forces betwen the fragments at scission would induce such angular momenta in the fragments if the fragments are formed in axially asymmetric configurations. Although the de-excitation mechanism of the fission fragments has been a subject of many investigations in the past, information regarding gamma ray emission, such as its dependence on the single particle properties, pairing, deformation and spin distribution, is still lacking.

The experimental observables in gamma ray measurements are the first moment $\langle N_\gamma \rangle$, and the higher moments $\langle N_\gamma^n \rangle$ of the multiplicity distributions. The first moment is the average number of gamma rays emitted by the fragments, the second moment is related to the width

of the distribution and the third moment gives the skewness of the distribution[10]. On each one of these, a differential measurement with respect to the mass, charge or kinetic energy of the fragment can be made. Alternatively, one can measure these quantities averaged over any one of these quantities or over all of them. One can also measure the anisotropy in gamma ray emission with respect to the fragment direction averaged over the fragment properties or differentially as a function of any one of them.

In this chapter, we present our work which aims to measure the average multipicity and the width of the multiplicity distribution of gamma rays as a function of the charge ratio of the fission fragments. We have also measured the anisotropy in gamma ray emission with respect to the fragment direction as a function of gamma ray energy. Using the available expressions for the branching ratios for neutrons and gamma ray emission from fission fragments, we have written a statistical model code based on the Monte Carlo technique which traces the history of the de-excitation of the fission fragments which have excitation energy of about 15-20 MeV and angular momentum of 10-15 $\hbar$.

This chapter is divided in five sections. In Sec.[2.2], we describe the details for the measurement of the multiplicity and the width of the multiplicity distribution of the gamma rays emitted from fission fragments(in spontaneous fission of ^{252}Cf) as a function of their charge ratio. In Sec.[2.3], we present the anisotropy in prompt gamma rays from fission fragments of ^{252}Cf with respect to the fragment direction of motion as a function of gamma ray energy. In Sec.[2.4], we describe the Monte Carlo based

statistical model code to simulate the gamma ray and neutron emission from the hot rotating fission fragments. Here, we investigate the role played by shell structure, excitation energy and the angular momentum carried by the fission fragments on the mean multiplicity and the width in the gamma ray multiplicity distribution in the spontaneous fission of ^{252}Cf. Lastly, based on our theoretical calculations, we have made an attempt to calculate the initial spin distribution of the fission fragments. Sec.[2.5] contains the conclusions drawn from the above studies.

[2.2] MULTIPLICITY MEASUREMENTS

[2.2](a) Introduction

There have been a number of measurements in low energy fission on the average multiplicity of the gamma rays and the average energy taken by them in order to investigate the nature of de-excitation of the fission fragments[11,12]. Pleasanton[13] measured the multiplicities of the gamma rays in thermal neutron induced fission of ^{235}U in the time range of 5 ns, 70 ns and 275 ns. His value of the multiplicity agree well with the value obtained by Verbuisky[11]. This implies that most of the gamma rays are emitted within 5 ns of the fission process. Mehta etal.[12] measured the average multiplicities and the average energy taken by the gamma rays in the ternary fission of ^{252}Cf. The average energy taken by the gamma rays is not much different than in the case of binary fission. There have been some measurements[14] which are in contradiction to the results of Mehta etal.. Increased $\bar{N}_\gamma$ indicates

that the spin of the fragment is more but in ternary fission, due to stretched scission configuration, the spin should be less. However, Ramamurthy etal.[15,16] have also found that the $\bar{N}_\gamma$ does not show any significant variation in ternary and binary fission. This may imply that the average excitation energy and the spin of the fragments remain the same irrespective of the emission of light charged particles. These results are well documented and the average energy taken by the gamma rays is 7.0±0.5 and the average number is 9.7±0.4[17].

It has also been observed that there is a positive correlation between the number of neutrons and the average number and the energy of the gamma rays emitted by the fission fragments while de-exciting. Johansson[18] observed that the gamma ray multiplicity as a function of fragment mass shows a prominent saw tooth structure which is similar to the structure exhibited by the neutrons[19]. The gammma ray multiplicity increases linearly with fragment mass till the doubly closed shell at mass 132. It then falls sharply and then again increases linearly with the fragment mass. In case of neutrons, this saw tooth stucture is destroyed as the energy of the fissioning nucleus increases. However, experimental information on the variation of multiplicity with the excitation energy in the case of gamma rays does not exist. Nifenecker[20] obtained a closed form expressions for the correlation between the number of neutrons emitted and (i)the average energy and (ii)the average number of gamma rays respectively:

$$\langle E_\gamma(m,E_K)\rangle = 0.75\ \bar{\nu}(m,E_K) + 2$$

$$\langle N_\gamma(m,E_K)\rangle = 1.1\ \bar{\nu}(m,E_K) + 1.75$$

where E_γ is the average energy taken by the gamma rays .

N_γ is the average number of gamma rays emitted.

$\bar{\nu}$ is the average number of neutrons emitted.

m is the mass of the fission fragments.

E_K is the kinetic energy of the fission fragments.

However, all these measurements have been made as a function of fragment mass which is obtained by measuring the energy of the two correlated fission fragments and then invoking mass and momentum conservation principles[21]. The mass resolution obtained by this technique is of the order of 4 amu. The pairing effect, if playing a role in the gamma emission process, is expected to be absent. The deformation effects are also expected to be diluted becuse of the poor mass resolution.

There has only been one measurement on the width of the gamma ray distribution[15,16] where the width was measured as a function of single fragment kinetic energy in the spontaneous fission of ^{252}Cf. The measurements were done both for binary[15] as well as ternary fission[16]. The results indicate that width in case of ternary fission is larger than that in binary fission. This, according to the authors, is because the average spin in case of ternary fission is small leading to less number of cascade gamma rays. However, in measurements as a function of single fragment kinetic energy the shell properties are expected to be diluted. The second moment of the multiplicity distribution as in heavy ion reactions is expected to yield information about the original spin distribution of the nucleus[10]. The present experiment was performed with the aim to see the effects of pair correlations and deformations on the average

multiplicity and the width of the multiplicity distribution. The charge of the emitting fragment was identified by measuring the characteristic K X-ray it emitted[22]. By this technique, we could get a single charge resolution.

[2.2](b) Experimental Details

A californium 252 source with a strength of 5μ Curie was mounted in a vacuum chamber. A solid state surface barrier detector was kept at a distance of 3 cms. from the ^{252}Cf source to detect the fission fragments. A high purity germanium (HPGe) detector was kept in a direction perpendicular to the direction of fragment motion to detect the K X-rays. The distance of the HPGe detector was around 4 cms from the source. The Californium source was mounted in such a way that it subtended an angle of 45° to both the fission detector and the HPGe detector. Two sodium iodide (NaI) scintillation detectors were kept in the plane perpendicular to the X-ray direction. One of the sodium iodide detectors was a 2" X 2" crystal and the other was a large 5" X 5" crystal. The two scintillation detectors were kept such that one subtended an angle of 160° to the direction of fragment motion and the other an angle of 200° to the direction of fragment motion. Fig.[2.2] shows a schematic arrangement of the experimental set-up. The large sodium iodide detector was suitably shielded with lead bricks to avoid the detection of stray neutrons and cosmic ray particles. Before starting the experiment, it was ensured that this shielding was

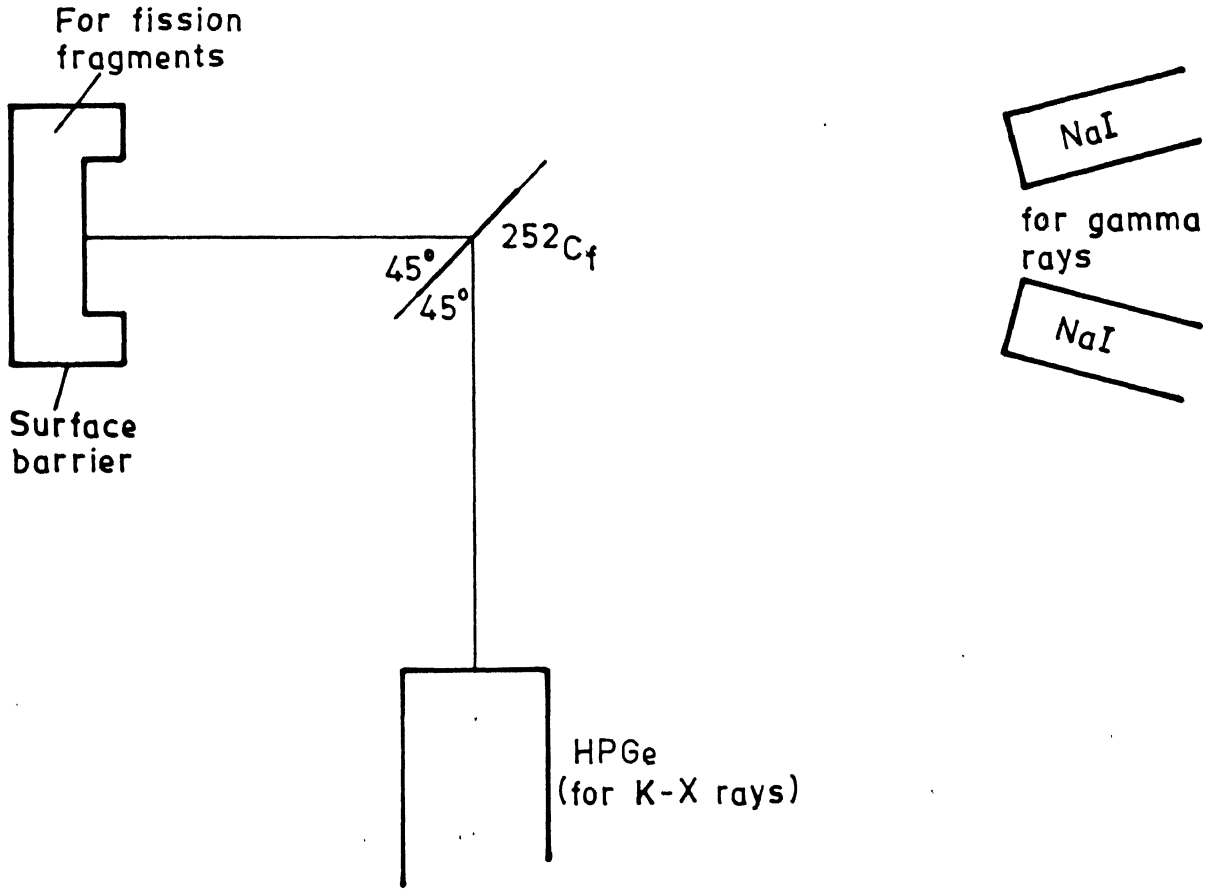

Fig. 2.2. Geometrical setup for the measurement of the multiplicity and width of the multiplicity distribution of prompt gamma rays emitted from fission fragments in spontaneous fission of ^{252}Cf .

effective by recording a K X-ray spectrum in coincidence with fission and gamma ray without the Californium source.

To measure the average number of gamma rays emitted per fission, it is sufficient to employ just one gamma ray detector of known detection effeciency and of known solid angle factor for a fixed number of fission events. To measure the width of the gamma ray distribution, it is essential to employ one more gamma ray detector. In fact, the number of detectors needed is directly related to the moment of distribution one is aiming to measure. This is made clear by the set of equations that we present in the next paragraph.

The equations given below connect the coincidence rates to the multiplicity distribution P_n [10]:

$$C_i = \sum_n [1 - (1 - \Omega_i)^n] P_n \qquad (2.1)$$

$i=1,2$

$$C_{12} = \sum [1 - (1 - \Omega_i)^n - (1-\Omega_j)^n + (1-\Omega_i-\Omega_j)^n] P_n \qquad (2.2)$$

$$i=1,2 \; ; \; j=1,2; \; i=j$$

where Ω_i is the detection effeciency and C_i is the coincidence rate of the i'th gamma ray detector. Ω_i includes both the detection effeciency as well as the solid angle factor. If we assume that the solid angle of gamma ray detectors is small and the probability of two gamma rays entering one detector simultaneously is small, then for a single fission event the number of gamma rays detected will be given by:

$$C_i = \langle n_\gamma \rangle \Omega_i$$

where $\langle n_\gamma \rangle$ is the average multiplicity.

The probability that after the first gamma ray detector has

detected one of the $\langle n_\gamma \rangle$ gamma rays, the second detector will detect one of the $\langle n_\gamma - 1 \rangle$ gamma rays is :

$$C_{ij} = \langle n_\gamma (n_\gamma - 1) \rangle \Omega_i \Omega_j$$

It is therefore seen that the count rate for single and double coincidence are related to $\langle n_\gamma \rangle$ and $\langle n_\gamma^2 \rangle$. Since Ω_is are the only unknown quantities, to eliminate them it is sufficient to have a priori knowledge of n_γ. (However, since we did not do an absolute efficiency calibration of our gamma ray detectors, we have taken the average number of gamma rays $\bar{n}_\gamma$ from the data by Skarsvag[17]. He has measured it for spontaneous fission of ^{252}Cf and according to him $\bar{n}_\gamma = 9.7$. In writing the expression for $\langle n_\gamma \rangle$ and $\langle n_\gamma^2 \rangle$ we make two assumptions :

(i)the two gamma rays are not correlated

(ii)the detection effeciency of our gamma ray detectors averaged over the gamma ray spectrum is nearly constant for single and double coincidence measurements.

Assumption (i), in light of the fact that only about 5 gamma rays in 4Π geometry are emitted from one of the fragments, is approximately correct. Assumption (ii) is also justified in light of the fact that the effeciency curve for the NaI detector for gamma ray energy below 5 MeV is almost flat and the number of gamma rays above 5 MeV emitted by fission fragments is very small.

Figure 2.3 shows the block diagram of the electronic set up used for this experiment. Pulses from the HPGe detector i.e. the K-Xray pulse was fed to a preamplifier and then to a linear amplifier. The pulse from the linear amplifier was fed to the input of the linear gate and stretcher. The fission fragment pulse from

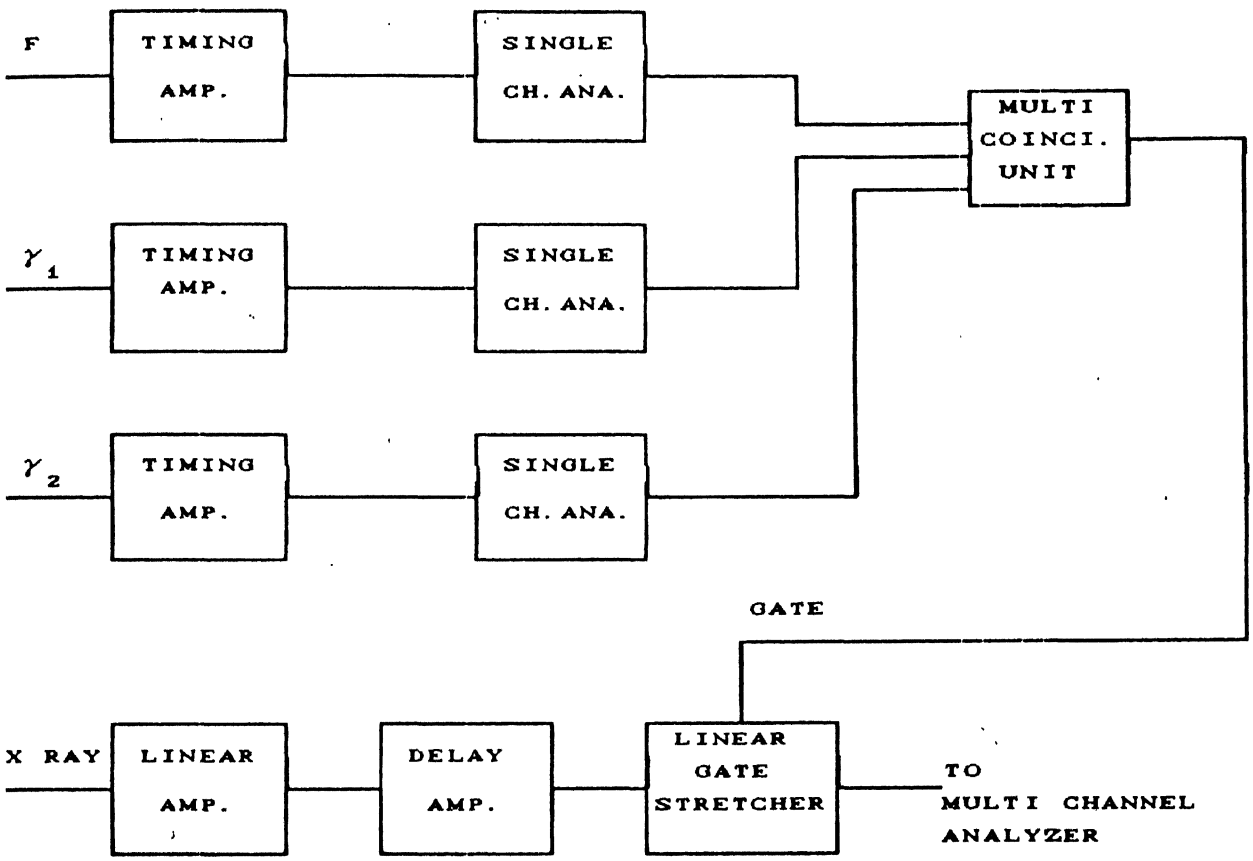

Fig.2-3. Electronic set up for the determination of the multiplicity and width in the mulplicity of gamma rays from fragments in spontaneous fission ^{252}Cf.

the solid state surface barrier detector was passed through a preamplifier-amplifier combination and then to a single channel analyzer, which was used to cut off the natural alpha particles. The pulses from the two gamma ray detectors were also processed similarly. The single channel analyzer in case of gamma ray detectors were adjusted to cut off gamma ray energies below 80 keV. The pulse from these single channel analyzers were fed to a multicoincidence unit which had the option of switching off or on any one of these pulses.

[2.2](c) Results

First the K-Xray spectrum was recorded in a multi channel analyzer in coincidence with fission fragments. We will call this spectrum the double coincidence spectrum, which is shown in Fig.[2.4]. The triple coincidence spectrum was recorded by switching on the multicoincidence unit by the gamma pulse from either one of the NaI crystals alongwith the fission fragments. The triple coincidence spectrum obtained by the larger sodium iodide crystal is shown in Fig.[2.5] Finally, we recorded the K-Xray spectrum in coincidence with the pulse from the two gamma ray detectors and the fission detector. This we will call the four fold coincidence spectrum. The four fold coincidence spectrum is shown in Fig.[2.5].

These spectra were then unfolded to get the intensity due to various charges. For this, a fitting program was used which required the energy and the relative intensity of the K_α and K_β X-ray lines of the various charges[23]. The program also required the

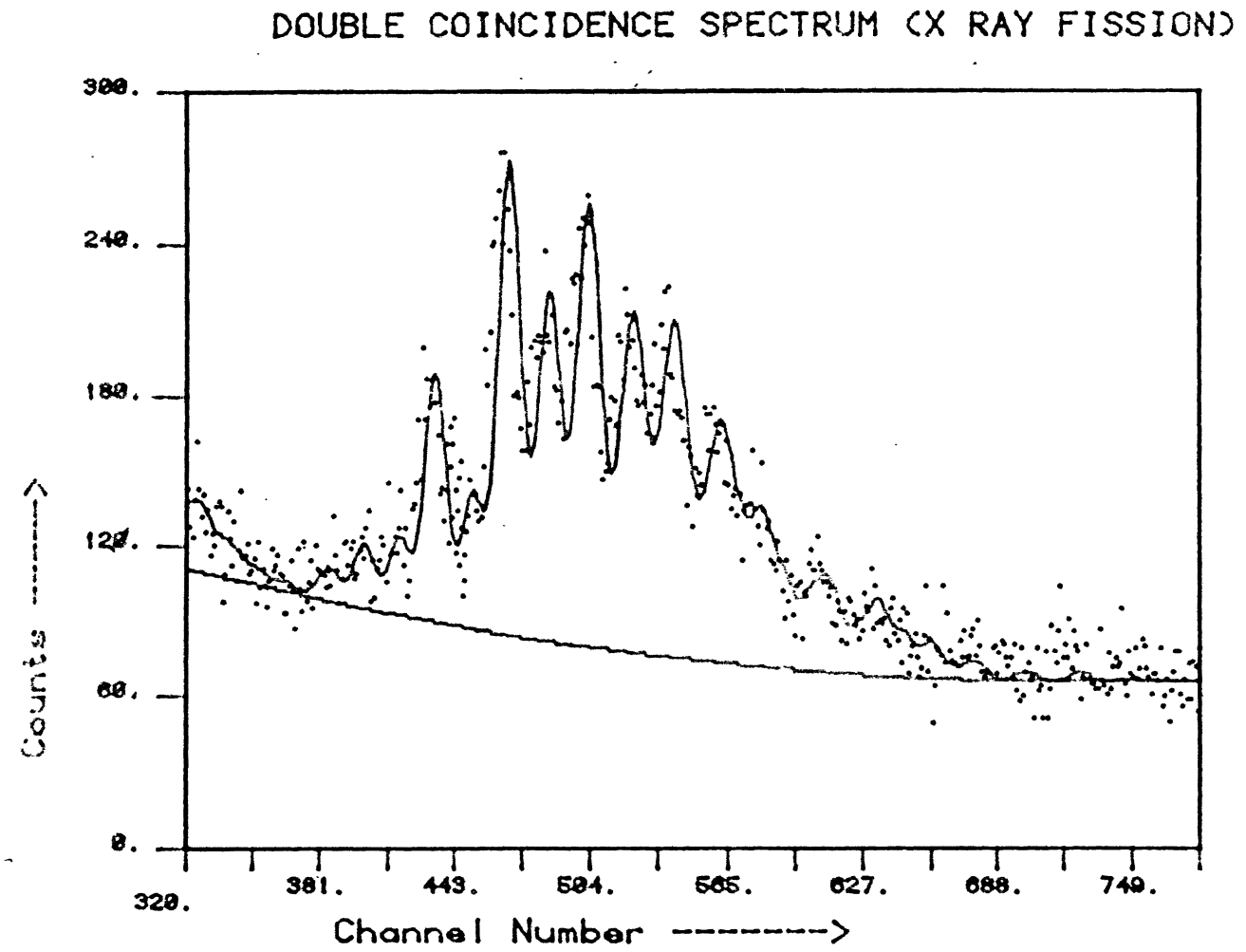

Fig. [2.4] The double Coincidence Spectrum.

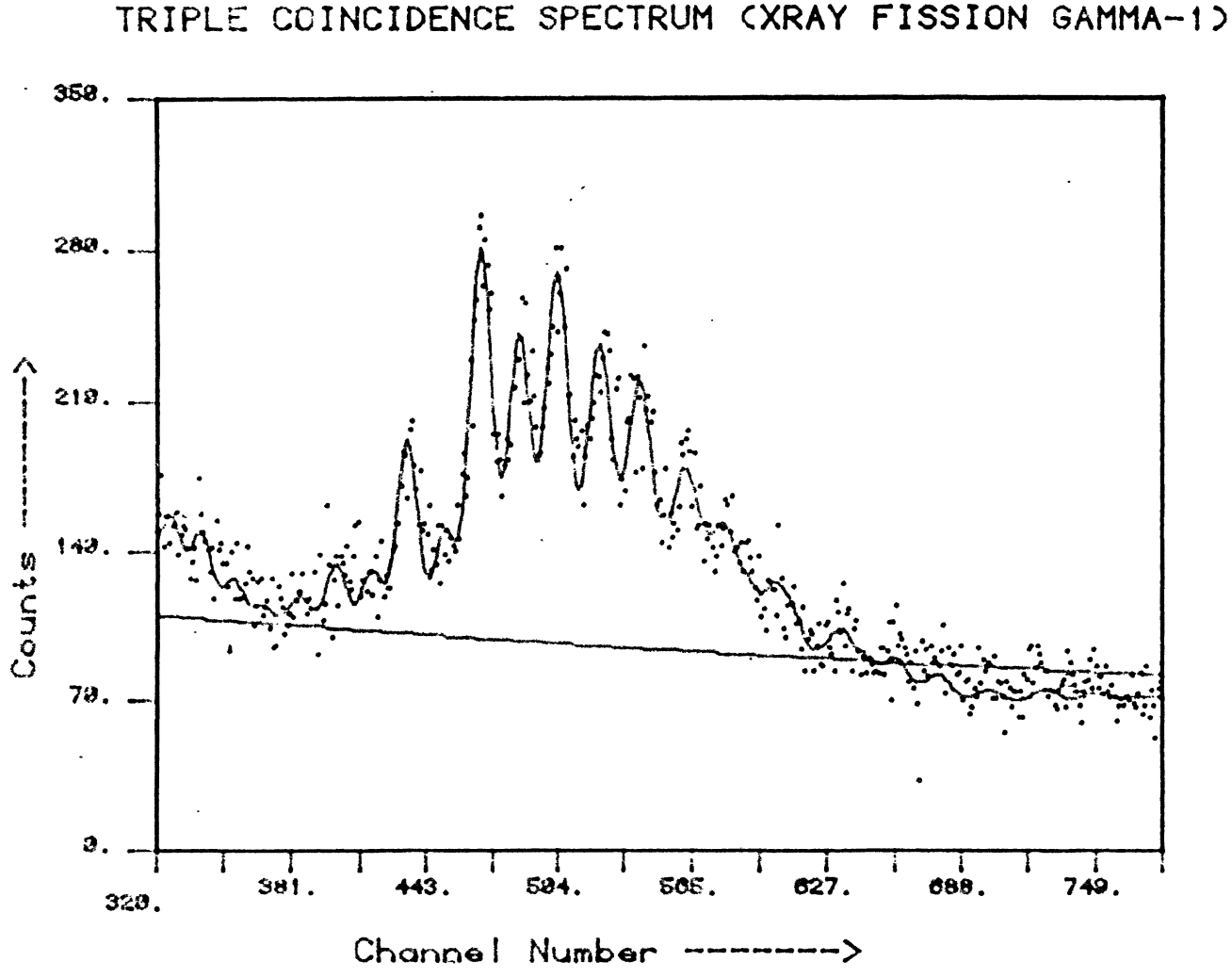
TRIPLE COINCIDENCE SPECTRUM (XRAY FISSION GAMMA-1)
350.
280.
210.
140.
70.
0.
Counts ------>
320.
381.
443.
504.
565.
627.
688.
749.
Channel Number ------->
Fig. [2.5] The Triple Coincidence Spectrum.

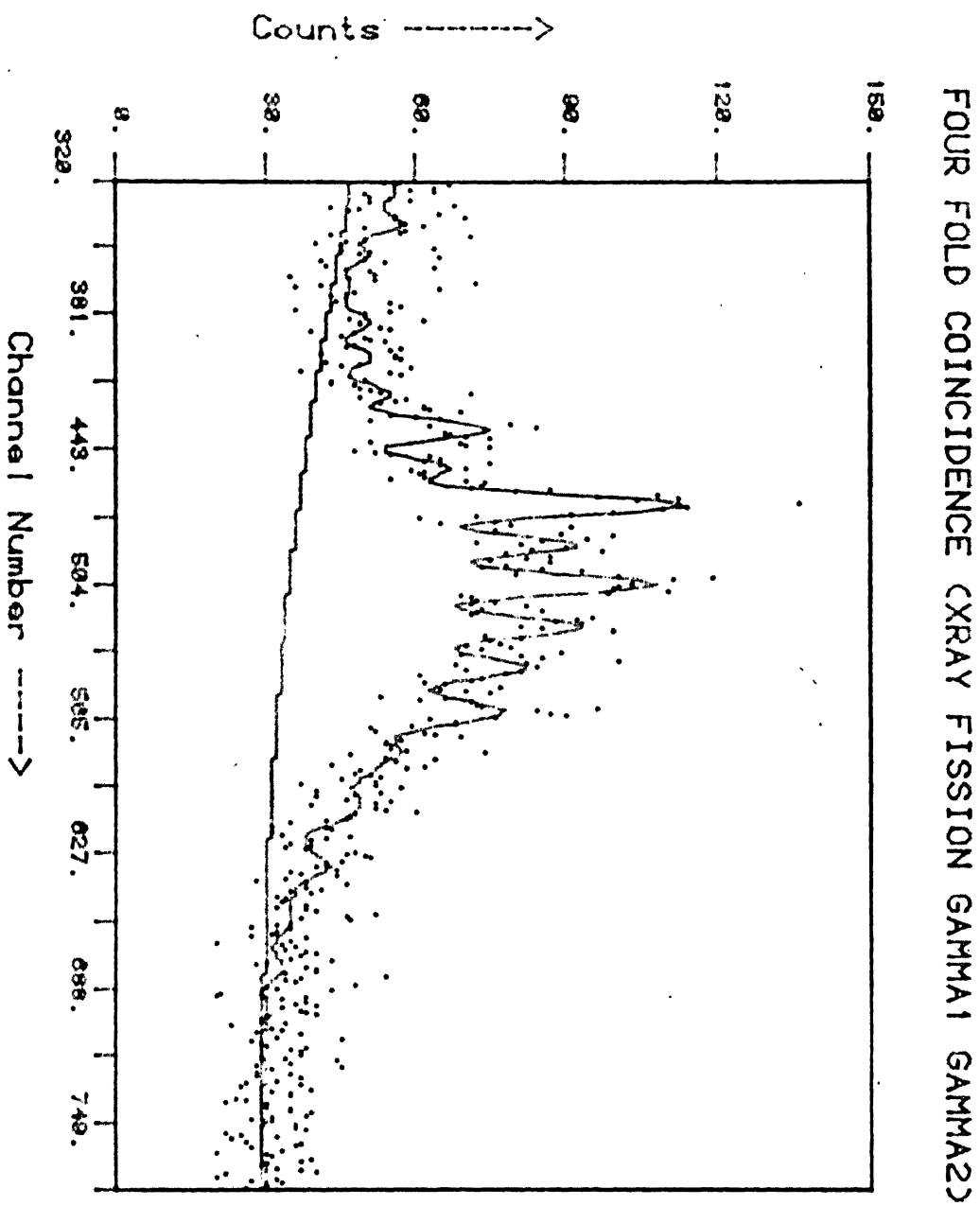
FOUR FOLD COINCIDENCE CXRAY FISSION GAMMA1 GAMMA2)
Counts ------->
0.
30.
60.
90.
120.
150.
320.
381.
443.
504.
565.
627.
688.
749.
Channel Number ----->
Fig. [2.6] The Four Fold Coincidence Spectrum.

detector response function. The background was fitted with a second order polynomial fit. χ^2 minimisation was done to get the proper unfolding of the spectra. The area under each of the charges gives the contribution of that charge for either the double, triple or four fold coincidence spectra. From the measured K X-ray intensities due to various charges in the double, triple and four fold coincidence spectra, we have derived the average gamma multiplicity $\langle N_\gamma \rangle$ and the width of the gamma multiplicity distribution as a function of the charge ratios of the fission fragments. The procedure followed is simple but for the sake of completeness we will describe it. For a particular charge if $\overline{N_f^Z}$ is the average number of fission events that the fission detector has detected; $\overline{N_x^Z}$ is the average number of X-rays emitted per fission and $\overline{N_\gamma^Z}$ is the average number of gamma rays emitted per fission, then the intensity of that charge in the double triple and four fold coincidence spectra is given by

$$C_D^Z = \overline{N_f^Z N_x^Z \Omega_x}$$

$$C_T^Z = \overline{N_f^Z N_x^Z N_\gamma^Z \Omega_x \Omega_\gamma^1}$$

$$C_F^Z = \overline{N_f^Z N_x^Z N_\gamma^Z (N_\gamma - 1) \Omega_x \Omega_\gamma^1 \Omega_\gamma^2}$$

and

$$\overline{N_\gamma^Z} = \frac{C_T^Z}{C_D^Z \Omega_\gamma^1}$$

$$\overline{N_\gamma^z(N_\gamma^z-1)} = \frac{C_F^z}{C_D^z \Omega_\gamma^1 \Omega_\gamma^2}$$

Fig.[2.7] shows the intensities obtained due to various charge ratios (C_D^z, C_T^z, C_F^z) in the double triple and four fold coincidence spectra.

Fig.[2.8] shows the average multiplicity as a function of charge ratio of the fission fragments. The multiplicity seems to indicate some odd even differences, for example, multiplicity for charge 54 is larger than that for 55 and again it is larger for charge 56 than for 57. However, since the error bars are large any definite statements cannot be made on average multiplicity as a function of fragment mass.

Fig.[2.9] shows the width of the multiplicity distribution as a function of the charge ratio of the fission fragments. The width clearly shows a dependence on the odd even nature of the fragments. The widths corresponding to charge 52 is larger than for charge 53, for charge 54 it is again large and then for charge 55 it is small. As we pass over to the region of deformed nuclei (Z= 57-59), the odd even character seems to vanish. Slightly lower values of the width observed and the vanishing of the odd even structures can be attributed to the fact that the nucleus in this region is a rapidly spinnig object. We can deduce from our experimental observations that the magnitude of the rotation is such as to destroy the pairing correlations. Secondly , a substantial amount of energy is now stored as the rotational energy of the fragment. The fragment dissipates this rotational energy and angular momentum by the

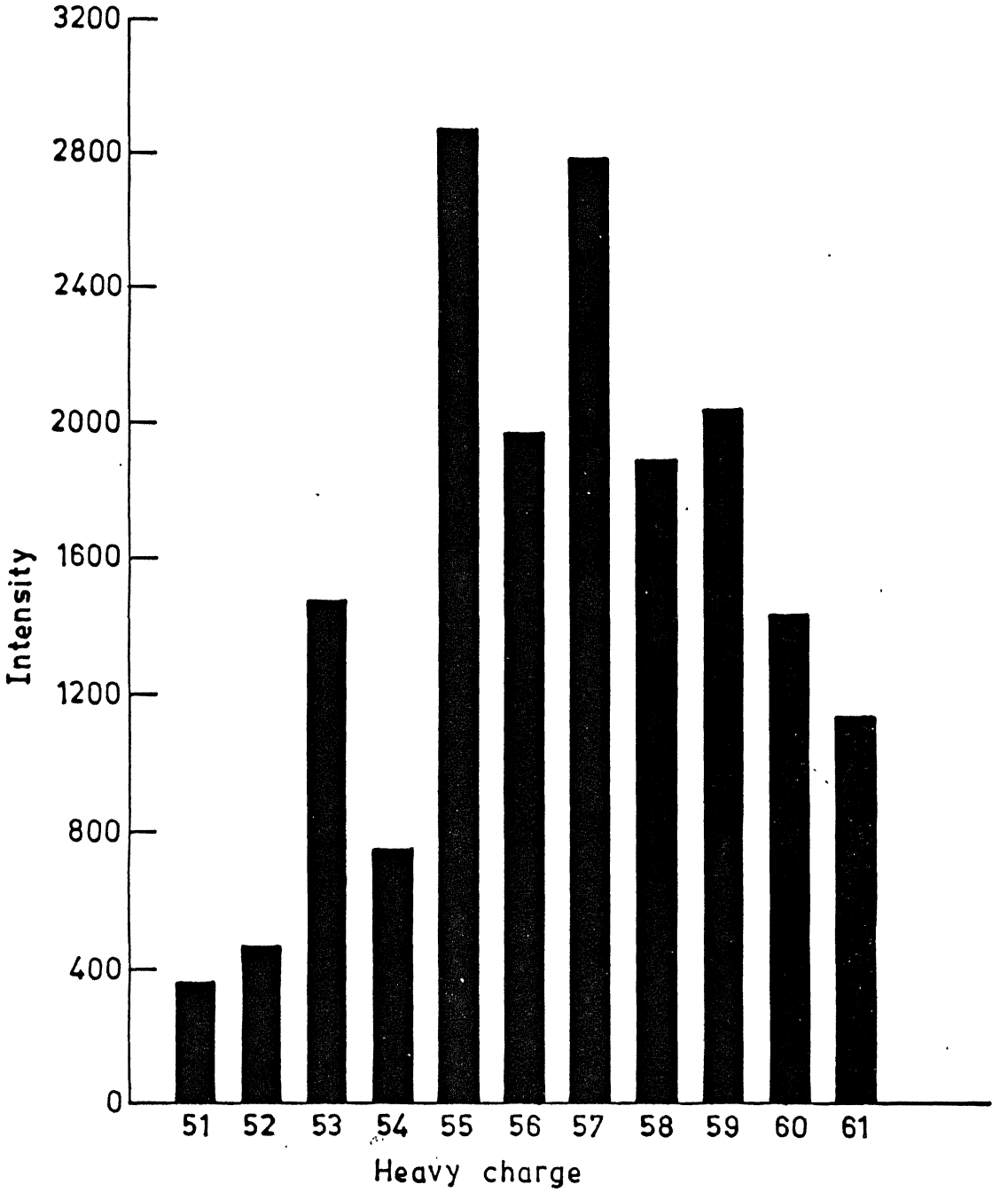

Fig. 2.7(a). Bar chart showing the intensity of various charges in double coincidence spectrum.

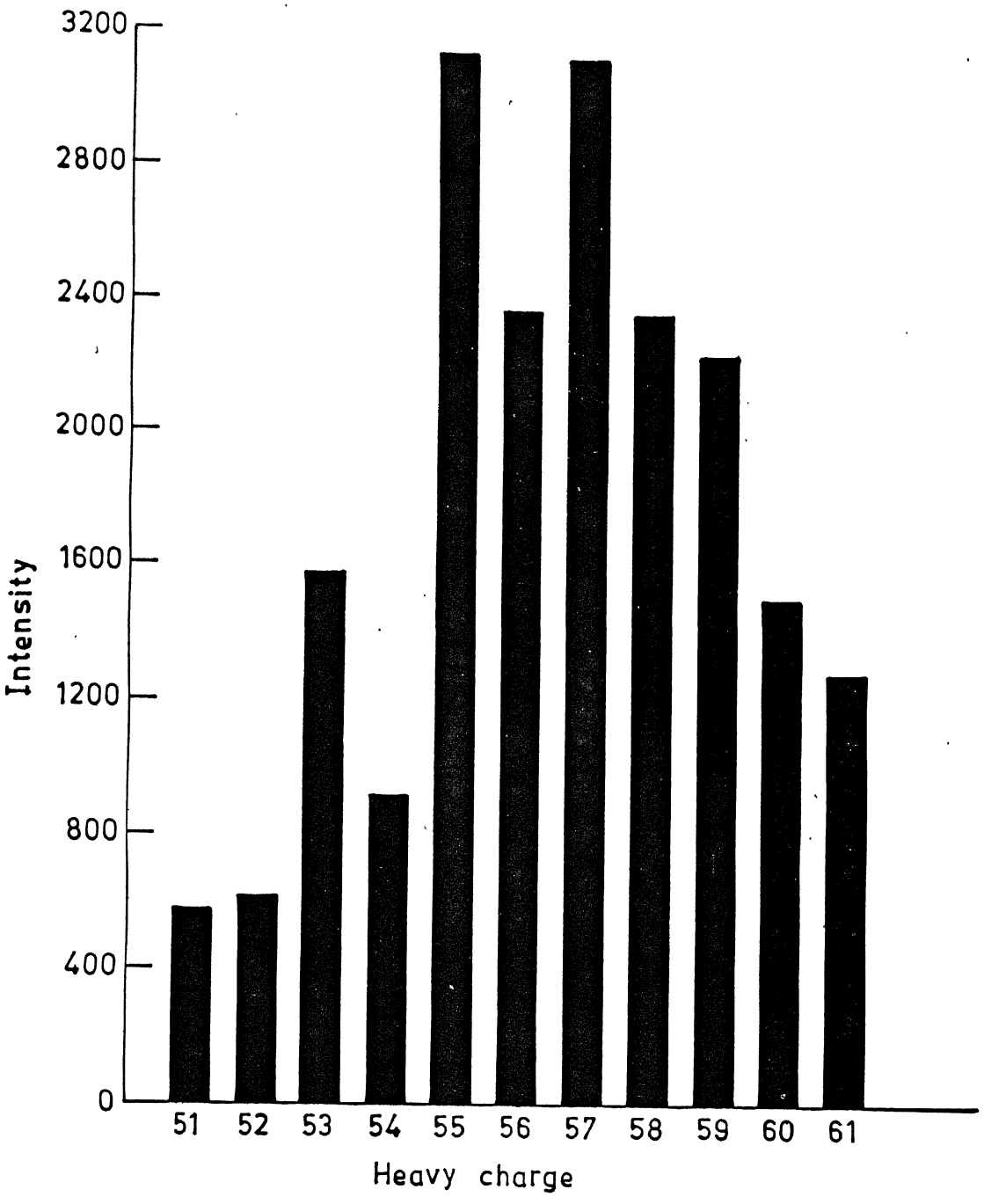

Fig. 2.7(b). Bar chart showing the intensity of various charges in triple coincidence spectrum.

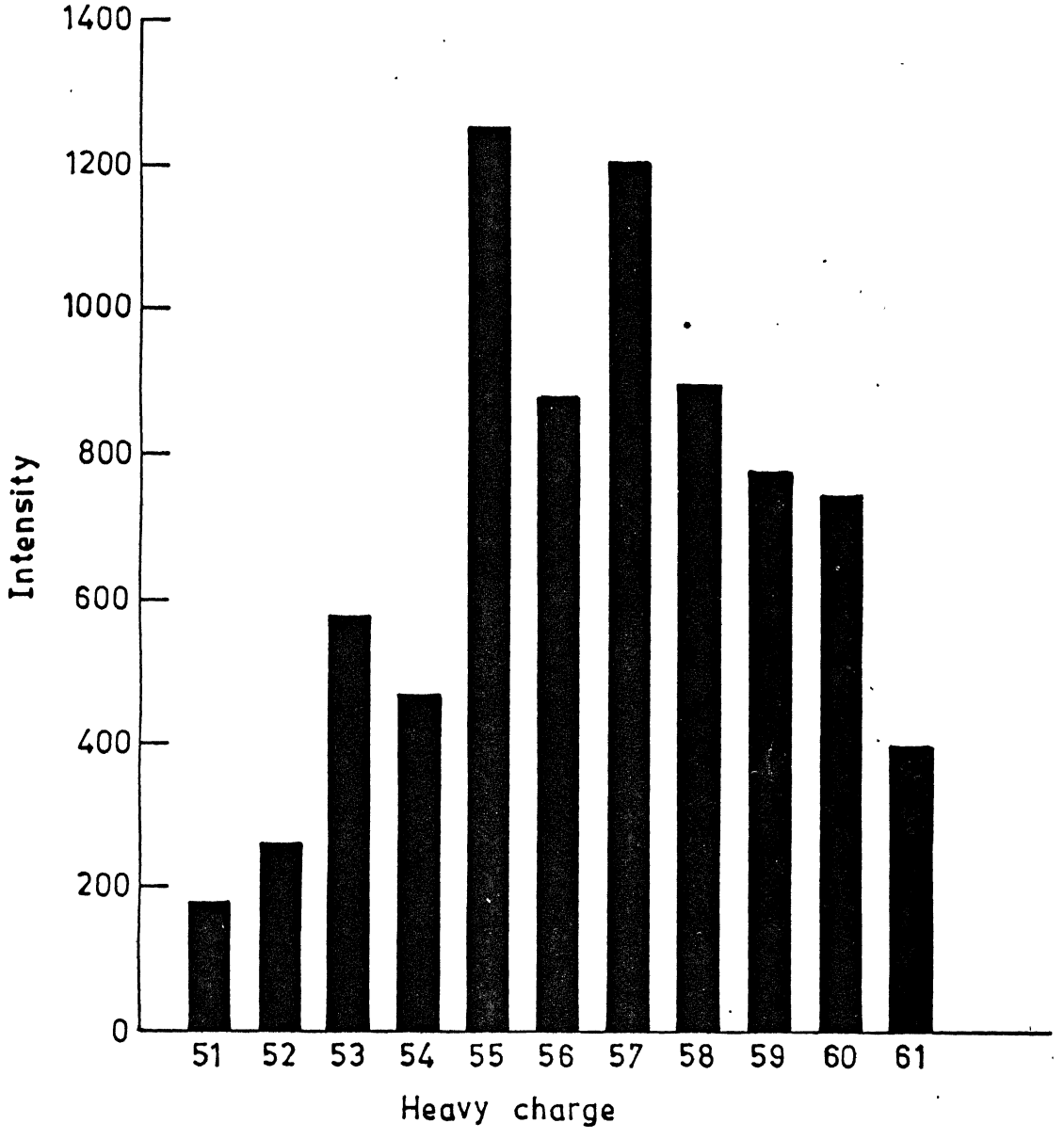

Fig. 2.7(c). Bar chart showing the intensity of various charges in four fold coincidence spectrum.

emission of E2 rotational cascades. These are transitions from fixed energy states with very little statistical variations associated with them. The contribution to the width comes from the statistical nature of emission of neutrons and the dipole transitions. The spherical nuclei are expected to de-excite by the emission of neutrons and then by statistical gamma rays. Being rotationally degenerate systems, the emission of E2 rotational cascades is inhibited. Thus the width of multiplicity distribution for spherical nuclei is expected to be more than that for a deformed nuclei. This is supported by our experiment also.

If we assume that the nuclear temperature at the scission point is 0.5 to 1 Mev and the moment of inertia of the fission fragment is between 100-200 MeV. Then the value of the experimental width obtained is in general agreement with the value of the width obtained by Moretto[24] assuming that the energy is partitioned equally amongst the various angular momentum bearing modes. The angular momentum bearing modes are the (i) bending mode (ii) tilting mode (iii) twisting mode and (iv) wriggling mode. The expression given by Moretto is

$$4\sigma_s^2 = \frac{2\mathcal{I}\mu r^2 T}{\mu r^2 + 2\mathcal{I}}$$

$$= \frac{10}{7}\,\mathcal{I}T$$

We will discuss the results in more detail in the last section of this chapter after we have presented our results for the statistical model calculations.

[2.3] ANISOTROPY STUDIES

[2.3](a) Introduction

The angular distribution of the γ rays emitted from the fission fragments with respect to the fragment direction can give information about quantities such as the multipolarity of radiation and the alignment of the angular momentum of the fission fragments. An angular correlation between the fission fragments and the prompt γ rays has been observed, with the emission in the direction of the fragments more probable by about 15% than emission perpendicular to the direction of the fragments[4,9]. There are two reasons for the anisotropy in the fission gamma ray angular distribution. One is due to the Doppler effect, i.e. an isotropic distribution of γ rays in the frame of reference of the fragments will give rise to a distribution in the laboratory system due to Doppler effect given by:

$$W(\theta) = W\,[1+(2+r)v/c\,\cos\theta]$$

where v is the velocity of the fragment, c is the velocity of light, θ is the angle with respect to fragment direction and r a small correction factor accounting for the change in energy of the γ rays. The Doppler anisotropy disappears if the experiment does not distinguish between the fragments or if the fragments are stopped before they emit γ rays.

The other cause of the anisotropy is of our interest. It is a consequence of a preferential orientation of the fragment spin with their direction of flight. The nature of anisotropy is a pointer to

the fact that γ emission is predominantly of quadrupole nature. Any angular momentum present in the original fissioning system appears later in the final fragments (but with the axis of rotation tending to lie in the direction of fragment motion) and as relative angular momentum between the fragments. The initial angular momentum, for low values of the projection of angular momentum on symmetry axis (which is expected for spontaneous and thermal neutron induced fission) is expected to appear as orbital angular momentum between the fragments. It has also been found that the magnitude of the anisotropy is insensitive to the initial compound nucleus spin. This along with the non appearance of the initial compound nucleus spin in the orbital angular momentum implies that the origin of the anisotropy with respect to fragment direction lies in the descent of the nucleus from the saddle to scission, a fact that can be utilized to study the dynamics of the fission process.

According to Strutinsky[25], axially asymmetric scission, gives rise to a transverse component of coulomb repulsion between the nascent fragments, which will cause them to rotate after fission in opposite directions. He has also derived a simple expression for the anisotropy of the radiation. Assuming that the de-excitation proceeds statistically, the angular distribution is given by

$$W(\theta) = 1+K(j/ IT) \sin \theta$$

where K = + 1/8 for dipole radiation

= - 3/8 for quadrupole radiation

Here, j is the angular momentum of the fission fragments

I is the moment of inertia of the fission fragments

T is the nuclear temperature.

There is always an admixture of dipole and quadrupole radiations. The assumption of pure quadrupole radiation leads to an under estimation of spin. The assumption that the relative probabilities of decay to states of higher or lower spins than the emitting state are dependent on a statistical level density weighting factor is also not quite correct for the last steps of the cascade where there are no final states of higher spin available.

Wilhelmy[26], by measuring the angular distributions of several $2 \longrightarrow 0$ transitions in the ground state band of even fission isotopes, had established that there is a preferential alignment of fragment spin with respect to their direction of flight. They found a preferential emission of E2 radiations along the direction of the fragment motion with anisotropies ranging between 8.3% to 33.4%. Hoffman[27] had done an early analysis of gross angular distribution of the fission γ rays. Wilhelmy's result agrees with that of Hoffman that the initial spins of the fragment are preferentially aligned perpendicular to the fragment's path.

Ivanov[28] has studied the fission γ rays as a function of fragment kinetic energies, mass ratios and also as a function of γ ray energy inc slow neutron induced fission of ^{235}U. They found that the γ anisotropy as a function of total kinetic energy shows a definite increase for all mass ratios. But γ anisotropy averaged over total kinetic energy is rather insensitive to mass ratios. Ambruster[29] has studied anisotropy of γ rays, emitted between 10 and 100 ps after the fission process, as a function of fragment

mass. Their results are in confirmation with that of Ivanov. They find that the anisotropy is approximately 20% for the heavy fragment mass whereas it is only 14% for the light fragment mass.

Skarsvag's[17] work is one of the few available in literature where differential measurement of γ anisotropy has been done as a function of γ ray energy. They find that total γ rays emitted within 12 ns after fission with energies greater than 0.114 MeV is 9.7 ± 0.3 per fission and the total γ ray energy released is (7.0 ± 0.3) MeV per fission. They have measured γ anisotropy as a function of γ energy from 0.114 MeV to 3.5 MeV. They find that the dipole and the quadrupole components are about equally strong at high γ ray energies, the dipole moment predominates at low energies and the quadrupole component at intermediate energies.

In the present work, we have measured γ anisotropy as a function of γ ray energy from 50 KeV to 5 MeV.

[2.3](b) Experimental Details

A spontaneously fissile source ^{252}Cf of 5μ Curie strength was kept in a vacuum chamber. Two solid state surface barrier detectors were mounted in the chamber such that both were at 90° with respect to each other and each of them saw the source symmetrical and at nearly equal solid angles. A NaI(Tl) scintillation detector was used to detect the γ rays and was kept at a distance of 60 cms from the source in line with one of the fission detectors, henceforth called as the F_o detector, and at an angle of 90° to the other fission detector, henceforth called the F_{∞} detector. Thus, the coincidence between the F_o detector and the NaI detector signalled

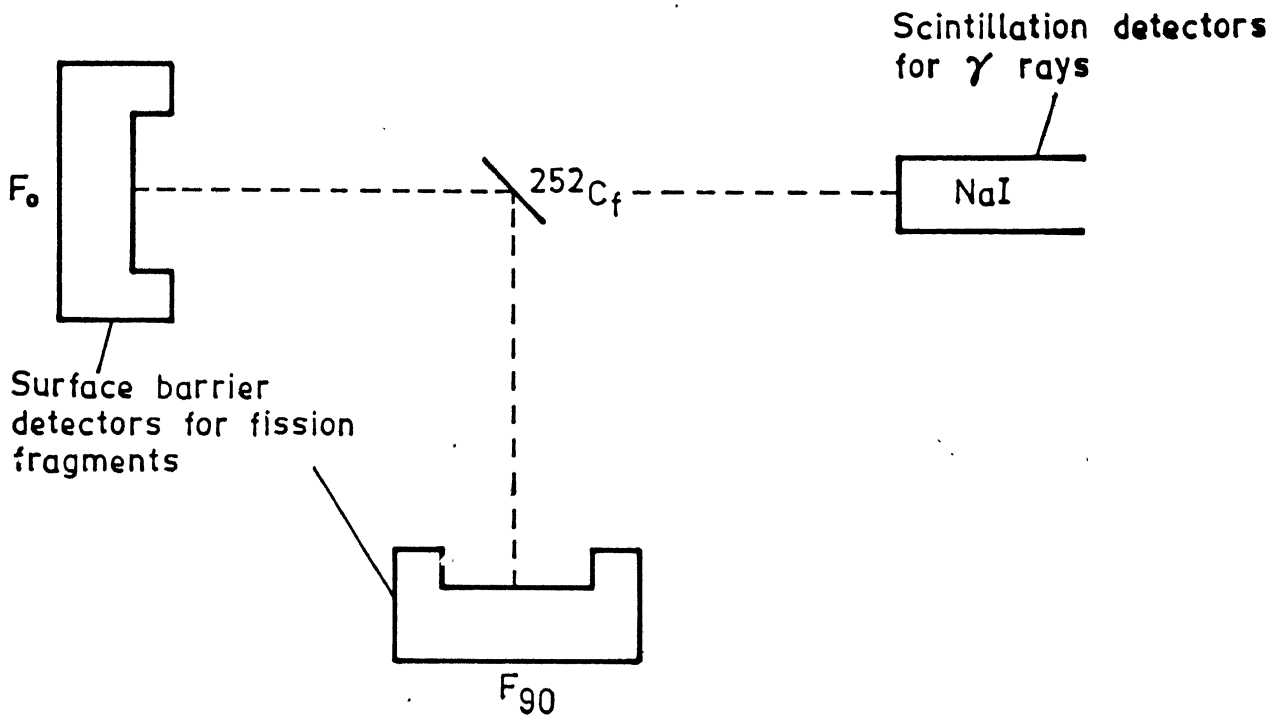

Fig. 2.10. Geometry of the experimental arrangement for the study of prompt gamma ray anisotropy as a function of gamma ray energy in spontaneous fission of ^{252}Cf.

γ ray emitted in the direction of the fission fragment, while the coincidence between the F_{∞} detector and the NaI detector signalled a γ ray emitted perpendicular to the direction of fragment motion.

The fission detectors were ORTEC F series heavy ions detectors. Each detector had an area of 300 mm^2 with a depletion depth of 60 μ. The sodium iodide detector was of 5" x 5" size with a resolution of 10% at 600 keV. Since the neutrons emitted from the fragments are strongly correlated to the direction of the fragment motion and thereby show a large anisotropy, it was necessary to eliminate them by the time of flight technique. Since we had a very large NaI crystal, it had to be properly sheilded from stray neutrons and cosmic rays. The shielding was tested with a run without the source and the background contribution was found to be negligible.

Fast coincidence was taken between either of the fission pulses and the γ ray pulse. To do this, the timing pulse from the preamplifiers of the fission detectors were passed through a fast timing filter amplifier, the output of which was fed to a constant fraction discriminator which was operated in the external delay mode. Walk adjustments were made to optimize the timing resolution. The pulse from the dynode of the photomultiplier coupled to NaI detector was processed in a similar fashion. The outputs of the two constant fraction discriminators being fed by the F_o and F_{∞} pulses were ORED and were used as a stop pulse for the Time to Amplitude converter, the start pulse being given by the γ ray pulse.

The energy pulse from the two fission detectors was passed

through a research amplifier which could give a −2V maximum signal (a requirement of the ADCs). The energy pulse from the γ ray detector was passed through a Spectroscopy Amplifier. Suitable delays were introduced to ensure coincidence between the analog pulses and the gate. The electronic block diagram used for the experiment is shown in Fig.[2.11]. The fission counts in the two fission detectors were monitored after every 12 hours. This was done to normalize the data such that both the detectors detected equal number of fission events.

A delay of 50 ns was introduced in the timing channel of F_{∞} detector to seperate the γ pulses due to F_o and F_{∞}. This resulted in a clean separation between the true peaks due to gamma emission along the direction of fragment motion and perpendicular to the direction of fragment motion. A timing resolution of 2.5 ns was obtained. The TAC peaks obtained are shown in Fig.[2.12]. The figure shows the TAC peak due to the F_o and the F_{∞} Channels. Also shown in the figure are the neutron humps in the direction of fragment motion and perpendicular to the direction of fragment motion.

The digital pulse from TAC which was +5 V was fed to a gate and delay generator to get a −2 V, a requirement of the CAMAC A to D converters being used. This −2 V logic pulse formed the master pulse and gated the camac ADC's Four parameters, namely the two analog pulse of the fission detectors, the cathode pulse from photomultiplier carrying information about γ ray energy and analog pulse from the TAC. These were recorded in the list mode on a magnetic tape on a camac based data acquisition system. The

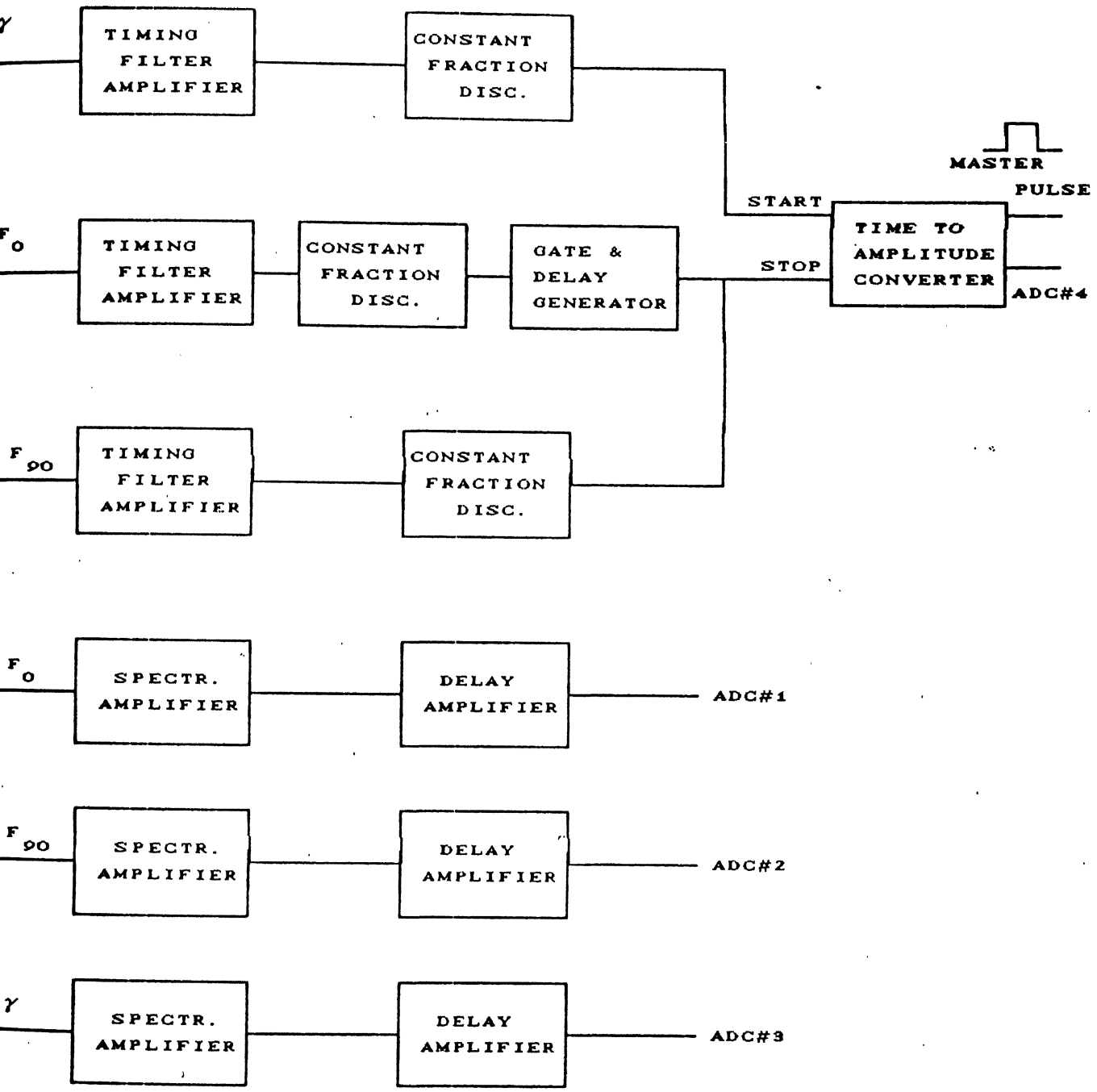

ig.2.11 Electronic set-up for the determination of anisotropy of prompt gamma ray w.r.t fragment motion as a function of gamma ray energy.

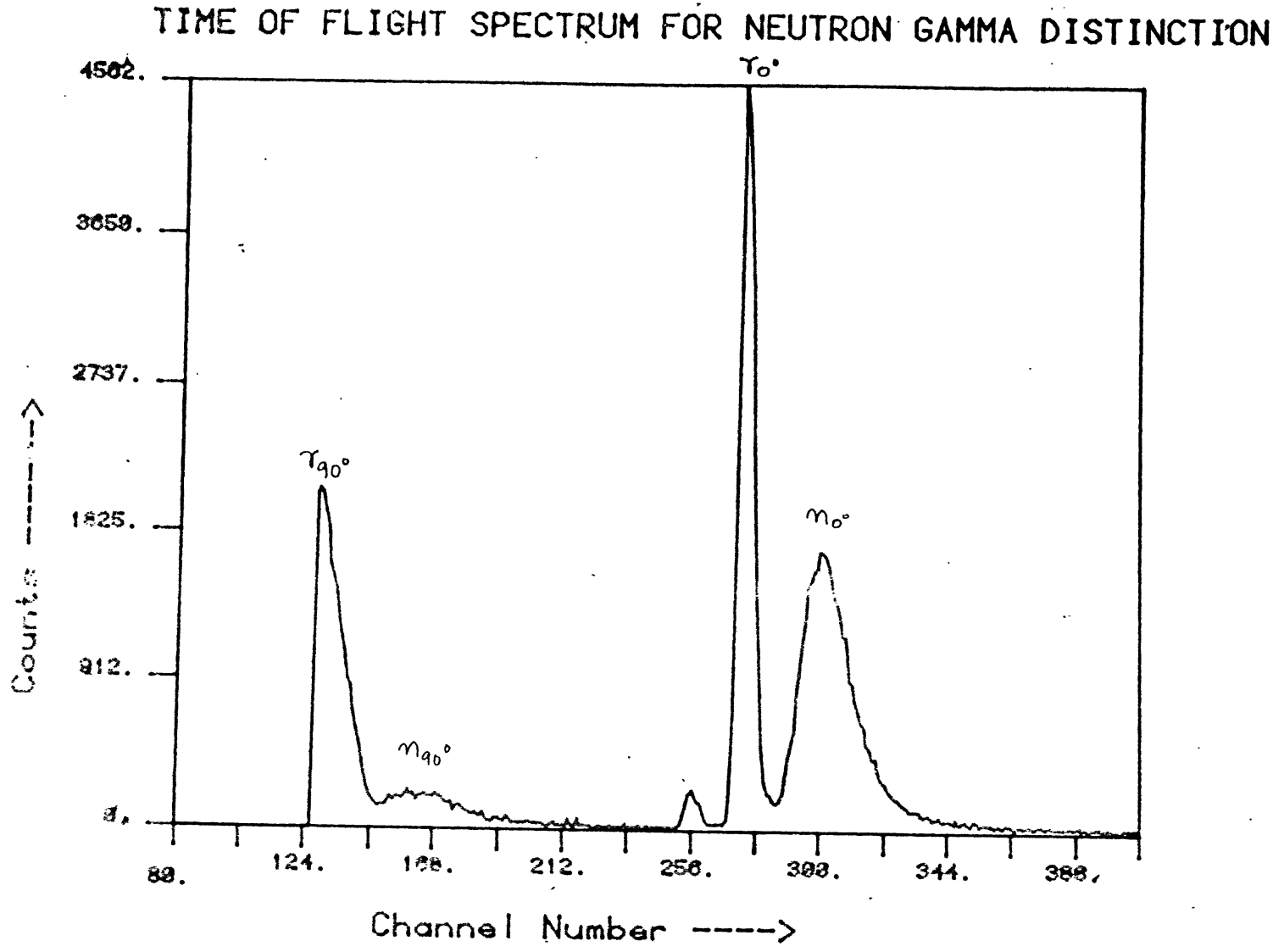
TIME OF FLIGHT SPECTRUM FOR NEUTRON GAMMA DISTINCTION
4562.
3650.
2737.
1825.
912.
0.
Counts ---->
$\gamma_{90°}$
$n_{90°}$
$\gamma_{0°}$
$n_{0°}$
80.
124.
168.
212.
256.
300.
344.
388.
Channel Number ---->
Fig. [2.10] Time of Flight Spectrum for Neutron Gamma Distinction

external delay in the F_{∞} timing channel resulted in clear separation of the two true TAC peaks. The γ spectrum due to F_o and due to F_{∞} were separated during the off line analysis. Above 180 keV γ energy cut off, a clear separation between the true γ peak and the neutron hump was achieved.

[2.3](c) Results

From the TAC peaks due to gamma rays in the direction of fragment motion and in the direction perpendicular to the fragment motion with suitable normalization (as defined in the earlier section), we could obtain the anisotropy in the gamma emission as a function of gamma energy. The nature of our curve is very similar to that obtained by Skarsvag[17]. Fig.[2.13] shows the anisotropy as a function of the gamma ray energy. We find that in the energy region between 200 keV and 700 keV, anisotropy shows a strong correlation with the fragment direction being a maximum of 1.26±0.01 at 520 keV. This is a typical yrast bump seen in the gamma rays from heavy ion reaction residues too. The value obtained by Skarsvag in the energy interval 0.491 to 0.566 is 1.27± 0.04. The similarity of the curve obtained by us and that by Skarsvag extends further also. We have made measurements beyond that done by Skarsvag and we find that the nature of the curve does not change. The anisotropy always remains more than one which implies that there are more number of E2 transitions than E1. This is true at gamma ray energies even beyond 2.5 MeV.

For energies greater than 0.7 MeV, one does not expect any rotational E2 transitions. We expect the nucleus to decay by

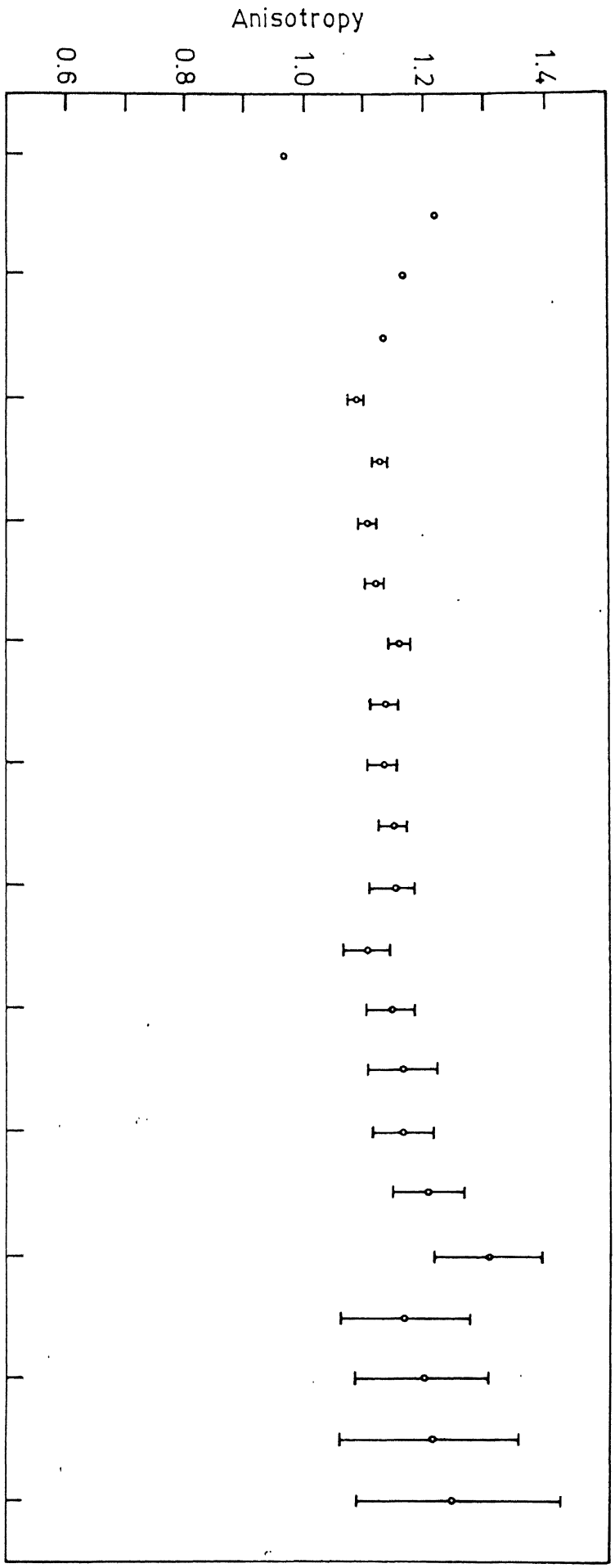

Fig. 2.13. Anisotropy in γ emission with respect to fragment direction of motion as a function of γ-ray energy.

neutrons or E1 transitions. Since the fission fragments carry a moderate amount of excitation energy and spin it is difficult to conjecture the emission of E2 vibrational transitions. However, if the transitions were predominantly dipole in nature, then by Strutinsky's[25] prescription, anisotropy should have been less than one. One conjecture is that these transitions contributing towards increase of anisotropy are either E2 vibrational lines in the even-even fragments or they are E2 statistical gamma rays. The anisotropy shows a similar behaviour in case of heavy ion data[30,31]. The nature of these transitions, there also is not known. The angular distributions studies alone cannot distinguish the various possibilities and some more experimentation is needed to establish the multipolarity of these transitions.

[2.4] STATISTICAL MODEL CALCULATIONS

The nucleus, given a small excitation energy, being a complex many body system can exist in many different states. This is utilized by the statistical models of nuclear structure and nuclear reactions. The fact that the density of quantum mechanical states increases rapidly with the excitation energy has not only made the statistical models appropriate but also essential for the comprehension and prediction of many nuclear phenomena.

One can use statistical model for calculating the average properties of a nucleus and also for the decay of fully equilibrated system such as the compoud nucleus. The essential assumption in all statistical models is that all possibilities for

the decay are intrinsically equally likely. Physical process is governed by factors such as the density of final states and the barrier penetration factors. The probability for a particular decay to occur is thus inversely proportional to the total number of possilble decays.

In heavy ion induced reactions, because of high excitation energy and spin, the reaction products have many decay possibilities. The decay possibilities may to some extent depend on the entrance channel parameters which are also many[33]. This has resulted in a number of computer codes to simulate the statistical decay of these hot rapidly spinning reaction products depending on the type of information the user wants to extract. These model can broadly be classified in two categories:

(i) the single step processes (ii)the multistep processes

In the multistep processes, gamma emission, particle evaporation and fission are included explicitly. The popular ones are *Alice*[34,35], *Cascade*[36,37] *Julian*[38], *Roulette*[39] etc. (for more details see Ref.[33]).

All these models have been developed for heavy ion reactions where a nucleus is given a lot of excitation energy and angular momentum. In case of low energy fission, the fission fragments are populated with a moderate amount of excitation energy and spin. Thus, the decay of these fission fragments is slightly different from a nucleus prodouced in heavy ion reactions. To analyze our multiplicity data, we have therefore written a statistical model code to trace the history of decay of the fission fragments having 15-20 MeV of excitation energy and around 10-15 units of angular

momentum.

Our primary aim in developing the code was to estimate the spin distribution of the fission fragments. The hot rotating fission fragments first cool by the emission of neutrons and then they further cool by the emission of the E1 statistical gamma rays till they reach the yrast line. After reaching the yrast state the fission fragments dissipate angular momentum by the emission of E2 rotational cascades.

The fission fragments are expected to de-excite by emitting

(i) neutrons

(ii) E1 statistical gamma rays

(iii)E2 statistical gamma rays

(iv) E2 rotational cascades

While the neutrons and the E1 and E2 statistical gamma rays cool the nucleus, most of the angular momentum is dissipated by the E2 collective rotational lines. E1 statistical gamma rays can also take away one unit of angular momentum, but the most probable transitions are the ones which leave the nucleus in the same angular momentum state as the initial one. While E2 statistical gamma rays can take away two units of angular mometum, their emission probability is much smaller. Therefore, most of the angular momentum is dissipated by the E2 rotational transitions.

Monte Carlo procedure, is used to calculate the number and energy of the gamma rays and the neutrons emitted by a fragment given some excitation energy and spin. Following steps illustrate the method briefly:

Step 1: It calculates the partial decay width for the possible

decays using the following expressions:

$$\Gamma_n = (D/2\pi)(2mR^2g)\int_0^{E-B_n} \varepsilon\rho(E-B_n-\varepsilon)d\varepsilon$$

$$\Gamma_\gamma = C_\lambda \varepsilon^{2\lambda+1}\rho(E_f,J_f)/\rho(E_i,J_i)$$

where D is the level spacing.

m is the mass of a nucleon.

R is the radius of the fragment.

g is the intrinsic neutron degeneracy.

B_n is the binding energy of the neutron.

λ is the multipolarity of the radiation.

C_λ is a constant, dependant on the multipolarity of the radiation.

ρ is the level density parameter; a function of the spin and the excitation energy of the fragment.

The level density parameter used was that of Ignatuk and Smirenkin[40] and is given by:

$$\rho(E_x) = a(1-f(x)\Delta_{gs}/E_x)$$

where $f(x) = [1 - e^{-\gamma E_x}]$

a is the asymptotic value of the level density paramater and is given by :

$$a = A(\alpha + \beta A^{-1/3}B_s)$$

$\alpha = 0.0730$; $\beta = 0.115$

Δ_{gs} is the ground state shell correction

$\gamma = 0.054 MeV^{-1}$

The spin dependence in the level density parameter was introduced by reducing the excitation energy by the amount of energy stored

as rotational energy.

Step 2: The partial decay widths for various particles are calculated which determine the weight factor for the various types of decays.

Step 3: Once the type of decay is decided, it determines the energy of the transition and reduces the excitation energy of the fragment by the amount of energy of the emitted transition. In case of neutron emission, the excitation energy is further reduced by the bindig energy of that neutron.

Step 4: The procedure is repeated with reduced excitation energy (and mass if a neutron is emitted).

The iterations are continued till the difference in the excitation energy of the fragment and the rotational energy is less than 0.5 MeV. The iterations are stopped at this difference because below this energy the decay may not be statistical due to scarcity of energy levels. In fact, placing a cutoff less than this distorts the gamma energy spectrum at low energy. The probability for low energy transition becomes very high, giving a spurious peak in the gamma ray energy spectrum.

For calculating the average multiplicity and width in the multiplicity distribution, the history of a particular fission fragment, having a fixed excitation and spin, was traced a hundred times. The same was done for the complimentary fragment having the same value of spin and excitation energy. The calculation for the multiplicity and width of the multiplicity as a function of charge ratios was done by simply adding the average N_γ due to each of them, while the widths were added in quadrature.

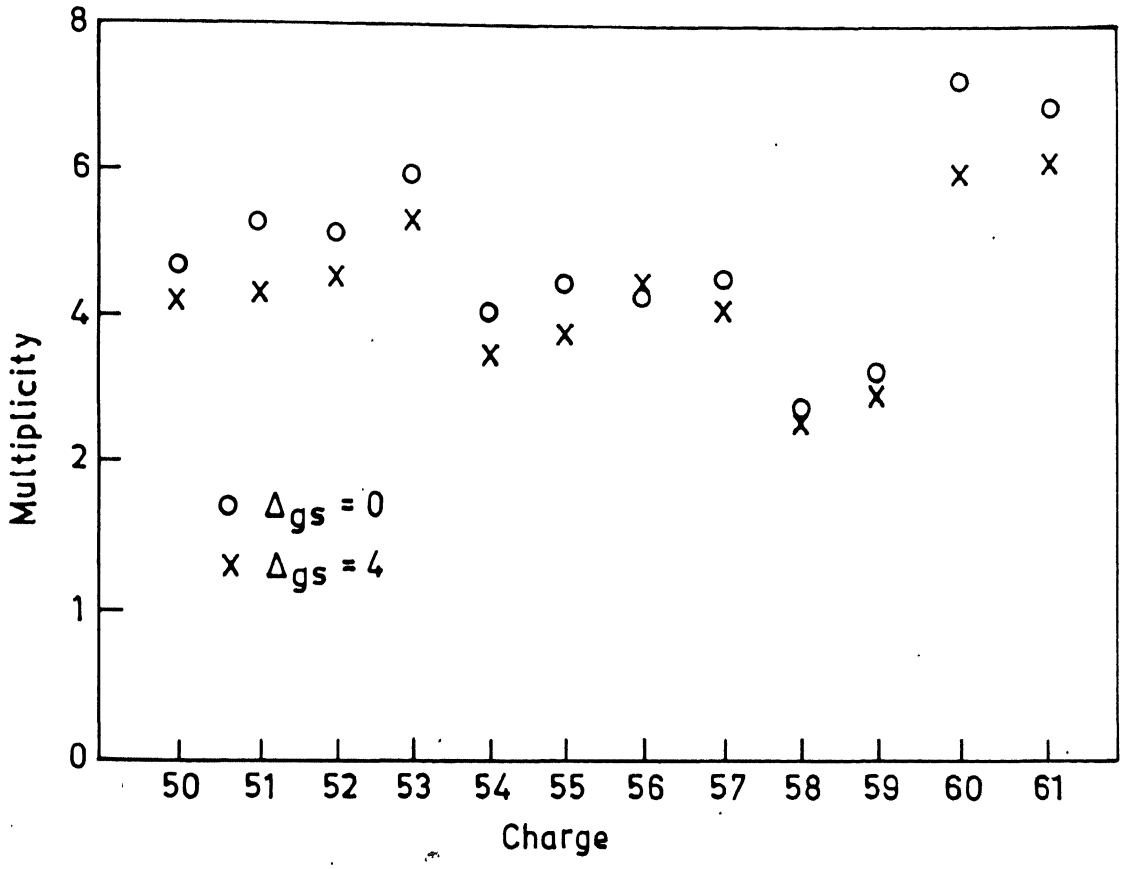

Fig. 2.14. Variation of multiplicity with the charge of the fission fragments for two values of Δ_{gs} (ground state shell correction in level density parameter).

The probability for the emission of E2 statistical gamma rays was found to be rather small. In a typical case of thousand iterations, the frequency of emission of an E2 statistical gamma ray was barely 3 or 4. Hence, we did not find it necessary to calculate the probability of emission of E2 statistical gamma rays and they were removed from the calculations.

To investigate the role played by the shell structure in gamma emission process, we performed the calculations for the variation of $\langle N_\gamma \rangle$ as a function of charge ratio for two values of the shell correction parameter Δ (Δ=0 and Δ=4). Fig.[2.12] shows the average multiplicity as a function of charge ratio for the two values of Δ. It shows that the shell correction parameter does not alter the average number of gamma rays appreciably.

The calculations for the average multiplicity and width were done for a wide range of excitation energies and spins. Table.[2.1] shows the average multiplicity for excitation energy equal to 20, 15 and 10 MeV. The calculations were repeated for three different values of spin i.e. 15$\hbar$, 10$\hbar$ and 5$\hbar$. Table[2.1] shows the average multiplicity for the above mentioned values of excitation energy and spin for fission fragment pairs having a charge of 56 and 42. We find that as the spin of the nucleus is reduced, the multiplicity increases. This is expected as the excitation energy locked up in rotation is now available for the emission of one more gamma ray. The calculation estimates a value of average multiplicity which is in close agreement with our experimental result.

Table[2.1] Showing the variation of the multiplicity with the excitation energy and spin for the fragment pair having charge Z(H)=56 & Z(L)=42

EXCITATION ENERGY	SPIN	Δ=4 AVERAGE MULTIPLICITY	Δ=0 AVERAGE MULTIPLICITY
20	15	3.79	3.99
	10	4.44	5.00
	5	3.58	3.75
15	15	3.22	3.84
	10	3.43	3.99
	5	2.40	2.90
10	15	2.74	2.75
	10	2.75	4.38
	5	4.57	5.08

We also calculated the width of the multiplicity distribution as a function of excitation energy for different values of spin as for the calculation of average multiplicity. Table[2.2] shows the average width as a function of excitation energy again for three values of excitation energy i.e.20, 15 and 10 MeV and three values of spins i.e. 15ħ, 10ħ and 5ħ.

Table[2.2] Showing the variation of width of the multiplicity distribution with excitation energy and spin for pairs having charge Z(H)=56 & Z(L)=42

EXCITATION ENERGY	SPIN	Δ=4 AVERAGE WIDTH	Δ=0 AVERAGE WIDTH
20	15	1.13	1.18
	10	1.18	1.34
	5	1.71	1.80
15	15	1.20	1.28
	10	2.40	2.55
	5	1.80	1.93
10	15	0.86	0.82
	10	0.94	0.95
	5	0.94	1.02

The point worth attention is that the average width is very much underestimated by the theory as compared to the experiment. The difference is not wiped out even for a wide range of excitation energy and spin.

Table [2.3] gives the calculated values of the $\langle N_\gamma \rangle$ and $\langle \sigma_n \rangle$ for the various charges. The table reported here is for a spin of each fragment being 10 and having an excitation energy of 15 MeV.

Table[2.3] Showing the multiplicity and the width of the gamma ray distribution.

$\Delta = 4$

CHARGE	AVERAGE MULTIPLICITY	WIDTH OF THE MULTIPLICITY
51	2.92	1.75
52	2.19	1.76
53	2.97	1.66
54	2.97	1.54
55	2.75	1.06
56	2.67	1.14
57	2.61	1.01
58	2.70	1.18
59	2.04	1.54
60	1.98	1.05

$\Delta = 0$

CHARGE	AVERAGE MULTIPLICITY	WIDTH OF THE MULTIPLICITY
51	2.54	1.93
52	2.26	1.88
53	2.34	1.89
54	2.73	1.91
55	3.04	1.22
56	2.89	1.09
57	3.00	1.08
58	3.13	1.26
59	2.30	1.68
60	2.72	1.08

The salient features of the results of the statistical model calculations can be summarised as :

(i) The probability for the emission of E2 statistical gamma rays

was found to be rather small.

(ii) Whereas the calculations do reproduce the average multiplicity, the width is very much underestimated by the theory.

(iii) We find that the average multiplicity is not a very crucial function of the shell correction parameter Δ in the level density.

(iv) We find that the average width does not change significantly for a wide range of excitation energies and spins.

[2.5] DISCUSSION AND CONCLUSIONS

In the light of our calculations showing that the probability for emission of E2 statistical gamma rays with tha available expression is very small, we are unable to explain the anisotropy exhibited by the gamma rays at higher gamma ray energies to be more then one. At high gamma ray energies, our experimental results on anisotropy indicate that there are more number of E2 transitions than E1 transitions. The possibility of emission of E2 rotational cascades of energies greater than 2.5 MeV seems very remote. The enhancement of the anisotropy could come from the emission of E2 gamma transitions, vibrational in nature. Before any conclusive statements can be made, one will have to study the multipolarity of the these radiations of higher energy. If the nature of these radiations is E2 vibrational in nature then one would like to investigate as to why theoretically their emission is hindered.

We have also found that the width in the gamma ray

multiplicity distribution is very much underestimated by the theoretical calculations. The width in the gamma ray multiplicity distribution is primarily because of two reasons:
(i) Statistical nature of emission of neutrons and gamma rays of E1 nature. (ii) Fission fragments originally having some spin distribution.

If the fission fragments originally have some spin distribution, then, depending on the initial spin of the fragments, the number of E2 rotational gamma rays emitted to dissipate angular momentum will be different. This will then again contribute to the width of the multiplicity distribution.

The width in the gamma ray multiplicity distribution due to the initial spin distribution can calculated if we subtract in quadrature the contribution to the width due to statistical nature of neutrons and E1 gamma rays from the experimentally measured widths. Since we have calculated the width associated with the statistical nature of emission of E1 transitions and neutrons we present in the Table(2.4) the width due to the initial spin distribution of the fission fragments.

Table(2.4) The width due to the initial spin distribution of the fission fragments.

CHARGE	WIDTH IN THE MULTIPLICITY DUE TO SPIN DISTRIBUTION
52	4.9 ± 0.7
53	3.8 ± 0.5
54	6.0 ± 0.6
55	3.8 ± 0.3
56	5.7 ± 0.5
57	3.9 ± 0.3
58	2.8 ± 0.6
59	2.8 ± 0.7
60	6.6 ± 1.0

The calculated width, as we see from the Table[2.4], is also very much different for the spherical fragments from the measured experimentally measured widths. The origin of this difference is not understood. In our calculations we have assumed that even a spherical nucleus dissipates angular momentum by the emission of rotational cascades after reaching the yrast state. There are two points we would like to make regarding this assumption:

(i) The Yrast state is not well defined for a spherical system. So the assumption that it dacays along the yrast line is not rigorous.

(ii) These are rotationally degenrate systems and hence decay by E2 rotational cascades should be inhibited.

However, in absence of any viable theory this was the only alternative available at our disposal. In fact, one uses this kind of assumption in the statistical de-excitation of the reaction products of the heavy ion reactions even if they are spherical. One possibility is that they dissipate angular momentum by the emission of E2 gamma rays vibrational in nature. This conjecture would

support our anisotropy results also.

Our analysis has revealed that the theory in its present form is unable to answer the following questions:

(i) How do spherical and deformed nuclei differ in their de-excitation mechanism. In particular, by what mechanism does a spherical nucleus dissipate angular momentum.

(ii) How is the angular momentum partitioned between the aligned single particles degrees of freedom and collective rotations.

A theory taking the above mentioned facts into account can only explain the mechanism of de-excitation of a hot spinning nucleus.

[2.6] REFERENCES

1. A.Johnson, A.Ryde and J.Sztarkier, Phys. Lett.B34 (1971) 605.

2. F.S.Stephens and R.S.Simons, Nucl. Phys. A183 (1972) 257.

3. H.Warhanek and R.Vandenbosch, J. Inorg. Nucl. Chem. 26 (1964) 669.

4. R.Vandenbosch and J.R.Huizenga, *"Nuclear Fission" Academic press, New York and London (1973)* and references therein.

5. F.S.Stephens, J.E.Draper, C.Bacelar, E.M.Deleplanque and R.M.Diamond, Phys. Rev. C37 (1988), 2927.

6. R.A.Broglia, T.Dossing, B.Lauritzen and B.R.Mottelson, Phys. Rev. Lett. 58 (1987) 326.26.

7. J.E.Draper, E.L.Dines, E.M.Deleplanque R.M.Diamond and F.S.Stephens, Phys. Rev. Lett. 56 (1986), 307.

8. J.C.Bacelar, G.B.Hageman, B.Herskind, B.Lauritzen, A.Holm, J.C.Lisle and P.D.Tjon, Phys. Rev. Lett. 55 (1985) 1858.

9. T.D.Thomas and J.R.Grover, Phys. Rev. 159 (1967) 980.

10. D.L.Hillis, J.D.Garrett, O.Christensen, B.Fernandez, G.B.

Hagemann, B.Herskind, B.B.Back and F.Folkmann, Nucl. Phys. A235 (1979) 216. 16.

R.J.Liotta and R.A.Sorensen, Nucl. Phys.A297 (1978) 136.

11. V.V.Vebuisky, H.Weber and R.E.Sund, *Proc. Phys. and Chem. of fission*(IAEA Vienna 1969) 929.

12. G.K.Mehta, J.Poitou, M.Ribarg and C.Signarbieux, Phys. Rev. C7 (1973) 373.

13. F.Pleasonton, R.L.Ferguson and H.W.Schmitt, Phys. Rev. C6 (1972) 1023.23.

14. N.N.Ajitanand, Nucl. Phys. A133 (1969) 625.

15. V.S.Ramamurthy, R.K.Choudhury and J.C.Mohankrishna, Pramäna 8 (1977) 322.

16. V.S.Ramamurthy, R.K.Choudhury and J.C.Mohankrishna, Pramäna 9 (1977) 623.

17. K.Skarsvag, Phys. Rev. C22 (1980) 638.

18. S.Johansson, Nucl. Phys. 60 (1964) 378.

19. J.S.Fraser and J.C.D.Milton, Ann. Rev. Nucl. Sci. 16 (1966) 379.

20. H.Nifenecker, C.Signarbieux, R.Babinet and J.Poitou,*Proc. Phys. and Chem. of fission* (IAEA Rochester 1973).3).

21. F.Plasil, R.L.Ferguson, F.Pleaston and H.W.Schmitt, Phys. Rev. C7 (1973) 1186.

22. R.L.Watson, H.R.Bowman and S.G.Thompson, Phys. Rev. 162 (1967) 1169.

23. C.M.Lederer, J.M.Hollander and I.Perlman, Tables Of Isotopes (John Wiley & Sons.)

24. L.C.Moretto, Ann. Rev. Nucl. Sci. (1984)

25. V.M.Strutinsky, Sov. Phys. JETP 10 (1960) 613.

26. J.B.Wilhelmy, E.Cjiefetz, R.C.Jared, S.G.Thompson, H.R.Bowman and J.O.Rasmussen, Phys. Rev.C5 (1972) 204.

27. M.M.Hoffman, Phys. Rev. 133 (1964) B714.

28. O.I.Ivanov, Y.A.Kushnir and G.N.Smirenkin ZhETF Pisma 6 (1967) 898.

29. P.Ambruster, H.Labus and K.Reichett, Z.Naturforsch 26A (1971)

512.

30. G.V.Val'skii, B.M.Aleksandrov, I.A.Buranov, A.S.Krivokhatskii, G.A. Petrov and Y.Pleva, Sov. J. Nucl. Phys. 10 (1969) 137.

31. A.Lajtai, L.Jeki, G.Kluge, I.Vinnay, F.Engard, P.P.Dyachenko and B.D.Kuzminov, *Proc. Phys. and Chem. of fission* (IAEA, Vienna 1974) 249.

32. R.M.Diamond and F.S.Stephens, Ann. Rev. Nucl. Sci. 30 (1980) 85.

33. R.G.Stokstad in *Treatise on Heavy Ion Science (Plenum Press* Ed. D.A.Bromley) 83.83.

34. R.S.Simon, R.M.Diamond, Y.Elmasri, J.O.Newton, P.Sarva and F.S.Stephens, Nucl. Phys. A313 (1979) 209.

35. J.O.Newton, S.H.Sie and B.D.Dracolous, Phys. Rev. Lett. 40 (1978) 625.25.

36. F.Plasil, Phys. Rev. C17 (1978) 823.

37. F.Pühlhofer, Nucl. Phys. A280 (1977) 267.

38. Y.Eisen, I.Tserruya, Y.Eyal, Z.Fraenkel and M.Hillman, Nucl. Phys. A291 (1977) 459.59.

39. M.Wakai and A.Faessler, Nucl. Phys. A307 (1978) 349.

40. A.V.Ignatuk, K.K.Istekov, G.N.Smirenkin, Sov. J. Nucl. Phys. 29 (1979) 450. 50.

CHAPTER III

THE VARIATION OF THE TOTAL KINETIC ENERGY WITH EXCITATION ENERGY IN THE REACTION $^{238}U(\alpha,\alpha'F)$

[3.1] INTRODUCTION

Fission of the nucleus results from a "*run away*" large amplitude collective motion. Even in low energy fission, though large energy release is involved, its observables such as fragment mass yields and their energies are known to be very strongly influenced by shell and pairing effects[1]. The mass distributions are known to be asymmetric in the case of actinide nuclei.

It is known for a long time that the fragment shell structure at scission plays a dominant role in deciding the nature of mass asymmetry. However, attempts to quantitatively calculate the mass and energy distribution on the basis of scission configurations have not been successful. This is ascribed to the difficulties in the description of the dynamics of the fission process between the saddle and the scission point.

The mass distributions are one of the most important charateristics of the fission process. Although there is a large amount of experimental data on the mass distribution[2] and their dependence on excitation energy of the fissioning system for a variety of nuclei, a suitable theory to explain the observed characteristics is yet to come. It is known that the actinide

nuclei fission asymmetrically leading to two humps in the mass distribution. It is also known that the peak to valley ratio in the mass distribution is a decreasing function of the excitation energy of the fissioning system and at sufficiently high excitation energy, the dominant mode of fission becomes symmetric. This can be qualitatively explained as due to vanishing of the shell effects. The initial excitation energy of the fissioning system, therefore plays a crucial role in determining the mass distributions. The determination of the mass distribution of the fission fragments as a function of excitation energy is important on two counts:

(i) It tells us as to what role the shell effects play in the determination of the mass distribution.

(ii) While calculating the total kinetic energy as a function of excitation energy, it helps us to eliminate the effect of excitation energy on the mass distribution by studying the total kinetic energy variation as a function of excitation energy for mass separated fragments.

During the last few years, the studies of the dynamical aspects of the fission process have rejuvenated, so to say, receiving tremendous stimulus from the data from heavy ion reaction studies. The discovery of the other modes of large scale collective motion, their relation to fission and a unified description is one of the arduous tasks before the nuclear physicists today.

The dynamical aspects play an important role in the last phase of the fission process during which the system crosses the fission barrier and descends from the saddle point to the scission point.

The theoretical models[3], present in literature to explain the descent of the nucleus from the saddle to scission, have neither been explored in detail nor are sufficiently free from curve fitting to be generally accepted. The models can be broadly classified in two groups, depending on whether the motion from the saddle to scission is adiabatic with respect to particle degrees of freedom or not.

If the collective motion towards scission is sufficiently slow, so that single particle degrees of freedom can easily readjust to each new deformation as the distortion proceeds, then viscosity plays a significant role in the descent of the nucleus from the saddle to scission. In this case, the statistical approximation[4,5] may be valid. Here, it is assumed that the nucleus is in statistical equilibrium at all points in the deformation space. In that case decrease in potential energy from the saddle to scission appears, primarily, as the deformation energy of the fragments. On the other hand, if the motion from the saddle to scission is fast, then there is no transfer of energy from collective motion to single quasi particle excitation. In this case, the adiabatic models[6-8] are valid and viscosity is assumed to play an insignificant role in the descent. The difference in potential energy from the saddle to scission appears as the relative kinetic energy of the system.

Particle excitations, when dealt with macroscopically, appear in the form of nuclear friction, which is a natural extention of the concept of collective coordinates, inertia and potential along the lines of classical friction. Hill and Wheeler[9], looking for a

possible explanation of mass asymmetry, in 1953, suggested a microscopic derivation of viscous forces acting during the descent from the saddle to scission. In their theory, level slippages caused by some residual interaction give rise to time dependent single particle occupation numbers which, in turn, prevent the nucleus from fissioning in its lowest state. Their conjecture that viscosity may entail asymmetry in the actinide region in low energy fission was, however, belied.

Wilet[10] gave a full treatment of the interaction betwen collective and intrinsic degrees of freedom by time dependent Schrödinger equation. Unfortunately, at that time his idea did not receive full attention and it was only by the impact of data from heavy ion experiments which brought the idea of deep inelastic scattering, fast fission etc. to the forefront that the idea of nuclear friction or viscosity received a fresh breath of air.

Deep inelastic collisions[11,12] exhibit features very similar to those displayed by fission fragments. Here, when a heavy nucleus with energy above coulomb barrier and having a large degree of mass asymmetry in the target projectile combination, collides with an impact parameter $b > R$, (where $R = R_1+R_2$, R_1 and R_2 being the radii of the target and the projectile nuclei) with another heavy nucleus, it gets scattered inelatically. This scattereing is unlike the usual inelastic scattering known in light ion induced reaction. In the exit channel, there is a lot of dissipation of the centre of mass energy. The final projectile energy is continuously distributed between the bombarding energy of the projectile and the fully relaxed value, very nearly equal to the coulomb energy

between the target and the projectile. The masses of the two reaction products are close to the masses of the target and the projectile. A naive picture is that, as the nuclear densities of the two nuclei overlap, damping takes place dissipating the entire kinetic energy above the coulomb barrier energy. The two nuclei then spin together, when the exchange of a few nucleons becomes possible, and after about half a revolution, they separate under the coulomb repulsion with very little relaxation in the mass asymmetry degree of freedom. The fully relaxed total kinetic energy of *the target and the projectile like fragments* is not given by the two spherical nuclei in contact but by those of deformed spheroids as in the case of fission fragments. The average time scale for the process is around 10^{-21} seconds. The energy loss is strongly correlated with the scattering angle[13,14]. There were some early attempts to explain the viscous effect[15]. Wilezynski[14] suggested an interpretation of, then newly discovered, deep inelastic collisions in terms of negative angle scattering and frictional forces. The deep inelastic collisions is a subject in itself and we would not refer to it anymore. Our objective was only to show that there are other examples of large scale nuclear motion which are viscous and for a more detailed study, the reader is referred to Ref.[16] and references therein.

In the case of fission fragments, viscous forces are expected to affect the fragment kinetic energies. The fission fragment kinetic energy has been measured from compound nucleus ^{101}Rh (Namboodiri[16]) upto ^{278}110 (Sikkeland[17], Borderie[18]). If plotted against $Z^2/A^{1/3}$, they follow systematically a straight line. This

behaviour is expected for the lighter compound nucleus upto $A \simeq 135$ or $Z^2/A^{1/3} \simeq 650$ because the saddle points of nuclei with fissility smaller than approximately $\chi \simeq Z^2/50A = 0.5$ almost coincide with their scission points and hence, the total kinetic energy of symmetric fission fragments is well approximated by the mutual coulomb interaction energy of two spheres in contact, however, the trend seems to be valid even beyond. Fig.[3.1], taken from Ref.[19], shows the experimental points of total kinetic energy as a function of $Z^2/A^{1/3}$ (a property of the fissioning system). The figure also shows the results of theoretical calculations[20,21]. The calculations have been made both by assuming that the system is viscous and also without putting any viscosity in the calculations. The nature of viscosity assumed for the calculations was of *ordinary hydrodynamical kind*. While looking at these calculations one might say that the nuclear matter is only slightly viscous, the heavy ion data is a pointer to the fact that the viscosity is large. Thus we can conclude say that the analysis is not unique. In fact, Prakash et.al[22]. have shown that as the fragments separate at scission there is considerable dissipation of relative kinetic energy in the initial stages due to the proximity friction and a free separation in the coulomb field starts only after the surface separation distance exceeds about 2 fm. This gives rise to a kinetic energy value smaller than the initial energy at scission. With the inclusion of this effect they could explain Viola systematics[23] at scission.

Medium and heavy fissioning nuclei are deformed at their scission points and have less Coulomb energy than if they were

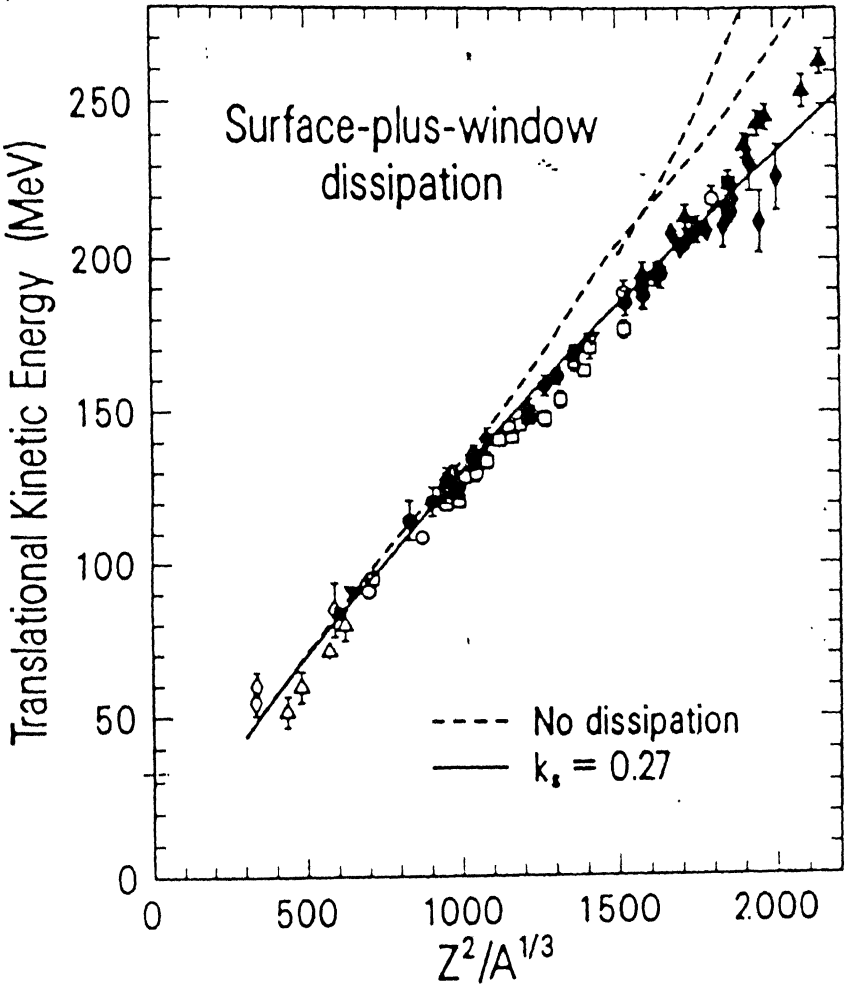

FIGURE 3.1 Reduction of average fission-fragment kinetic energies by surface-plus-window dissipation, compared to experimental values.

spherical. But simultaneously, their saddle shapes become less deformed and nucleus might accumulate prescission kinetic energy. The prescission kinetic energy must be smaller for viscous fluids as the amount of energy that is dissipated into heat is very crucially dependent on the nautre and magnitude of viscosity prevalent in the process. In this way, estimation of nuclear viscosity can be made by systematics of total kinetic energy of symmetrically fissioning nuclei as a function of excitation energy of the fissioning nucleus.

The degree of dissipation of collective energy into excitation energy is also important in another context. Though the principal contribution to the kinetic energy comes from mutual coulomb repulsion, the collective energy of the vibrational states can also be transferred to the kinetic energy of the fission fragments. The translational energy of the descent of nucleus can also contribute to the TKE. The single particle states also affect the final TKE. The contribution due to each can vary substantially depending on the assumption regarding viscosity. Problem of separating from total kinetic energy of fragments all their component parts is very difficult. The experimental study for the effect of transition states of the fissioning nucleus on the total kinetic energy consists of the study of correlation between the mean total kinetic energy of the fragments and other characteristics of the fission process in which the properties of the transition state are reflected.

The variation of the total kinetic energy as a function of excitation energy is available for a few fissioning systems. For

example[24], in the case of ^{240}Pu, we have the data for spontaneous fission and isomeric fission, and neutron induced fission of ^{239}Pu provide systematics upto 10 MeV of excitation energy. In isomer and resonance fission the excitation energy shows up entirely as an increase in kinetic energy. This led Swiatecki [15] to the conclusion that such a fission process must be non-viscous. For neutron induced fission with excitation energies at or above 4.5 MeV there is a sharp drop in kinetic energy by about 2.5 MeV followed by a gentle decrease. By simultaneous measurements of neutron energy with the assumption that average γ energy remains the same, it was found that average internal excitation energy is increased by 5.4 MeV, whereas kinetic energy by 1.15 MeV. This type of fission process is highly damped. The sharp drop in kinetic energy at the excitation energy of 4.5 MeV can be attributed to the breaking of the nucleon pairs. The decrease in the average kinetic energy with excitation energy might be attributed either to the washing out of shell effect or to larger viscosity. Since breaking of nucleon pair is responsible for transition from adiabatic to damped fission, adiabatic fission process should show odd-even effect in mass yield and kinetic energy distributions. Wahl etal[25] and Amiel and Feldstein[26] measured the abundance of even Z products in thermal neutron fission of ^{235}U and found it to be 20-50% larger than the relative average yield. Unik[27] found that fine structure vanishes as we go to heavier nuclei ^{246}Cm to ^{256}Fm. David etal[28-32] have made extensive measurements on the variations of total kinetic energy as a function of excitation energy of the fissioning nuclei. They have employed the $(\alpha,\alpha'f)$ reaction on several isotopes of

Uranium and Thorium to study this variation. In case of Uranium nucleus, they find that the slope of the $\overline{TKE}$ versus E_x curve is a small negative number. The bar on the total kinetic energy shows the average value. For Th they find that $\overline{TKE}$ as a function of excitation energy has a positive slope. David has also investigated the nature of the slope for mass separated fragments. They found that the slope of the $\overline{TKE}$ versus E_x curve is independent of the mass of the fission fragments. Hence, they conclude that the difference in the sign of the slope mentioned above is a property of the fissioning system. They suggest that this may have to do with the relative difference in height between inner and outer barriers. Back etal.[39] measured the variation of total kinetic energy as a function of excitation energy for ^{238}U in the excitation energy range of 5 to 50 MeV. Their low energy results corroborate with that of David's and at energies above 22 MeV they find a small positive slope for the $\overline{TKE}$ versus E_x curve. Choudhury etal.[34] have also measured the slope of the $\overline{TKE}$ versus E_x curve in Pu. They studied the reaction (α,f) and not (α,α',f) as that studied by David and Back. Moreover, they have measured the slope at energies much above the barrier. They also find a small positive slope for the curve.

Although there is a plethora of experimental results available still it is not clear as to how the system becomes more viscous when it is given more excitation energy. Another open question is at what stage the system passes from a non-viscous fluid to a viscous fluid. If the total kinetic energy decreases with increase in the excitation energy, then how the system becomes more viscous

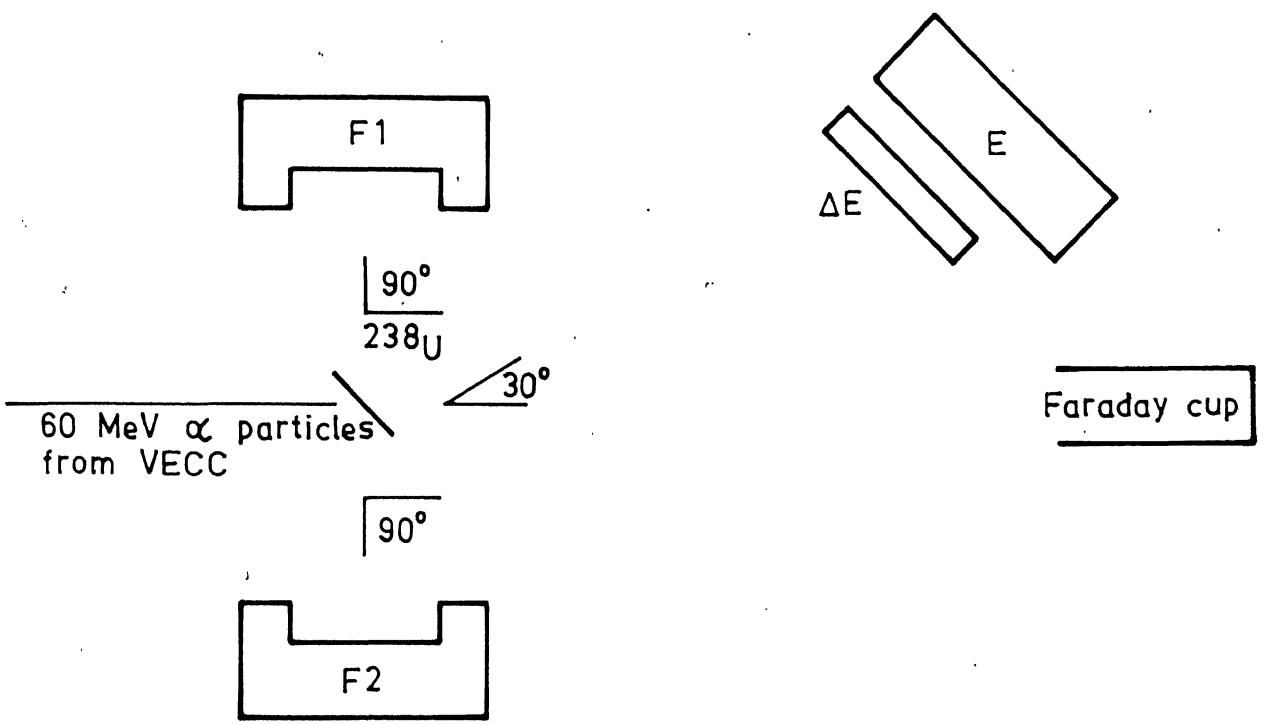

Fig. 3.2. Geometry of the experimental arrangement for the study of variation in total kinetic energy as a function of excitation energy of ^{238}U .

at the detector laboratory of the VECC. The solid angle subtended by the telescope was 5 msr. The resolution of the E-ΔE particle telescope was about 1 MeV for the inelastically scattered alpha particles from the carbon backing.

Two heavy ion surface barrier detectors F_1 and F_2 were placed as shown in the figure to detect the fission fragment pairs. They were placed at 180° to each other and each of them was approximately at 90° to the beam axis. One of the detectors i.e. F_1 was placed very close to the target such that it caught fragments complimentary to those detected by F_2 irrespective of the non colinearity introduced due to the centre of mass motion and neutron evaporation from nascent fragments. The solid angle subtended by the fission detector F_1 was 33 msr. The solid angle subtended by F_2 fission detector was 14 msr.

The angular distribution for inelastic scattering of an energetic ion on a target material, due to incomplete momentum transfer, exhibits a $(1-\cos\theta)$ behaviour. The detection of these inelastically scattered alpha particles, if done at larger cross sections would help in increasing the count rate. Higher count rates would also result in a better true to chance ratio. Thus a proper positioning of the telescope is very important. For this a DWBA calculation was performed to calculate the cross section for the inelastically scattered alpha particles from ^{298}U. It was found that the angular distribution is peaked at forward angles. However, a competing process, which contributes significantly to the deterioration of the true to chance ratio, is the inelastic scattering of alpha particles from the carbon backing which is also

peaked at forward angles. Thus there is a trade off involved between higher count rates and contributions to chance coincidences. The optimum angle was fixed at 30° by actually taking the ratio of the two aforementioned quantities during the actual run. A 7 mg/cm^2 thick alumunium foil was mounted in front of the detector telescope to prevent the radiation damage of ΔE detector due to fission fragments reaching the detector. Magnets were also placed in front of the detector to suppress low energy electrons from the target.

The electronic block diagram used for the experiment is shown in Fig.[3.3]. Fast coincidence was taken between the pulse from the fission detector which was further away and the ΔE detector while the geometry ensured the coincidence between E stop detector and nearer fission detector. The coincidence between the four pulses was further ensured software wise at the time of analysis.

For the fast pulse, timing output from the preamplifier was fed to timing filter amplifier. The output from this was fed to a constant fraction discriminator in external delay mode. Walk adjustments were made to get a good timing resolution. The pulse from the preamplifier in the ΔE channel was processed in a similar fashion. An external delay was put in the ΔE circuit to bring the true TAC peak in the middle region of the TAC spectrum. The fission pulse started the time to amplitude converter and the ΔE pulse provided the stop pulse.

Fig. [3.4] shows the TAC spectrum. The second peak is due to both the true and the random events whereas the other peaks are due to random events only. A random event is one in which an

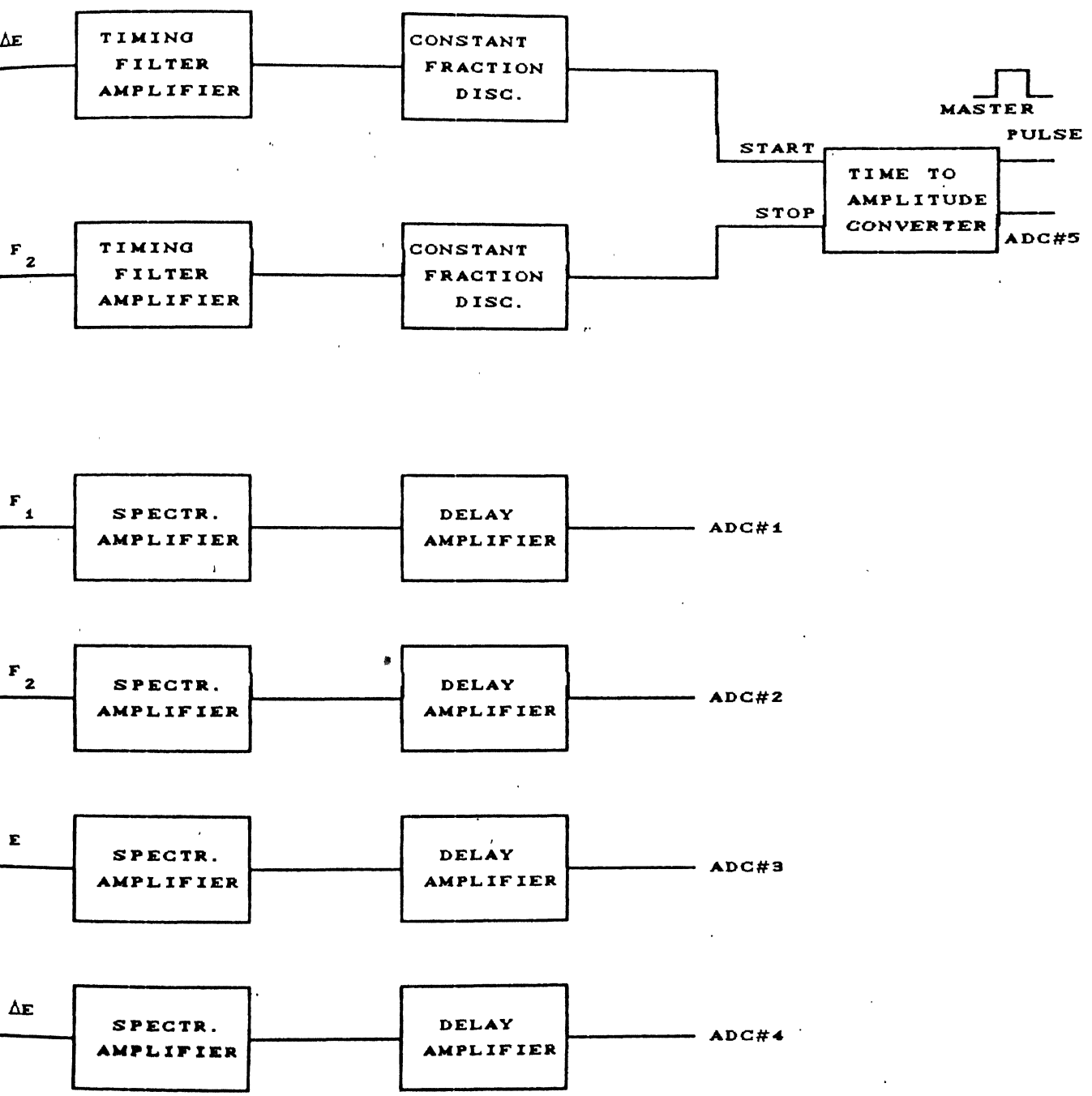

Fig.3.3 Electronic set-up for the study of the mass energy correlations in the reaction $^{238}U(\alpha,\alpha'f)$.

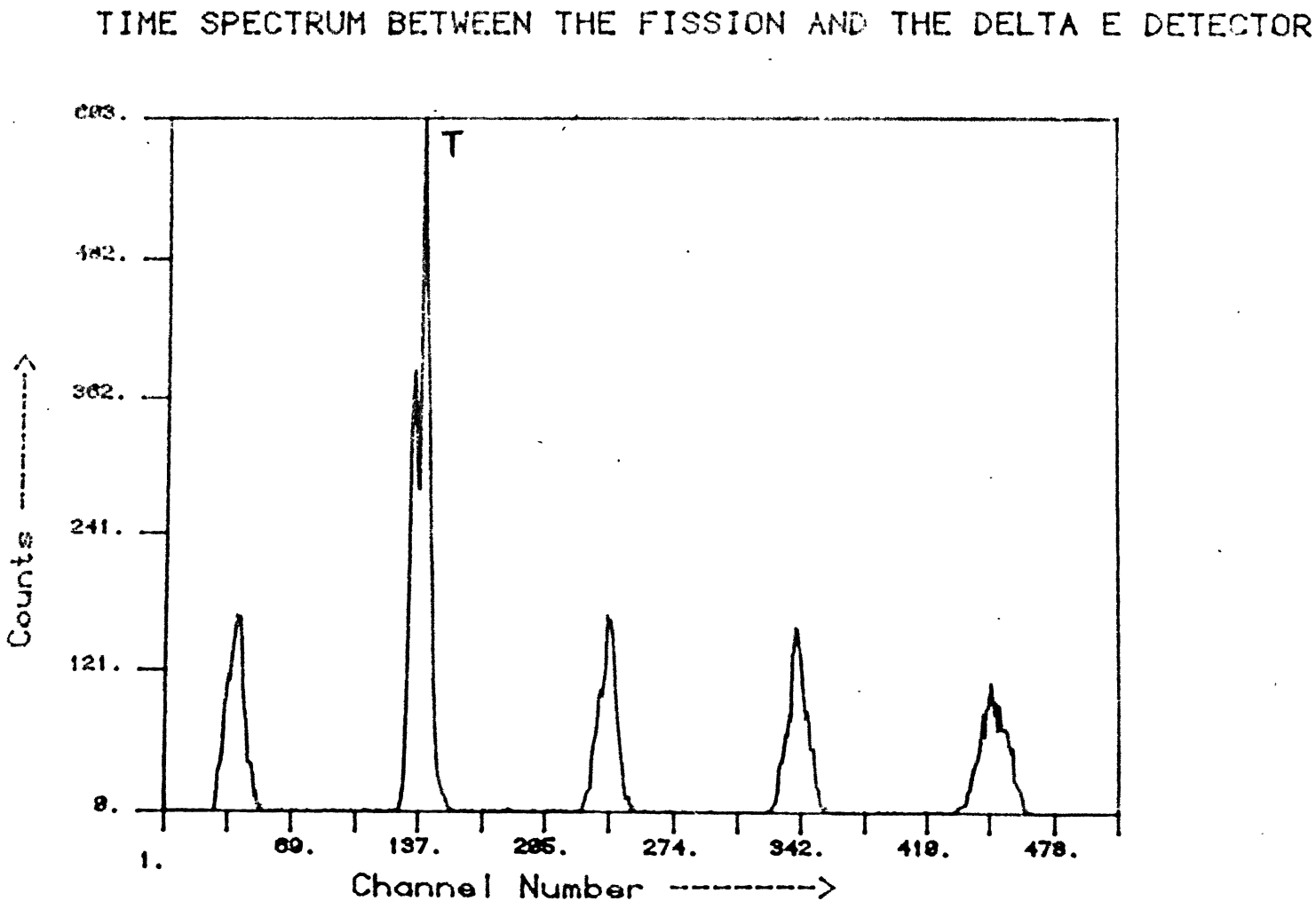

Fig. [3.4] Time of Flight Spectrum Between the Delta E and the Fission Detector.

inelastically scattered alpha particle from carbon is detected in coincidence with fission resulting from the (α,f) process. As can be seen from the figure, the cross section for this kind of event is much larger than the events resulting from the (α,α'f) process.

The energy pulses from the two fission detectors, F_1,F_2 and from the telescope E-ΔE, was fed to spectroscopy amplifiers. The pulses from the amplifiers were fed to analog to digital converters (ADC) which were of the Willkinson type, requiring a maximum analog signal of +8 volts.

The TAC also provided a digital gate which was used as the master pulse which gated all the ADC's and started the data acquisition cycle. Five pulses F_1, F_2, E, ΔE and TAC were acquired in list mode on a magnetic tape using a camac based data acquisition system.

The experiment was continuously monitored on line by building (i)5 singles spectra namely F_1, F_2, ΔE, E and TAC (ii)3 dual spectra namely:

(a)between F_1 and F_2 : to monitor the correlated fission events.

(b)between E and ΔE : to monitor the particle identification spectrum.

(c)between ΔE and TAC : to monitor the true to chance ratio in the experiment.

One conditional TAC spectrum was also built by cutting the elastic peak from the E spectrum to see the real true to chance ratio after eliminating the elastically scattered alpha particle.

The beam current was kept at 5-10 ηA to avoid pile up in

fission as well as the ΔE detectors. The rate of true events was around 8–10 per minute.

[3.3] ANALYSIS PROCEDURE

Mass spectrum from the correlated pulse height spectrum of the two fission fragment detectors is obtained after calibrating the detectors and correcting the energies for :

(a) energy loss suffered by the fragments due to finite target and backing thickness.

(b) the centre of mass motion of the fissioning nucleus.

(c) neutron evaporation from primary fragments.

The analysis is involved as each of these corrections and the calibration depends on the mass of the fragment, something which we have set out to determine. We invoke the momentum and mass conservation to determine the mass of the fission fragments, and then apply these corrections iteratively till the mass of the fragments comes out to be the same in subsequent iterations. Appendix [2] gives the details of the analysis programme. It was found that after two iterations the value of the mass converges.

[3.3](a) Energy Calibration:

The output pulse height due to the energy lost by an energetic charged particle in a detector medium is a function of the particle energy, its mass and charge. For the lighter ions, the pulse produced in solid state surface barrier detectors is very nearly

proportional to the energy of the particle but in the case of fission fragments and other heavy ions, particles having same energy but different masses do not produce the same pulse height and thus the linearity between the pulse height and the energy is lost. The pulse height produced in the solid state detector due to lighter ion is higher than due to a heavier ion of the same energy. The departure in linearity due to this dependence is known as the *pulse height defect*. This has to be taken into account in the energy calibration.

It was found that once the mass is fixed the relationship between the pulse height and energy was unique. Further, once the energy is fixed, the relationship between pulse height and mass is linear. This was demonstrated by Schmitt etal[35] using Br and Iodine ions. Based on the above facts, there are a number of calibration schemes, all empirical, but the one due to Schmitt etal has found the most widespread use. According to this procedure the calibration equation for a surface barrier detector reads as

$$E = (a + a'M)\ X + b + b'M$$

where X is the pulse height, M is the mass of the heavy ion, a,a',b,b' are the constants which have to be determined for each individual detector. Schmitt calibration provides a scheme by which, measuring the fission fragment spectrum of ^{235}U or ^{252}Cf, one can calibrate their detector, if we know P_L, the pulse height of the most probable light fragments and P_H, pulse height of the most probable heavy fragments. The constants are given by the following relations:

$$a = a_o/(P_L - P_H)$$

$$a' = a'_o/(P_L - P_H)$$

$$b = b_o - a.P_L$$

$$b' = b'_o - a'.P_L$$

where a_o, a'_o, b_o and b'_o are constants given by Schmitt which depend on whether one uses ^{235}U or ^{252}Cf for calibration.

Though this scheme is most widely used, the values of the total kinetic energy obtained by this energy calibration scheme in the double energy measurement and the one obtained due to the time of flight technique (i.e. the double velocity measurement), are known to be slightly at variance. To quote one result[36]; the average total kinetic energy release $\langle TKE^* \rangle$ for thermal neutron induced fission of ^{235}U as obtained with surface barrier detectors using this technique was reported to be $\langle TKE^* \rangle$ = 171.9 MeV. From double velocity measurement the figure turns out to be 168.3 MeV. Moreover, the calibration scheme of Schmitt was formulated in early sixties. Since then the detector technology has advanced much and the material of Silicon may be different. Another drawback of their scheme is that they tested it for Bromine and Iodine ions only.

Weissenberger etal[37] have recently reinvestigated the behaviour of solid state surface barrier detectors with ORTEC F series heavy ion detectors. They have also checked for ions other than iodine and bromine, and have arrived at the conclusion that the phenomenological ansatz by Schimitt etal for the pulse height response of surface barrier detectors to heavy ions covering the energy and mass range of fission fragments is perfectly well suited. They conclude that within the experimental and evaluational uncertainty of ± 150 keV, there is no need to go beyond the linear

parametrization of the response E(X,M). They have slightly modified the constants a_o,a_o',b_o and b_o' for the pulse height response of Californium fission fragments. We have used these set of constants in calibrating our detector:

$$a_o = 24.30$$

$$a_o' = 0.0283$$

$$b_o = 90.397$$

$$b_o' = 0.1150$$

For finding out P_L and P_H for the two detectors a ^{252}Cf calibration was taken separately for the two detectors and then Guassians were fitted to calculate the position of P_L and P_H, the peak positions for the light and heavy fragments.

The Calibration of the telescope detectors was done by taking the energy spectrum of the inelatically scattered alpha particles on carbon nuclei(^{12}C). Since the energy level scheme of this is known, the difference in the peaks of the inelastically scattered α particle spectrum is known, the calibration of the telescope could be done.

[3.3](b) Energy Loss Correction :

The energy lost by a charged particle in a material medium is a function of its energy, mass and charge. Fission fragments with large A and Z and energy of the order of 1 MeV/nucleon lose a substantial amount of energy in the finite thickness of the target and the backing material. Apart from the energy loss, there is also energy straggling which is also dependent on the Z of the material. This energy spread degrades the energy resolution which, in turn,

spoils the mass resolution. Thus in these experiments, where one measures mass distribution by double energy measurements in a typical back to back detector arrangement, the target and the backing should be thin and backing should be of low Z material. Initially, when the fragments are emitted they are fully ionized but as they transverse the medium they acquire electrons and lose their charge. Since the energy loss is a crucial function of the charge, in calculating it the term effective charge is used.

There is a multitude of empirical relations for the stopping power calculations but unfortunately, there is a dearth of experimental results and most of the tables extrapolate into the regions uncovered by experiment. The rather extensive tables of NorthCliffe and Schilling[38] present their data with unstated accuracy. Moreover, since their presentation, our knowledge of energy loss mechanism has improved. Hence, we have used the mechanism of Zeigler etal.[39], who have presented an extensive calculation for energy loss suffered by ions with different Z in different elements. For solid targets and ion velocities from 0.2 to 2 MeV/u the stated error, at best, in their formulation is 10%. The expression that they have used for Z_{HI}^{*}/Z_{H}^{*} is

$$Z_{HI}^{*}/Z_{H}^{*} = 1 - \exp(-A)[\ 1.034 - 0.1777\ \exp(-0.08114)Z_1\ ]$$

where

$$A = B + 0.0387\ \sin(\pi B/2)$$

$$B = 0.886\ (E/25M_1)^{1/2}/Z_1^{2/3}.$$

[Here E is energy in keV, M_1 is mass in a.m.u. and Z_1 is the charge. The expression for S_H is

$$(\text{Stopping})^{-1} = (S_{low})^{-1} + (S_{high})^{-1}$$

for E/M < 999 keV/a.m.u.

where $S_{low} = A_2 E^{0.45}$

$S_{high} = (A_3/E)\ \ln [\ 1 + A_4/E + A_5/E\ ]$

Stopping $= A_6/\beta^2 [\ \ln (\quad) - \beta^2 - \sum A_i (\ln E)^i\ ]$

The coefficients $A_1, \ldots A_{12}$ are given for different elements.

E is the energy of the ion traversing the medium

Z is the charge of the medium

$\beta = v/c$ where v is the velocity of ion and c is the velocity of light.

[3.3](c)Centre Of Mass Motion:

The α particle that hits the ^{238}U nucleus imparts some energy and momentum to it and gets inelastically scattered. Then, if the moving nucleus has energy above the fission barrier, it breaks into two fission fragments. The energy of the fission fragments that we measure is in the lab frame. We are interested in the energy of the fragments in the centre of mass frame. To convert the lab energy to the centre of mass energy a small correction is required. Fig 3.4 illustrates how the centre of mass motion was taken into account. It is taken from Ref.[40] where such an iterative calculation for the mass of the fission fragments from double energy measurements has been described. If the compound nucleus was stationary the fragments would have been emitted at 180° with respect to each other, but since it is moving, they are emitted at an angle. The angle formed by the direction of their motion in the lab frame is known as the folding angle.

Since we know the energy of the scattered α particle, thereby

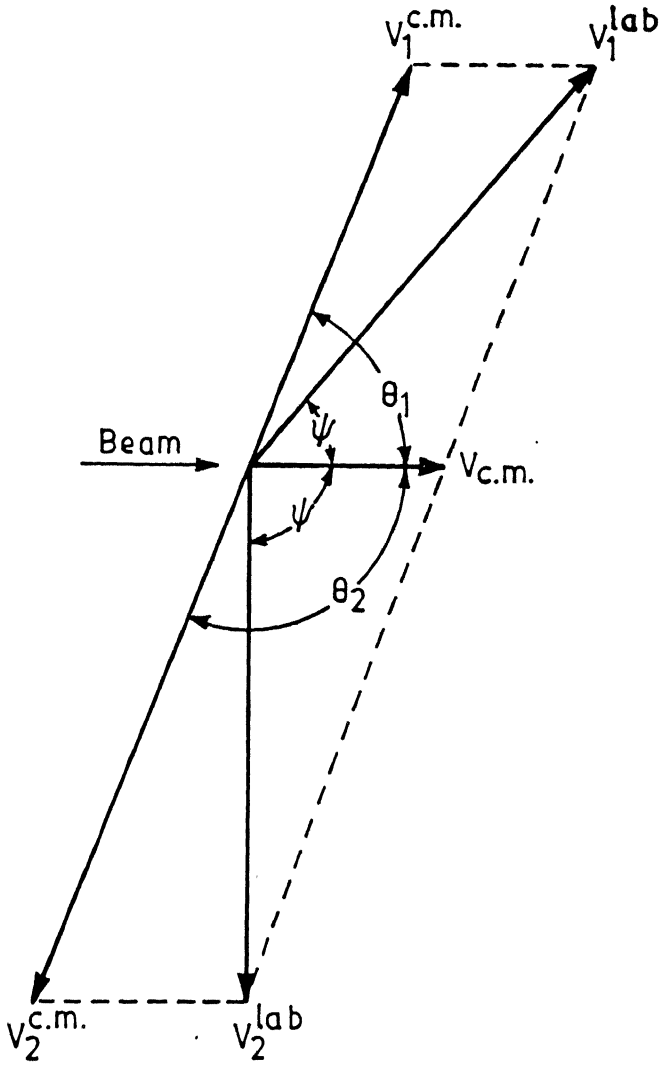

Fig. 3.5. Centre of mass correction for the velocities of fission fragments.

the energy imparted to the fissioning nuclei, we can calculate the velocity by formula

$$v_{CN} = 1.389 \sqrt{E_{CN}/M_{CN}}$$

Since we have measured the E_1^{lab} and E_2^{lab}, the fission fragment kinetic energies, we can calculate v_1^{lab} and v_2^{lab} using the above relation between velocity, energy and mass.

The velocity of the fragments , then, in the centre of mass frame is

$$v_1^{c.m.} = \sqrt{(v_1^{lab^2} + v_2^{lab^2} - 2v_1 v_{CN} \cos\theta_1)}$$

$$v_2^{c.m.} = \sqrt{(v_1^{lab} + v_{CN}^2 - 2 v_1 v_{CN} \cos\theta_2)}$$

It is sufficient to know the angle of emission of one of the fission fragments. The angle of emission of the other fragment can be calculated by simple vector algebra. Knowing the velocities one can transfer them back to energy to get the centre of mass energy.

[3.3](c) Neutron Correction:

The major fraction of the energy released, not appearing as kinetic energy of the fragments, is dissipated by the emission of neutrons. The neutron anisotropy studies have established that most of the neutrons are evaporated from fully accelerated fission fragments. The neutrons that are emitted from the fission fragments modify the energy and mass of the fragments. Since we are interested in the mass and energy distributions before neutron evaporation, we have to make corrections for the energy and mass as measured by our detectors for the energy taken away by the emitted neutrons. This correction is applied on the basis of previously

measured neutron numbers.

The number of neutrons that are emitted from the fission fragments is a function of excitation energy of the target nuclei and the kinetic energy of the fission fragments. At low energies i.e. energies near the fission barrier, number of neutrons is a non linear function of fragment mass. The average neutron yields are non integral implying thereby some variation in neutron yield from one fission event to another fission event.

At low excitation energy of the compound nucleus, the most interesting aspect of neutron emission is the variation in neutron yield as a function of fragment mass. The first evidence for structure in the dependence of neutron yield on fragment mass was obtained by Fraser and Milton[41]. There are unequal number of neutrons emitted from two complimentary fragments. Fig.[3.6(a)] (taken from Ref.[42] shows the variation of the neutron yield as a function of fragment mass for two different excitation energies for the fission of ^{238}U. This behaviour is exhibited by almost all fission fragments resulting from the fission of all actinides. This led Terrel[43] to the conclusion that the neutron yields are closely related to deformabilities of the nascent fragment. Closed shell or near closed shell nuclei prefer spherical shapes and are unusually resistant to deformation. If the complimentary fragment of such a nuclei is not close to a closed shell, most of the deformation energy will be in the complimentary fragment. The number of neutrons depends on the amount of deformation energy stored at scission. Once the energy is increased, shell effects are diminished or get washed away and the closed shell nuclei are also

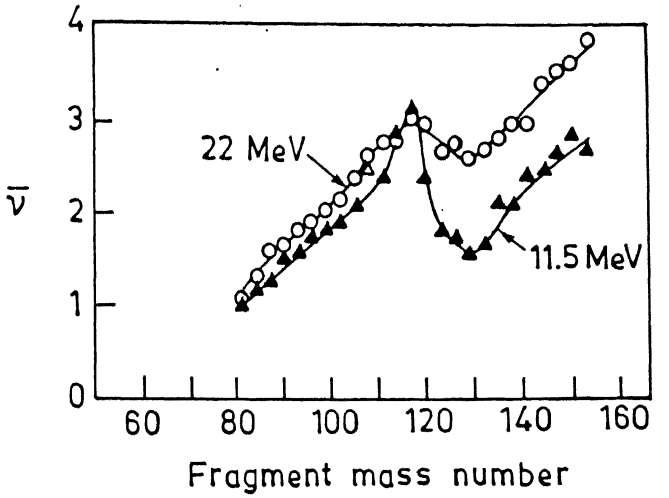

Fig. 3.6(a). Variation of neutron yield as a function of fragment mass in ($p + ^{238}U$) fission for proton energies of 11.5 MeV and 22 MeV.

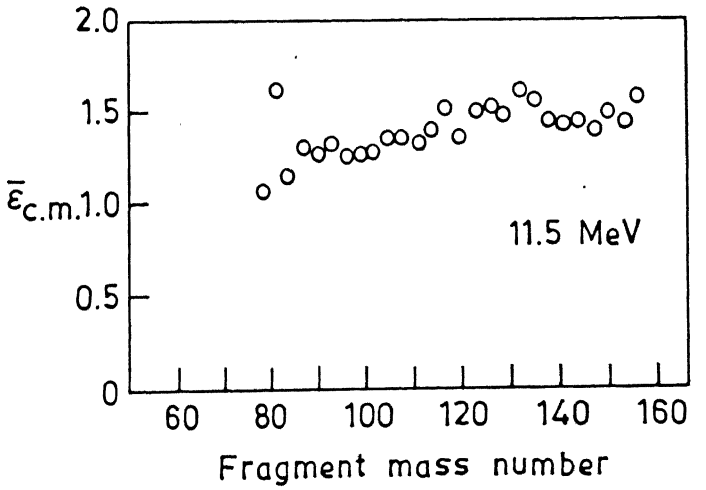

Fig. 3.6(b). Variation of neutron energy with fragment mass.

able to share deformation energy, Fig.[3.6(a)] shows that the saw tooth nature of neutron yield gets diminished as the excitation energy of the fissioning nuclei is increased. In our calculation, we require $\nu(A, E_x)$, where ν is the number of neutrons, A is the fragment mass and E_x is the excitation energy. Unfortunately, there is a dearth of experimenal results and there is no emperical relation to give the number of neutrons as a function of fragment mass and excitation energy of the fissioning nuclei. We have therefore, extrapolated or intrapolated linearly the results of obtained by Bishop etal depending on the excitation energy of the Uranium nuclei by fitting least square fits.

The average energy taken by the neutrons in the lab frame is about 2 MeV. Since most of the neutrons are emitted from moving fission fragments, the energy given to them by virtue of fragment motion is 2/3 MeV. Fig.[3.6(b)] shows the average neutron energy as a function of fragment mass. The data is again from Bishop etal[49]. The least square fit to this data has a very small slope. Though within the experimental resolution and the evaluational uncertainties we could have assumed that the energy is constant, yet we have taken a small slope. The energy is given by the relation

$$(M_i - 50) \times 4.4117647 \cdot 10^{-3} + 1.1268382$$

where M_i is the mass of the fragment.

[3.4] RESULTS AND DISCUSSION

Fig.[3.7] shows the variation of average total kinetic energy

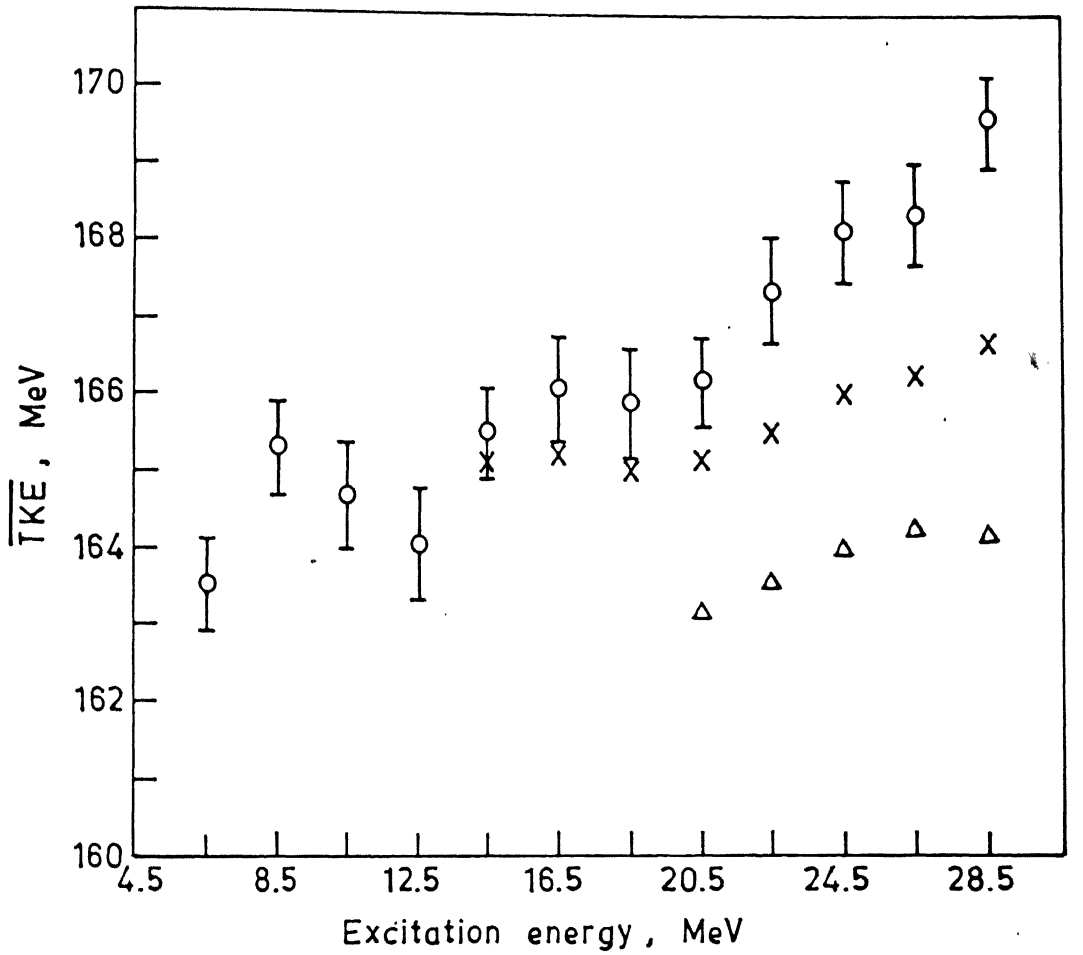

Fig. 3.7. The variation of total kinetic energy with excitation energy. The o show the experimental data, the X shows the data corrected for neutron from saddle to scission, the Δ shows the data further corrected for scission neutrons.

($\overline{TKE}$)as a function of the excitation energy of the fissioning nucleus. We observe that the total kinetic energy in the excitation energy region of 8.5 to 12.5 shows a decrease with excitation energy. Here, we have neglected the point at the excitation energy of 6.5 MeV because the error due to chance coincidence is very large due to the inelastic peak from the carbon in the backing interfering at this value of the excitation energy. This implies that as the excitation energy is increased, the viscosity of the system increases. This has been observed by Back etal[33] and also by David etal.[29]. The total kinetic energy then remains constant till 22.5 MeV and then it shows an increase with the excitation energy. At high excitation energies Back etal. also observe a positive slope. The positive slope has also been measured by Choudhury etal[34], though in a different system and at slightly higher excitation energies of the fissioning system. A possible explanation for this change of slope as more excitation energy is given to the system could that at lower excitation energies the shell effects are prevalent and giving a small amount of excitation energy to the system may amount to breaking of paired nucleons. At 22 Mev the pairing correlation is destroyed and the shell effects get diluted. They are not yet completely wiped out as is evident from the fact that the mass distribution still shows two humps. The peak to valley ratio averaged over all the values of excitation energy is 1 is to 1.5. The dilution of shell effects may weaken the coupling of the internal degrees of freedom to the external degrees. The excitation energy of the fissioning system then may manifest itself in the relative kinetic energy of the fragments.

($\overline{TKE}$)as a function of the excitation energy of the fissioning nucleus. We observe that the total kinetic energy in the excitation energy region of 8.5 to 12.5 shows a decrease with excitation energy. Here, we have neglected the point at the excitation energy of 6.5 MeV because the error due to chance coincidence is very large due to the inelastic peak from the carbon in the backing interfering at this value of the excitation energy. This implies that as the excitation energy is increased, the viscosity of the system increases. This has been observed by Back etal[33] and also by David etal.[29]. The total kinetic energy then remains constant till 22.5 MeV and then it shows an increase with the excitation energy. At high excitation energies Back etal. also observe a positive slope. The positive slope has also been measured by Choudhury etal[34], though in a different system and at slightly higher excitation energies of the fissioning system. A possible explanation for this change of slope as more excitation energy is given to the system could that at lower excitation energies the shell effects are prevalent and giving a small amount of excitation energy to the system may amount to breaking of paired nucleons. At 22 Mev the pairing correlation is destroyed and the shell effects get diluted. They are not yet completely wiped out as is evident from the fact that the mass distribution still shows two humps. The peak to valley ratio averaged over all the values of excitation energy is 1 is to 1.5. The dilution of shell effects may weaken the coupling of the internal degrees of freedom to the external degrees. The excitation energy of the fissioning system then may manifest itself in the relative kinetic energy of the fragments.

Table 3.1

EXCIT. ENERGY	MASS					
	130	135	140	145	150	155
6.5	169.9±1.4	169.0±1.7	164.4±1.6	161.4±1.3	158.0±1.6	159.2±1.4
8.5	168.8±1.5	168.6±1.4	164.4±1.1	162.2±1.4	157.0±2.5	154.0±1.8
10.5	162.4±3.2	167.4±1.6	166.2±1.6	162.2±1.0	157.0±1.8	154.0±1.8
12.5	162.4±2.7	169.2±2.0	165.4±1.8	161.4±1.4	157.6±1.5	155.4±1.8
14.5	168.6±2.6	169.4±1.4	164.6±1.4	162.2±1.0	160.8±1.2	156.8±1.6
16.5	167.2±2.8	167.6±2.0	167.6±1.6	164.0±0.8	162.0±1.4	155.8±9.0
18.5	169.0±2.4	168.4±2.0	165.2±1.8	163.6±1.4	158.8±1.2	157.0±2.6
20.5	168.6±2.0	166.2±2.0	166.0±1.2	164.2±1.6	161.8±1.2	157.8±2.0
22.5	169.0±2.6	168.4±2.0	169.6±1.4	164.2±1.0	161.8±2.0	160.8±1.8
24.5	168.0±1.4	169.8±1.6	169.2±1.8	167.2±1.8	160.4±1.6	157.0±2.0
26.5	165.0±2.4	169.8±1.4	169.2±1.4	167.8±1.2	162.0±1.8	163.9±2.2
28.5	169.6+2.2	169.0+1.8	169.2+1.2	165.8±1.4	164.8±1.4	163.6±2.0

Table.3.1 The variation of the total kinetic energy as a function of excitation energy for mass selected fragments.

Table.3.1 shows the variation of the total kinetic energy as a function of excitation energy for mass selected fragments. Fig.[3.8] shows the data of Table [3.1]. The figure shows the variation of $\overline{TKE}$ with excitation energy for mass selected fragments. For this kind of analysis the statistics of our data is very poor and consequently the error bars are very large.

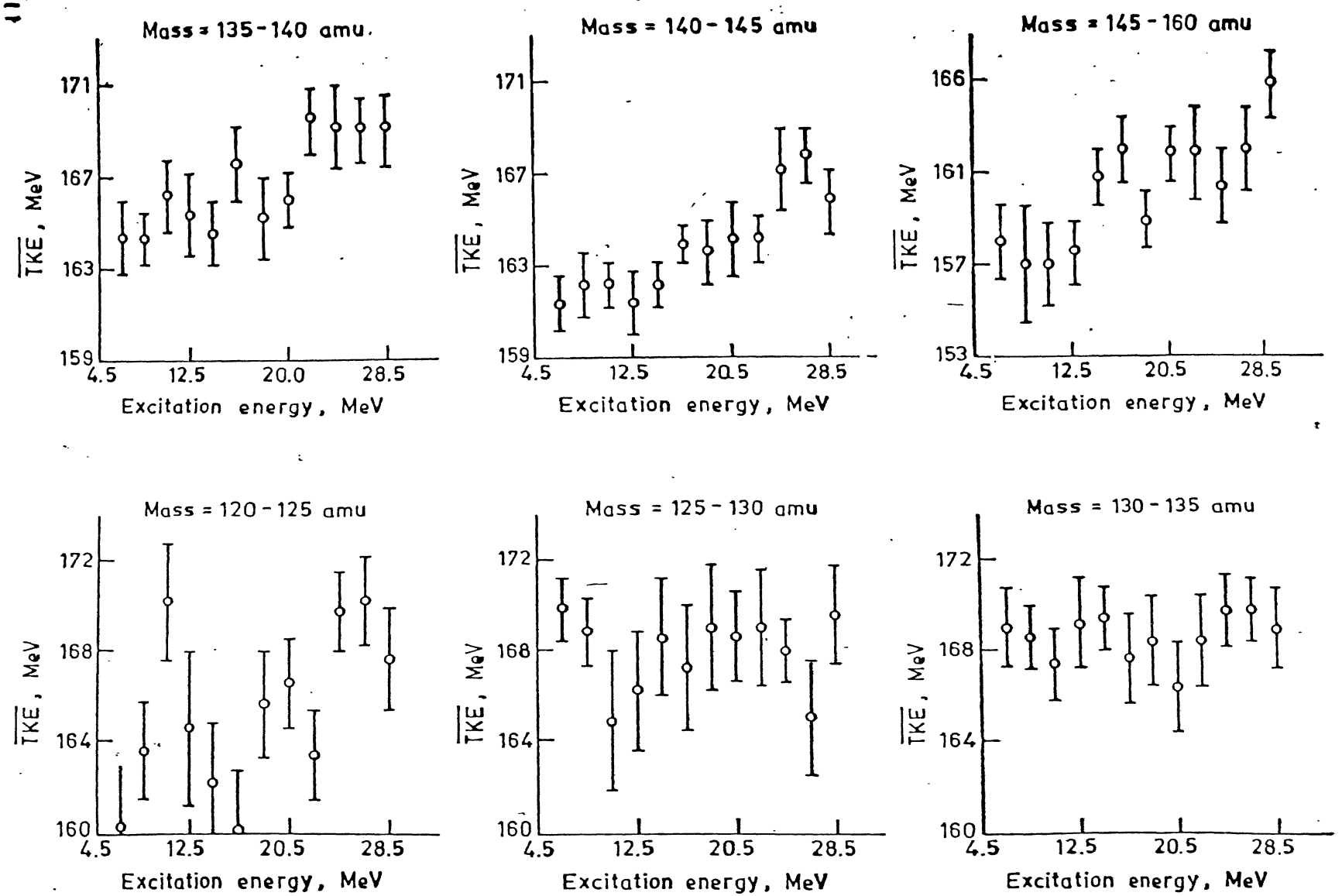

Fig. 3.8. Total kinetic energy variation with excitation energy for mass separated fragments. Mass window of 5 amu has been put.

Nevertheless, within the experimental errors one can say that for mass selected fragments near the doubly closed shell the total kinetic energy does not show any variation with excitation energy. For the highly asymmetric masses, the total kinetic energy increases with excitation energy of the fissioning nuclei. This implies that the coupling between the internal and the external degrees of freedom is stronger in case of spherical nuclei as compared to deformed nuclei.

Chance coincidence correction

One drawback of the earlier measurements[29-33] is the corrections applied to eliminate the effect due to chance coincidences. These chance coincidences, as mentioned earlier, arise due to alpha scattered from the carbon in the backing and fission due to (α,f) process. In earlier measurements, correction for the chance coincidence is made by subtracting the events under one of the random peaks from the events under the true + random peak after processing both the events as mentioned in Sec. [3.3]. This is improper because events under the random peak and random events in the true + random peak are due to the (α,f) process where the centre of mass and the neutron corrections apply differently than in the $(\alpha,\alpha'f)$ process. The random events under the true + random peaks have therfore to be processed in the same manner as those events under the random peak. This is not possible to do. In the earlier measurements, the correction for this effect has been done assuming that the data is the result of the direct reaction. This subtraction results, therefore, in biasing the data. Even if

the true to chance ratio is one is to ten, it introduces an error of 10% in their results. We have therefore not done this subtraction as this results in undue biasing of the data.

Thus we suggest that this experiment should be done with a self supporting foil of the target nucleus. This has not been done earlier because the target would have to be much thicker. Being a high Z material, the fragments will loose a substantial portion of their energy in the foil. This again will increase the uncertainity in the results. However, if one uses a gas detector to measure the energy and also the angle of emission of the fragments, the error will then be only due to the energy straggling which is of much smaller magnitude. The measurement of angle will also result in substantial improvement of the mass resolution since the averaging over the angle, which is done to correct for the energy loss correction and centre of mass motion in the experiments so far,spoils the mass resolution. If this experiment is done with mass resolution of the order of one mass unit, it may be possible to observe the effect of pair breaking on the total kinetic energy - an effect which has not been seen earlier due to poor mass resolution.

Neutron Correction:

We have made corrections for the number of neutrons emitted by the fully accelerated fragments. The number of neutrons emitted by the fragments at low excitation energy of the target is a function of their mass as well as the excitation energy of the fissioning nuclei. These neutrons can be classified into three categories

depending on the mechanism of their emission:

(i) neutrons emitted from the compound neucleus

(ii) neutrons emitted when the fissioning nucleus descends from saddle to scission

(iii)neutrons emitted from fully accelerated fragments

The study of prompt neutrons and their angular distributions in early sixties[44-46] had revealed that a small fraction of neutrons do not come from the fragments, but are emitted by the fissioning nucleus by the first two mechanisms mentioned above. The neutrons emitted before scission are nearly isotropic in the c.m system of the compound nucleus, whereas neutrons emitted by fully accelerated fragments are strongly correlated to the direction of fragment motion.

The measured fragment energies have to be corrected for neutron emission because the neutrons are emitted with some kinetic energy and in addition to this have some energy due to emission from fragment motion.

The results are corrected using the experimental results of Bishop etal[42]. They have measured the number of neutrons emitted in the proton induced fission of Uranium for two different proton energies. We have interpolated or extrapolated for the number of neutrons basing our results for these two energies following a procedure very similar to the one used by David[29]. Unfortunately the data of Bishop etal does not distinguish between the neutrons emitted before scission and the ones evaporated from fully accelerated fragments. Neutrons emitted from fully accelerated fragments are to be taken into account for the correction of the

single fragment kinetic energies. This experimental data does not exist. So far all the existing results on TKE measurements suffer from this uncertainity of making a correction to single fragment of the type (1+ ν/M) E_f (where ν is the number of neutrons, M is the mass and E_f is the energy of the fragment which is overestimated because it includes contributions from mechanisms 1 and 2 which do not modify the single fragment kinetic energy.

To correct for the number of neutrons emitted by the fissioning nucleus from compound nucleus to the saddle point stage, we have made a calculation of number of neutrons emitted from compound nucleus using Γ_n and Γ_f values from Vandenbosch[46]. The computer code to calculate this is given in Appendix [3]. If we incorporate this $\bar{\nu}$ calculation in our experimental curve showing $\overline{TKE}$ vs E_x, the curve which was having a positive slope becomes nearly a constant. The value of the $\overline{TKE}$ as a function of excitation energy, after correcting for this effect, is shown in Fig.[3.7] with a x. Our calculations do not include neutrons emitted from the saddle to scission.

There is a lot of data in heavy ion physics on prescission neutrons[47-49]. Gavron etal have found that theory always underestimates the value and most of the excitation energy goes into the emission of prescission neutrons. There is, however, one experimental result in α induced fission by Scobel etal,[50] which has direct bearing on our experimental results. They have studied prescission neutrons from fission fragments from α induced fission of Uranium. They find that nearly half of the excitation energy appears in the form of enhancement in prescission neutrons. We have

again corrected our results based on the results of Scobel which also gives the average energy taken by the scission neutrons as a function of excitation energy. This we show in the Fig.[3.7] with Δ. However, they have not measured the average energy and the multiplicity in low excitation energy region. Thus to quote the value of slope for $\overline{TKE}/E_x$ one requires the measurement of the prescission neutrons in this excitation energy range. For depending on the multiplicity of these neutrons the curve can have a negative, positive or zero slope.

[3.5] REFERENCES

1. B.D. Wilkins, E.P. Steinberg and R.R. Chasm, Phys. Rev. C14 (1976),1832.
2. K.F.Flynn and L.E.Glendenin, *Rep. ANL-7749 Argonne Nat. Lab. Argonne, Illinois.*
3. L.Wilet, "*Theories of Nuclear fission*" (Clarendon Press Oxford 1964).
4. P.Fong Phys. Rev. 135 (1964), B1338.
5. P.Fong, "*Statistical theories of nuclear fission*",
6. J.R. Nix, Ann Phys. 41 1967, 1.
7. J.R. Nix and W.J. Swiatecki Nucl. Phys.71 (1965), 1.
8. J.R. Nix, Nucl. Phys.A130 (1969), 241.
9. D.L. Hill and J.A. Wheeler,Phys. Rev. 89 (1953),1102.
10. L.Wilets, Phys. Rev.116 (1959),372.
11. R.Kaufmann and R.Wolfgang, Phys. Rev. 121 (1961),192.
12. T.Sikkeland, E.L.Haines and V.E. Viola Jr., Phys. Rev. 121 (1962) 1350.

13. D.H.E.Gross, Nucl. Phys. A240 13.

14. J.Wilczynski, Phys. Lett. 27B (1968) 277.

15. W.J.Swiatecki, *Proc. Int. Conf. Nucl.Reactions induced by heavy ions* Heidelberg (1969) North Holland.

16. J.R.Huizenga and W.U.Schöder, *Treatise in Heavy Ion Science Vol. 2* Plenum Press (1984).

17. M.N.Namboodiri, J.B.Natowitz, E.T. Chulick, K.Das and L.Webb, Nucl. Phys. A252 (1976) 163.

18. T.Sikkeland, Phys. Lett. 27B (1968) 277.

19. B.Borderie, F Hanappe, C. Ngo, J. Peter and B. Tamain, Nucl. Phys. A220 (1974) 93.

20. J.R.Nix, Proc. Nucl. Data Basic and App. Sci. Vol.1 (Gordon and Breach Publishers).

21. J.R.Nix and A.J.Sierk, Proc. Int. Conf. Nucl. Phys. Bombay 1984 (World Scientific Publishers).

22. M.Prakash, V.S.Ramamurthy, S.S.Kataria and S.S.Kapoor, Phys. Lett B81 (1979)136.

23. V.R.Viola,Jr.,Nucl. Data Sect.A1 (1966) 391.

24. W.J.Swiatecki and S.Björnhölm, Phys. Rep. 4C (1972) 326.

25. A.C.Wahl, A.E.Norris, R.A. Rouse and J.C. Williams, Proc. Phys. and Chem. of fission (IAEA Vienna 1969).

26. S. Amiel and H.Feldstein, Phys. Rev. C11 (1975) 845.

27. J.P.Unik, J.E.Gindler, L.E.Glendenin, K.F.Flynn, A. Gorshi and R.K.Sjoblom, Proc. Phys. and Chem. of fission (IAEA Rochester 1974)

29. P.David, J.Debrus, F.Lübke, H.Mommsen, E.Schmitt, R. Schoenmackers and H. Simons, Phys. Lett. 61B (1976) 158.

30. P.David, J.Debrus, F.Lübke, R. Schoenmackers and J. Schulze, Phys. Lett. 77B (1978) 178.

31. P.David, J.Debrus, H.Janszen, J.Schulze, M.N. Harakeh, J. Van der plicht and A Van der Woude,Nucl. Phys. A380 (1982) 27.

32. P.David, J.Debrus, P.Hartfiel, H Janszen and R Von Mutius, Nucl. Phys. A412 (1984) 24.

33. B.B.Back, A.C. Shotter, T.J.M Symonds, A.Bice, C.K.Gelbke T.C.Awes and D.K.Scott, Phys. Rev. C23 (1981) 1105.

34. R.K.Choudhury, A.Saxena, V.S.Ramamurthy, D.M.Nadkarni and S.S. Kapoor, Nucl. Phys. A463 (1987) 597.

35. H.W.Schmitt, W.M. Gibson, J.H. Neiler, F.J. Waiter and T.D. Thomas, Proc. Phys. and Chem. of fission (IAEA Vienna 1965) 531.

36. H.W.Schmitt, J.H.Neiler and F.J.Walter, Phys. Rev. 141 (1966) 47.

37. E.Weissenberger, P.Geltenbort, A.Oed, F.Gönnenwein and H. Faust, Nucl. Inst. Meth. A248 (1986) 506.

38. L.C.Northcliffe and R.F.Schilling, Nucl. Data Tables A7 (1970) 129.

39. Z.A.Zeigler, Handbook for stopping power of all ions Vol 5 (Pergamom Press).

40. F.Plasil, R.L.Fergueson, F.Pleasonton and H.W.Schmitt, Phys. Rev. C7 (1970) 233.

41. J.S.Fraser and J.C.D.Milton, Ann. Rev. Nucl. Sci. 16 (1966) 379.

42. C.J.Bishop, R.Vandenbosch, R.Alley, R.W.Shaw Jr. and I.Halpern, Nucl. Phys. A150 (1970) 129.

43. J. Terrel, *Proc. IAEA Symp. Phys. and Chem. Fission* Salzburg (1965).

44. K.Skarsvag and K.Berghein, Nucl. Phys. 45 (1963)

45. S.S.Kapoor, R.Ramanna and P.N.Rama Rao, Phys. Rev. 131 (1963) 283

46. R.Vandenbosch and J.R.Huizenga, *Nuclear Fission (Academic Press, New York 1973).*

47. H.A.Widenmûler and J.S.Zhang, Phys. Rev. C29 (1984) 879.

48. A.Gavron, J.R.Beene, B.Cheynis, R.L.Ferguson, F.E.Obenshain, F.Plasil, G.R.Young, G.A.Petit, M.A.Jääskelläinen, D.G.Sarantites and C.F.Maguire, Phys. Rev. Lett. 47 (1981) 1255.

49. A.Gavron, A.Gayer, J.Boissevain, H.C.Britt, J.R.Nix, A.J.Sierk P.Grange, S.Hassani, H.A.Widenmûler, J.R.Beene, B.Cheynis, D.Drain, R.L.Ferguson, F.E.Obenshain, F.Plasil, G.R.Young, G.A.Petit, and C.Butler, Phys. Lett. 176B (1986) 312.

50. P.Plischke, R.Langkau, W.Scobel and R.Wein,Nukleonika 27 (1982) 282.

CHAPTER IV

SUMMARY AND CONCLUSIONS

The studies in this thesis were aimed at providing further insight into the fission dynamics during the descent of the fissioning nucleus from the saddle to the scission point. We have investigated the prompt gamma ray emission in spontaneous fission of ^{252}Cf and the total kinetic energy distribution in the fission of ^{238}U following inelastic alpha scattering.

The results obtained can be summarized as follows:

(i) The gamma ray multiplicity distribution measurements indicate that the spin distribution of the fission fragment spin has a width (variance) of $\sigma = 5.7 \pm 0.5$ is deduced from the data for the charge ratio 1.3 (heavy fragment charge=56 and light fragment charge=42). This is a new piece of information since all the earlier studies have yielded only the mean value of the fragment spin.

The value of the width obtained is in general agreement with the hypothesis (Moretto etal.[1]) that the different angular momentum bearing modes (namely (i)twisting (ii) bending (iii) tilting and (iv) wriggling) at scission are in equilibrium. This width has been compared with the expression given by Moretto assuming the scission temperature to be around 0.5 to 1.0 MeV.

Gamma ray angular distribution shows that the anisotropy with respect to the fragment direction has a strong quadrupole signature in the range of $300<E_\gamma<700$ keV the maximum being 1.26±0.01 around 500 keV. Beyond 700 keV the anisotropy decreases but remains more than one. Below 300 keV the anisotropy is less than one signifying a predominantly dipole emission.

The analysis of the gamma ray data has brought out a number of shortcomings of the existing statistical model calculations of gamma ray emission. This may have important consequences on the de-excitation mechanism of nuclei having a finite spin and excitation energy.

The anisotropy of the prompt gamma rays with respect to the fragment direction for gamma energies greater than 700 keV being more than one is not understood. The statistical model, with the available expressions for the decay widths of gamma emission, predicts that the emission is predominantly dipole in nature at energies beyond 700 keV. This should make the anisotropy less than one. The experimental data suggests about an equal admixture of dipole and quadrupole transitions with the probability of quadrupole being slightly more. The origin of these quarupole and their nature is presently not known.

Deformed nuclei and spherical nuclei having large excitation energy and spin differ in their deexcitation. The present statistical model simulation does not include any difference in the nature of de-excitation between the spherical and deformed nuclei. Also the fragments carry angular momentum both as aligned single particle spins and collective rotations (in case of deformed

fragments). The answer to how a given angular momentum is partitioned between the two is also not answered by the theory.

Investigations on the kinetic energy distribution of the fission fragments have brought out the following results:

The total kinetic energy in the excitation energy range of 8.5 MeV to 12.5 MeV shows a decrease with excitation energy. In the excitation energy range of 12.5 MeV to 22.5 MeV it remains constant. From 22.5 MeV to 28.5 MeV it shows an increase with excitation energy.

The excitation energy dependence of the mass distribution leads to an apparent dependence of the fragment kinetic energy on the excitation energy. To minimize this effect, we carried out the variation of total kinetic energy as a function of excitation energy for mass separated fragments. We found that for nuclei near the doubly closed shell, the total kinetic energy does not show as much variation with excitation energy as it does for more asymmetric masses. While our statistics for a complete detailed analysis of this kind was poor, within experimental errors we can say that the descent of the fissioning nucleus from the saddle to scission for near spherical fragments is more viscous than for more asymmetric fragments.

Further analysis has brought out the reliability of earlier results[2-5] in question. This relates to the correction to single fragment kinetic energy due to neutron emission. The multichance fission events do not modify the single fragment kinetic energy. However, these have been included in the correction for the single fragment kinetic energy in the previous results.

We have, unlike the previous measurements, corrected our curve of $\overline{TKE}$ versus excitation energy partly by excluding the neutrons emitted from compound nucleus to the saddle point. The correction was done on the basis of statistical decay widths for fission and neutrons. Once the neutrons emitted during this stage of the fission process are excluded from the neutron correction in the single fragment kinetic energy, the nature of the curve beyond 22.5 MeV changes considerably.

Another new dimension has been added by the presence of enhanced prescission neutron multiplicity observed in heavy ion reactions, an area which has received very little attention in the past but plays a very crucial role in the analysis of this kind of measurements. These neutrons like those emitted in multichance events do not modify the single fragment kinetic energy.

From the measurements of Scobel etal.[6], we have corrected our total kinetic energy variation with excitation energy for errors resulting due to inclusion of these neutrons in the correction of the single fragment kinetic energy. This makes the curve of $\overline{TKE}/E_x$ almost flat. A reliable information on the viscosity prevalent during the descent of the fissioning nucleus from the saddle to the scission point can be deduced from these results, if the experimental information on the dependence of scission neutron multiplicity on the excitation energy of the fissioning nucleus and the fragment mass is known.

REFERENCES

1. L.G. Moretto, Ann. Rev. Nucl. Sci. (1984).

2. P.David, J.Debrus, H.Janszen, J.Schulze, M.N.Harakeh, J. Van der plicht and A. Van der Woude, Nucl. Phys. A380 (1982) 27.

3. P.David, J.Debrus, P.Hartfiel, H.Janszen, J. Von Mutius, Nucl. Phys. A384 (1984) 24 and references therein.

4. B.B.Back, A.C.Shotter, T.J.M.Symonds, A.Bice, C.K.Gelbke, T.C.Awes and D.K.Scott, Phys. Rev. C23 (1981) 1105.

5. R.K.Choudhury, A.Saxena, V.S.Ramamurthy, D.M.Nadkarni and S.S.Kapoor, Nucl. Phys. A463 (1987) 597.

6. P.Pliscke, R.Langkau, W.Scobel and R.Wein, Nukleonika 27 (1982) 282.

APPENDIX 1

```
C       PROGRAM TO CALCULATE THE SPIN DISTRIBUTION
        PROGRAM WIDTH
        DIMENSION SNEU(1000),SE1S(1000),SE2S(100),SE2C(100),RAND(1000)
        DIMENSION NITE1(15),NITN(15),TAC(100),NSPEC(50),NN(10),NU(10)
        DIMENSION AZ(50)
        CHARACTER*10 NAME
        COMMON/AA/HCROS,PI,SQRPI,PISQR,DELTA
        COMMON/BB/A,Z,EINI2,JINI2,ABAR,RINER,BN(3,50),ITZ,INEU
        EXTERNAL FNEU,FE1S,FE2S,FE2C
        PRINT'(''$GIVE THE NAME OF THE OUTPUT FILE:'')'
        READ '(A10)',NAME
100     FORMAT(A10)
101     FORMAT(2X,'MASS OF THE NUCLEUS=',F5.0,2X,'CHARGE=',F5.0,2X,
     1  'EX. ENERGY=',F4.0,2X,'SPIN=',I4,2X,'DELTA=',F5.1)
102     FORMAT(5X,(4(14(1H-)),'X'))
103     FORMAT(4X,'INITIAL EX. ENERGY=',F8.3)
104     FORMAT(10X,'SPIN VALUE IS=',I3)
105     FORMAT(4X,' THE SHELL CORRECTION PARAMETER=',F6.3)
106     FORMAT(4X,'FIRST AND SECOND MOMENT OF THE MULTIPLICITY DISTRIBUT
     1ION OF GAMMA RAYS ')
107     FORMAT(8X,'FROM FISSION FRAGMENTS AT DIFFERENT EXCITATION ENERGY
     1 AND SPIN')
108     FORMAT(5X,'EX ENERGY',5X,'NEUTRON',5X,'STA E1',5X,'STA E2',5X,
     1  'COL E2')
109    FORMAT(2X,'NO.OF GAMMA RAYS=',I2,2X,'ENERGY OF THE E1 STATISTICAL
     1=  ',F5.3)
110     FORMAT(2X,'NO.OF NEUTRON=',I3,3X,'ENERGY OF THE NEUTRON=',F5.3
     1  )
        OPEN(UNIT=4,FILE=NAME)
        OPEN(UNIT=33,FILE='BIND:DAT',ACCESS='READ')
        DO FOR I=1,27
        READ(33,*)AZ(I),BN(1,I),BN(2,I),BN(3,I)
        ENDDO
        CLOSE(UNIT=33)
        WRITE(4,106)
        WRITE(4,107)
        WRITE(4,*)
        WRITE(4,*)
        IN=1
        PI=4.*ATAN(1.)
        PISQR=PI**2
        SQRPI=SQRT(PI)
        RMASS=1.04
        ITER=0
        PRINT'(''$GIVE A RANDOM NUMBER AN INTEGER :'')'
        READ*,IX
        ITER=0
        Z=62.0
```

```
      EINI1=20.0
      EINI=EINI1
      JINI1=15
      JINI=JINI1
      IAZ=1
      A=AZ(IAZ)
      AINI=A
      DELTA=4.0
      WRITE(4,101)A,Z,EINI1,JINI1,DELTA
      HCROS=6.5819
      IAZ=IAZ+1
      ITZ=1
      GO TO 18
10    IF(Z.LE.50.0)GO TO 60
      ITER=0
      Z=Z-1.0
      A=AZ(IAZ)
      AINI=A
      IAZ=IAZ+1
      WRITE(4,*)
      WRITE(4,*)
      WRITE(4,101)A,Z,EINI1,JINI1,DELTA
      ITZ=ITZ+1
      JINI=JINI1
      EINI=EINI1
C      WRITE(4,108)
      DO 11 IS=1,10
11    NN(IS)=0
      GO TO 18
12    ITER=0
      EINI=EINI-5.
      WRITE(4,103)EINI
      JINI=JINI1
      IF(EINI.LE.5.)GO TO 10
      GO TO 18
13    ITER=0
      JINI=JINI-5
      IF(JINI.LE.0)GO TO 12
      WRITE(4,104)JINI
C     PRINT 104,JINI
      GO TO 18
14    ITER=0
      MSUM=0
      NSUM=0
      DO 15 L=1,10
      NSUM=NSUM+NU(L)*(L-1)
15    MSUM=MSUM+NN(L)*(L-1)
      RSS=FLOAT(MSUM)
      SSS=FLOAT(NSUM)
      RSUM=RSS/100.
      SSUM=SSS/100.
      RTT=0.0
      STT=0.0
      DO 16 L=1,10
```

```
      ITER1=ITER1+1
      ZZ=RNDM(IX,IN)
      IF(ZZ.GT.0.0.AND.ZZ.LE.PWNEU)GO TO 20
      IF(ZZ.GT.PWNEU.AND.ZZ.LE.(PWE1S+PWNEU))GO TO 30
20    CONTINUE
      SNEU(1)=0.0
      DO 21 I=2,1000
      EPS=I*0.01
      GAM=FNEU(EPS)
21    SNEU(I)=SNEU(I-1)+GAM
      DO 22 I=2,1000
22    SNEU(I)=SNEU(I)/SNEU(1000)
      ZZ=RNDM(IX,IN)
      ZZ2=ZZ
      DO 23 I=2,1000
      IF(SNEU(I).GE.ZZ)GO TO 24
23    CONTINUE
      IF(I.GE.1000)THEN
      EN=EINI2
      NNEU=NNEU+1
      A=A-1.0
      GO TO 18
      ENDIF
24    EN=I*0.01
      NNEU=NNEU+1
      EINI2=EINI2-EN-BN(INEU,ITZ)
      INEU=INEU+1
      A=A-1.0
C     WRITE(4,110)NNEU,EN
      GO TO 19
30    CONTINUE
      SE1S(1)=0.0
      DO 31 I=2,1000
      EPS=I*0.01
      GAM=FE1S(EPS)
31    SE1S(I)=SE1S(I-1)+GAM
      DO 32 I=2,1000
32    SE1S(I)=SE1S(I)/SE1S(1000)
      ZZ=RNDM(IX,IN)
      ZZ3=ZZ
      DO 33 I=1,1000
      IF(SE1S(I).GE.ZZ)GO TO 34
33    CONTINUE
34    E1S=I*0.01
      NE1S=NE1S+1
      EINI2=EINI2-E1S
C      WRITE(4,109)NE1S,E1S
      GO TO 19
40    CONTINUE
      SE2S(1)=0.0
      DO 41 I=2,100
      EPS=I*0.1
      GAM=(EPS**5)*WEJ(EINI2-BN(INEU,ITZ)-EPS,JINI2)
41    SE2S(I)=SE2S(I-1)+GAM
```

```
      DO 42 I=2,100
42    SE2S(I)=SE2S(I)/SE2S(100)
      ZZ=RNDM(IX,IN)
      ZZ4=ZZ
      DO 43 I=1,100
      IF(SE2S(I).GE.ZZ)GO TO 45
43    CONTINUE
45    E2S=I*0.1
      IF(I.EQ.101)THEN
      E2S=0.1
      NE2S=NE2S+1
      WRITE(4,*)'ENERGY OF THE E2 STATISTICAL',ITER1,E2S
      GO TO 18
      ENDIF
      NE2S=NE2S+1
      WRITE(4,*)'ENERGY OF THE E2 STATISTICAL',ITER1,E2S
      EINI2=EINI2-E2S
      GO TO 19
50    CONTINUE
      SE2C(1)=0.0
      DO 51 I=2,100
      EPS=I*0.1
      GAM=EPS**5
51    SE2C(I)=SE2C(I-1)+GAM
      DO 52 I=2,100
52    SE2C(I)=SE2C(I)/SE2C(100)
      ZZ=RNDM(IX,IN)
      DO 53 I=1,100
      IF(SE2C(I).GE.ZZ)GO TO 54
53    CONTINUE
54    E2C=I*0.1
      IF(I.EQ.101)THEN
      E2C=.1
      NE2C=NE2C+1
      WRITE(4,*)'ENERGY OF THE E2 COLLECTIVE',ITER1,E2C
      GO TO 18
      ENDIF
      NE2C=NE2C+1
      WRITE(4,*)'ENERGY OF THE E2 COLLECTIVE',ITER1,E2C
      EINI2=EINI2-E2C
      JINI2=JINI2-2
      GO TO 19
60    CONTINUE
      STOP
      END
      FUNCTION GINTEG(FF,A,B)
      DOUBLE PRECISION XX,WX
      DIMENSION XX(40),WX(40)
      DATA XX/0.0950125098D0,-0.0950125098D0, 0.2816035508D0,
     1        -0.2816035508D0, 0.4580167777D0,-0.4580167777D0,
     2         0.6178762444D0,-0.6178762444D0, 0.7554044084D0,
     3        -0.7554044084D0, 0.8656312024D0,-0.8656312024D0,
     4         0.9445750231D0,-0.9445750231D0, 0.9894009350D0,
     5        -0.9894009350D0, 24*0.D0/
```

```
      DATA WX/0.1894506105D0, 0.1894506105D0, 0.1826034150D0,
     1          0.1826034150D0, 0.1691565194D0, 0.1691565194D0,
     2          0.1495959888D0, 0.1495959888D0, 0.1246289712D0,
     3          0.1246289712D0, 0.0951585117D0, 0.0951585117D0,
     4          0.0622535239D0, 0.0622535239D0, 0.0271524594D0,
     5          0.0271524594D0, 24*0.D0/
      T=0.0
      DO 2 I=1,16
      XI=(B-A)*XX(I)*0.5+(B+A)*0.5
      T=T+FF(XI)*WX(I)
    2 CONTINUE
      GINTEG=T*(B-A)*0.5
      RETURN
      END
      FUNCTION WEJ(EX,J)
      COMMON/AA/HCROS,PI,SQRPI,PISQR,DELTA
      COMMON/BB/A,Z,EINI2,JINI2,ABAR,RINER,BN(3,50),ITZ,INEU
      ER=J**2/(2.*RINER)
      EF=EX-ER
      WEJ=0.0
      IF(EF.LE.0.0)RETURN
      FABAR=ABAR*(1-(DELTA/EF)*(1-EXP(-EF*0.054)))
      WEJ=(SQRPI*EXP(2.*((FABAR*EF)**0.5)))/(12.*(FABAR**.25)*
     1 (EF**1.25))
      RETURN
      END
      FUNCTION FNEU(X)
      DIMENSION YY(7)
      COMMON/BB/A,Z,EINI2,JINI2,ABAR,RINER,BN(3,50),ITZ,INEU
      COMMON/AA/HCROS,PI,SQRPI,PISQR,DELTA
      DATA YY/31.05,-25.91,342.4,21.89,0.223,0.673,617.4/
      Y=EINI2-BN(INEU,ITZ)-X
      SIGN=YY(3)*((A)**(1/3))+YY(4)*((A)**(2/3))+(YY(1)*((A)**(-1/3)
     1 +YY(2))*X+(YY(5)*((A)**(4/3))+YY(6)*((A)**(2/3))+YY(7))/X
      FNEU=(1./((PI*197.)**2))*940.*X*WEJ(Y,JINI2)*SIGN
C      FNEU=X*WEJ(Y,JINI2)
      RETURN
      END
      FUNCTION FE1S(X)
      COMMON/BB/A,Z,EINI2,JINI2,ABAR,RINER,BN(3,50),ITZ,INEU
      COMMON/AA/HCROS,PI,SQRPI,PISQR,DELTA
      ERR=34.*A**(-1/6)
      TA=6.
      SIGS=60.*((A-Z)*Z/A)*(2./(PI*TA))*(((TA*X)**2)/((TA*X)**2+(
     1 (X)**2-(ERR)**2)**2))
      FE1S=(1./(PI*197.)**2)*SIGS*(X**2)*WEJ(EINI2-X,JINI2)
C      FE1S=((X)**4)*WEJ(EINI2-X,JINI2)
      RETURN
      END
      FUNCTION FE2S(X)
      COMMON/BB/A,Z,EINI2,JINI2,ABAR,RINER,BN(3,50),ITZ,INEU
      FE2S=((X)**6)*WEJ(EINI2-X,JINI2)
      RETURN
      END
```

```
      FUNCTION FE2C(X)
      COMMON/BB/A,Z,EINI2,JINI2,ABAR,RINER,BN(3,50),ITZ,INEU
      FE2C=(X)**5
      RETURN
      END
      FUNCTION RNDM(IX,IN)
      INTEGER*4 JM,MM,IX,IC
C     PRINT *,IX
      IF(IN) 30,40,30
30    IN=0
      JM=2**10+3
      MM=2**( 20)
      FM=MM
40    IC=IX*JM/MM
      IX=IX*JM-IC*MM
      FX=IX
      XD=FX/FM
      RNDM=ABS(XD)
C     PRINT*,RNDM
      RETURN
      END
```

APPENDIX 2

```
      PROGRAM TAPETEST
      INTEGER*2 IBUF1(1024)
      INTEGER*4 IBUF2(80)
      DIMENSION NTKE(2,20,1550),NM1(2,20,1200),IE1(2,20,1200)
      DIMENSION RMEAN3(2,20),IE2(2,20,1200),IMEA(2,100,20)
      DIMENSION IMRE(2,20,100,100),IME(2,20,100,100),ITAC(750)
      DIMENSION IF1(20,200),IF2(20,200),IF3(20,250),IF4(20,200)
      DIMENSION IFIS1(2048),IFIS2(2048),IPAR(2048)
      COMMON/AA/EP
      COMMON/BB/SU(20)
      COMMON/CC/SC(20)
      COMMON/DD/EX
      COMMON/EE/THETA1,THETA2
      COMMON/EF/THETA
      COMMON/NEUT/ECM1,ECM2,E1N,E2N,RNU1,RNU2,AM1,AM2
      INTEGER*4 IERRNO
      CHARACTER*4 COMMAND(6),ANS
      CHARACTER*1 RAND
      DATA COMMAND/'BKSP','RWND','READ','EXIT','SKIP','WRIT'/
      ICOUNT=0
      JK=0
      OPEN(UNIT=5,FILE='POT:SYMB',ACCESS='READ',STATUS='OLD')
      OPEN(UNIT=6,FILE='MAS8:OUT',ACCESS='WRITE',STATUS='UNKNOWN')
      OPEN(UNIT=7,FILE='MAS9:OUT',ACCESS='WRITE',STATUS='UNKNOWN')
      OPEN(UNIT=8,FILE='TKE1:OUT',ACCESS='WRITE',STATUS='UNKNOWN')
      OPEN(UNIT=9,FILE='PARTI:OUT',ACCESS='WRITE',STATUS='UNKNOWN')
      OPEN(UNIT=10,FILE='TKEM:OUT',ACCESS='WRITE',STATUS='UNKNOWN')
      MTUR=40B
1000  FORMAT(/,'$GIVE FUNCTION BKSP/RWND/READ/EXIT/SKIP/WRIT ??')
1001  FORMAT(' Header Words Read:',I6)
1002  FORMAT(' No. of Blocks Read:',I5)
1003  FORMAT(120(1H-))
1004  FORMAT(25X,' VALUE OF TOTAL ENERGY=',I2)
1005  FORMAT(20I4)
1006  FORMAT(30X,' ENERGY=',I5)
1007  FORMAT(2X,I5,5X,'SUM=',F10.3,5X,'MEAN=',F10.3,5X ,'SIGMA=',F10.3)
1008  FORMAT(35X,'MASS =',I5)
1009  FORMAT(7X,I5,5X,'SUM=',F10.3,5X,'MEAN=',F10.3,5X,'SIGMA=',F10.3)
      READ(5,*)(SU(I),I=1,20)
      READ(5,*)(SC(I),I=1,20)
      CLOSE(UNIT=5)
      FM1=1174.;FM2=1204.;
C      FM2=1150.;FM1=1170.;
      AC1=1146.0
      BC1=1554.0
      AC2=1080.0
```

```
      BC2=1496.0
      EP=60.0
      PI=4.0*ATAN(1.0)
      THETA1=90.0
      THETA2=90.0
      EH1=78.42
      EH2=78.42
      EL1=102.64
      EL2=102.64
      TA1=(EL1-EH1)/(BC1-AC1)
      TA2=(EL2-EH2)/(BC2-AC2)
      TB1=EL1-TA1*BC1
      TB2=EL2-TA2*BC2
      ANOT=24.3
      ANOTP=0.0283
      BNOT=90.397
      BNOTP=0.1150
      A1=ANOT/(BC1-AC1)
      AA1=ANOTP/(BC1-AC1)
      B1=BNOT-A1*BC1
      BB1=BNOTP-AA1*BC1
      A2=ANOT/(BC2-AC2)
      AA2=ANOTP/(BC2-AC2)
      B2=BNOT-A2*BC2
      BB2=BNOTP-AA2*BC2
1     WRITE(1,1000)
      READ(1,*) ANS
      DO FOR I=1,6
      IF(ANS.EQ.COMMAND(I)) THEN
      GOTO (100,200,300,400,500,600) I
      ENDIF
      ENDDO
      GOTO 1
C.....BACKSPACE.....
100   CONTINUE
      MTUX=MTUR; ISTAT=MAGTP(15B,D,MTUX,D,D)
      GOTO 1
C.....REWIND........
200   CONTINUE
      MTUX=MTUR;ISTAT=MAGTP(13B,D,MTUX,D,D)
      IF(ISTAT.NE.0)THEN
      GOTO 999
      ENDIF
      GOTO 1
C.....READ........
300   DO FOR I=1,1024
      IBUF1(I)=0
      ENDDO
      IDUM=0;MTUX=MTUR;KOUNT=0
2     CONTINUE
      PRINT'(''$Do You Want to READ the HEADER:'')'
      READ'(A1)',RAND
      IF(RAND.EQ.'Y'.OR.RAND.EQ.'y')then
      ISTAT=MAGTP(OB,IBUF2,MTUR,80,IDUM)
```

```
      WRITE(1,1001)IDUM
      WRITE(1,'(20A4)')(IBUF2(I),I=1,40)
      ENDIF
      IJ=0
4     CONTINUE
      IF(IBLK.EQ.1000)GO TO 17
      ISTAT=MAGTP(0B,IBUF1,MTUR,60,IDUM)
      IF(ISTAT.EQ.3)THEN
      PRINT'('' EOF DETECTED'')'
      GO TO 17
      ENDIF
      IBLK=IBLK+1
      DO 16 I=1,56,5
      IRE=IBUF1(I)
      IRE1=IBUF1(I+1)
      IRE2=IBUF1(I+2)
      IRE3=IBUF1(I+3)
      IRE4=IBUF1(I+4)
      RE1=FLOAT(IRE)
      RE2=FLOAT(IRE1)
      IF(IRE4.GT.500.AND.IRE4.LT.649)THEN
          JKI=1
      ELSEIF(IRE4.GT.906.AND.IRE4.LT.1052)THEN
          JKI=2
      ELSE
          GO TO 16
      ENDIF
      E1=(RE1)*TA1+TB1
      KE1=E1+0.5
      E2=(RE2)*TA2+TB2
      KE2=E2+0.5
      EST=(FLOAT(IRE2))*0.032667-4.187703
      DEL=(FLOAT(IRE3))*0.022761-0.425054
      ETOT=DEL+EST
      IRE5=ETOT*10
      IF(IRE5.LT.1.OR.IRE5.GT.750)IRE5=1
      ITAC(IRE5)=ITAC(IRE5)+1
      EX=59.7-ETOT-5.8
      IF(ETOT.LT.30.5.OR.ETOT.GT.54.5)GO TO 16
      IF(KE1.LT.30.OR.KE1.GT.125)GOTO 16
      IF(KE2.LT.30.OR.KE2.GT.125)GOTO 16
      IJK=(ETOT-30.5)/2.0+1
      IF(IJK.LT.1.OR.IJK.GT.14)GO TO 16
      IF(IRE2.LT.150)GO TO 161
      MI=(ETOT**1.72-EST**1.72)+0.5
      IF(MI.LT.296.OR.MI.GT.340)GO TO 16
      IPAR(MI)=IPAR(MI)+1
161   TEMP1=E1
      TEMP2=E2
      AM1=238.*E2/(E1+E2);
      AM2=238.-AM1
      NIND=0
      GO TO 6
5     E1=(A1+AA1*AM1)*(RE1)+B1+BB1*AM1
```

```
      E2=(A2+AA2*AM2)*(RE2)+B2+BB2*AM2
      AM1=238.*E2/(E1+E2)
      AM2=238.-AM1
6     Z1=92.*AM1/238.
      Z2=92.-Z1
      IND=1
      TE1=E1
      CALL LOSS(E1,AM1,Z1,IND,E1F)
      TE2=E2
      IND=2
      CALL LOSS(E2,AM2,Z2,IND,E2F)
      ELL1=E1F-TE1
      ELL2=E2F-TE2
      E1=E1F
      E2=E2F
      AM1=238.*E2F/(E1F+E2F)
      AM2=238.-AM1
7     CALL KINEM(ETOT,E1F,E2F,AM1,AM2,ECM1,ECM2)
      ECM1=E1F
      ECM2=E2F
      CALL NEUT
      AM1=AM1-RNU1
      AM2=AM2-RNU2
      NIND=NIND+1
      IF(NIND.LT.2)GO TO 5
      IF(NIND.LT.3)GO TO 7
9     CONTINUE
      AM1=RNU1+AM1
      AM2=RNU2+AM2
      M1=AM1+0.5
      M2=AM2+0.5
      ENET=E1N+E2N
      NET=ENET+ 0.5
      NE1=E1N + 0.5
      NE2=E2N + 0.5
      IE1(JKI,IJK,NE1)=IE1(JKI,IJK,NE1)+1
      IE2(JKI,IJK,NE2)=IE2(JKI,IJK,NE2)+1
      IF(NET.LT.1.OR.NET.GT.250)GOTO 10
      NTKE(JKI,IJK,NET)=NTKE(JKI,IJK,NET)+1
10    IF(M1.LT.1.OR.M1.GT.200)GOTO 11
      NM1(JKI,IJK,M1)=NM1(JKI,IJK,M1)+1
11    IF(M2.LT.1.OR.M2.GT.200)GOTO 16
      NM1(JKI,IJK,M2)=NM1(JKI,IJK,M2)+1
12    INE=(NET-120)/10
      IF(INE.LT.1.OR.INE.GT.8)GOTO 13
13    IM1=(M1-60)/2 +1
      IF(IM1.LT.1.OR.IM1.GT.50)GOTO 14
      IME(JKI,IJK,IM1,INE)=IME(JKI,IJK,IM1,INE)+1
      IMEA(JKI,IM1,INE)=IMEA(JKI,IM1,INE)+1
14    IM2=(M2-60)/2 +1
      IF(IM2.LT.1.OR.IM2.GT.50)GOTO 15
      IME(JKI,IJK,IM2,INE)=IME(JKI,IJK,IM2,INE)+1
      IMEA(JKI,IM2,INE)=IMEA(JKI,IM2,INE)+1
15    JM1=M2
```

```
      IF(M1.GT.M2)JM1=M1
      KM1=(JM1-115)/5+1
      IF(KM1.LT.1.OR.KM1.GT.11)GOTO 16
      IN2=(NET-125)/2 +1
      IF(IN2.LT.1.OR.IN2.GT.40)GOTO 16
      IMRE(JKI,IJK,IN2,KM1)=IMRE(JKI,IJK,IN2,KM1)+1
16    CONTINUE
      J=J+1
      GOTO 4
500   PRINT'(''$ Want to SKIP File:'')'
      READ'(A1)',RAND
      IF(RAND.EQ.'Y'.OR.RAND.EQ.'y')THEN
      PRINT'(''$How Many Files to Skip:'')'
      READ*,IFILENO
      DO 502 IAS=1,IFILENO
      ISTAT=MAGTP(10B,IBUF1,MTUR,60,IDUM)
502   CONTINUE
      ENDIF
      IF(RAND.EQ.'N'.OR.RAND.EQ.'n')THEN
      PRINT'(''$How Many BLOCKS to Skip:'')'
      READ*,IBLKN
      DO FOR IAS=1,IBLKN
      ISTAT=MAGTP(16B,IBUF1,MTUR,60,IDUM)
      ENDDO
      ENDIF
      GO TO 1
17    WRITE(1,*)
      WRITE(1,1002)IBLK
      WRITE(1,*)
      PRINT'(''$Do You Want to CONTINUE -Y:Yes;N:No:'')'
      READ'(A1)',RAND
      IBLK=0
      IF(RAND.EQ.'Y'.OR. RAND.EQ.'y')THEN
      GO TO 2
      ENDIF
      GO TO 1
600   CONTINUE
C-----------------------
C      WRITE(9,1005)(IPAR(I),I=1,2048)
      DO FOR K=1,14
C-----------------------
C      WRITE(6,1004)K
      WRITE(6,*)' SINGLE FRAGMENT KINETIC ENERGY OF DETECTOR-1'
      WRITE(6,1005)(IE1(1,K,I),I=1,200)
      DO FOR I=1,200
      IE1(1,K,I)=IE1(1,K,I)-IE1(2,K,I)
      IF(IE1(1,K,I).LT.0)IE1(1,K,I)=0
      ENDDO
      WRITE(7,*)' SINGLE FRAGMENT KINETIC ENERGY OF DETECTOR-1'
      WRITE(7,1005)(IE1(1,K,I),I=1,200)
C      WRITE(6,1003)
      WRITE(6,*)' SINGLE FRAGMENT KINETIC ENERGY OF DETECTOR-2'
      WRITE(6,1005)(IE2(1,K,I),I=1,200)
      DO FOR I=1,200
```

```
      IE2(1,K,I)=IE2(1,K,I)-IE2(2,K,I)
      IF(IE2(1,K,I).LT.0)IE2(1,K,I)=0
      ENDDO
      WRITE(7,*)' SINGLE FRAGMENT KINETIC ENERGY OF DETECTOR-2'
      WRITE(7,1005)(IE2(1,K,I),I=1,200)
C      WRITE(6,1003)
      WRITE(6,*)' TOTAL KINETIC ENERGY'
      WRITE(6,1005)(NTKE(1,K,I),I=1,250)
      DO FOR I=1,250
      NTKE(1,K,I)=NTKE(1,K,I)-NTKE(2,K,I)
      IF(NTKE(1,K,I).LT.0)NTKE(1,K,I)=0
      ENDDO
      WRITE(7,*)' TOTAL KINETIC ENERGY'
      WRITE(7,1005)(NTKE(1,K,I),I=1,250)
      SUM1=0.0
      SUM2=0.0
      SUM3=0.0
      DO FOR I=150,220
      SUM1=SUM1+FLOAT(NTKE(1,K,I)*I)
      SUM2=SUM2+FLOAT(NTKE(1,K,I))
      ENDDO
      RMEAN=SUM1/SUM2
      DO FOR I=150,220
      SUM3=SUM3+NTKE(1,K,I)*((RMEAN-FLOAT(I))**2)
      ENDDO
      SIGM=SUM3/SUM2
      SIGM=SQRT(SIGM)
      WRITE(10,1004)K
      WRITE(10,1009)NTKE(1,K,NINT(RMEAN)),SUM2,RMEAN,SIGM
C      WRITE(6,1003)
      WRITE(6,*)' MASS DISTRIBUTION'
      WRITE(6,1005)(NM1(1,K,I),I=1,200)
      DO FOR I=1,200
      NM1(1,K,I)=NM1(1,K,I)-NM1(2,K,I)
      IF(NM1(1,K,I).LT.0)NM1(1,K,I)=0
      ENDDO
      WRITE(7,*)' MASS DISTRIBUTION'
      WRITE(7,1005)(NM1(1,K,I),I=1,200)
      ENDDO
      WRITE(8,*)' MASS DISTRIBUTION AS A FUNCTION OF TKE AVERAG. EX ENE'
      DO FOR K=1,8
      WRITE(8,*)'KINETIC ENERGY VALUE=',120+10*K
      DO FOR J=1,50
      IMEA(1,J,K)=IMEA(1,J,K)-IMEA(2,J,K)
      IF(IMEA(1,J,K).LT.0)IMEA(1,J,K)=0
      ENDDO
      WRITE(8,1005)(IMEA(1,J,K),J=1,50)
      ENDDO
       GO TO 1111
      DO FOR IJ=1,14
      WRITE(6,1004)IJ
      DO 20 I=1,8
      SM=0.0
      SAM=0.0
```

```
      SIGM=0.0
      NER=I*10+120
      WRITE(6,1006)NER
      DO FOR K=1,50
      IME(1,IJ,K,I)=IME(1,IJ,K,I)- IME(2,IJ,K,I)
      IF(IME(1,IJ,K,I).LT.0)IME(1,IJ,K,I)=0
      ENDDO
      WRITE(6,1003)
      WRITE(6,1005)(IME(1,IJ,K,I),K=1,50)
      RM=60.5
      DO 18 J=1,50
      SM=SM+IME(1,IJ,J,I)
      SAM=SAM+RM*IME(1,IJ,J,I)
      RM=RM+2.0
18    CONTINUE
      IF(SM.EQ.0.0)GOTO 20
      SAM=SAM/SM
      RJM=60.5
      DO 19 JJ=1,50
      SIGM=SIGM+IME(1,IJ,JJ,I)*(RJM-SAM)**2
      RJM=RJM+2.0
19    CONTINUE
      SIGM=SQRT(SIGM/SM)
      WRITE(6,1007)NER,SM,SAM,SIGM
20    CONTINUE
      ENDDO
      DO FOR IJ=1,14
      WRITE(7,1004)IJ
      DO 23 I=1,8
      SM=0.0
      SAM=0.0
      SIGM=0.0
      NER=I*10+120
      WRITE(7,1006)NER
      WRITE(7,1003)
      WRITE(7,1005)(IME(2,IJ,K,I),K=1,50)
      RM=60.5
      DO 21 J=1,50
      SM=SM+IME(2,IJ,J,I)
      SAM=SAM+RM*IME(2,IJ,J,I)
      RM=RM+2.0
21    CONTINUE
      IF(SM.EQ.0.0)GOTO 23
      SAM=SAM/SM
      RJM=60.5
      DO 22 JJ=1,50
      SIGM=SIGM+IME(2,IJ,JJ,I)*(RJM-SAM)**2
      RJM=RJM+2.0
22    CONTINUE
      SIGM=SQRT(SIGM/SM)
      WRITE(7,1007)NER,SM,SAM,SIGM
23    CONTINUE
      ENDDO
      DO FOR LM=1,14
```

```
      WRITE(6,1004)LM
      DO 26 I=1,14
      SE=0.0
      SFM=0.0
      SIGE=0.0
      RI=I
      MASS=120+I*5
      WRITE(6,1008)MASS
      WRITE(6,1003)
      DO FOR K=1,40
      IMRE(1,LM,K,I)=IMRE(1,LM,K,I)-IMRE(2,LM,K,I)
      IF(IMRE(1,LM,K,I).LT.0)IMRE(1,LM,K,I)=0
      ENDDO
      WRITE(6,1005)(IMRE(1,LM,K,I),K=1,40)
      RE=120.5
      DO 24 J=1,40
      SE=SE+IMRE(1,LM,J,I)
      SFM=SFM+RE*IMRE(1,LM,J,I)
      RE=RE+2.0
24    CONTINUE
      IF(SE.EQ.0.0)GOTO 26
      SFM=SFM/SE
      RJE=120.5
      DO 25 JJ=1,40
      SIGE=SIGE+IMRE(1,LM,JJ,I)*(RJE-SFM)**2
      RJE=120.5
25    CONTINUE
      SIGE=SQRT(SIGE/SE)
      WRITE(6,1009)MASS,SE,SFM,SIGE
26    CONTINUE
      ENDDO
      DO FOR LM=1,14
      WRITE(7,1004)LM
      DO 29 I=1,14
      SE=0.0
      SFM=0.0
      SIGE=0.0
      RI=I
      MASS=120+I*5
      WRITE(7,1008)MASS
      WRITE(7,1003)
      WRITE(7,1005)(IMRE(2,LM,K,I),K=1,40)
      RE=120.5
      DO 27 J=1,40
      SE=SE+IMRE(2,LM,J,I)
      SFM=SFM+RE*IMRE(2,LM,J,I)
      RE=RE+2.0
27    CONTINUE
      IF(SE.EQ.0.0)GOTO 29
      SFM=SFM/SE
      RJE=120.5
      DO 28 JJ=1,40
      SIGE=SIGE+IMRE(2,LM,JJ,I)*(RJE-SFM)**2
      RJE=RJE+2.0
```

```
28      CONTINUE
        SIGE=SQRT(SIGE/SE)
        WRITE(7,1009)MASS,SE,SFM,SIGE
29      CONTINUE
        ENDDO
        GOTO 1


C...ERR.......
999     WRITE(1,*) '*****'
        WRITE(1,*) 'ERRNO=',ISTAT
        GOTO 1111

C... EXIT ....
400     GOTO 1111
2345    CONTINUE
1011    ICNUM=ICNUM+1
        IF(ISTAT.EQ.3)THEN
        WRITE(1,*) ' END OF FILE'
        WRITE(1,*) ' BLOCK=',IBLK,' ISTAT=',ISTAT
        ICNUM=ICNUM+1
        IF(ICNUM.LT.INUM)GOTO 2345
        GOTO 1
        ELSE
        GOTO 999
        ENDIF
1111    CLOSE(6)
        CLOSE(7)
        CLOSE(8)
        CLOSE(9)
        CLOSE(10)
        STOP
        END
        SUBROUTINE KINEM(ETOT,E1,E2,AM1,AM2,ECM1,ECM2)
        COMMON/AA/EP
        COMMON/EE/THETA1,THETA2
        AM=238.0
        AP=4.0
        PI=4.0*ATAN(1.0)
        VP=1.389*SQRT(EP/AP)
        ETAR=59.7-ETOT
C        VCN=AP*VP/AM
        VCN=1.389*SQRT(ETAR/AM)
        VL1=1.389*SQRT(E1/AM1)
        VL2=1.389*SQRT(E2/AM2)
        ANG1=ACOS(VCN/VL1)
        ANG2=ACOS(VCN/VL2)
        VCM1=VL1**2-VCN**2
        VCM2=VL2**2-VCN**2
        ECM1=AM1*VCM1/1.929321
        ECM2=AM2*VCM2/1.929321
        RETURN
        END
        SUBROUTINE LOSS(ERES,AMF,ZF,IND,EF)
```

```
C**********THIS SUBROUTINE CALCULATES THE ENERGY LOSS SUFFERED*****
C***************BY FISSION FRAGMENTS*****************
      COMMON/BB/SU(20)
      COMMON/CC/SC(20)
      COMMON/EE/THETA1,THETA2
      COMMON/RR/BACK,THICK
      EL=0.0
      EF=0.0
      NCN=0
      PI=4.0*ATAN(1.0)
      NCN2=0
      GOTO (20,24)IND
20    THETA=THETA1-45.
      THETA=THETA*PI/180.
      TU=.05/COS(THETA)
      GOTO 69
24    THETA=THETA2-45.
      THETA=THETA*PI/180.
      TU=.05/COS(THETA)
69    EBM=ERES/AMF
      I=EBM/0.1
      ZALF=2.
      S1=SU(I)-(SU(I)-SU(I+1))*(EBM-0.1*I)/0.1
63    V=1.389*SQRT(ERES/AMF)
      V0=0.2188
      VR1=V/(V0*ZALF**.65)
      VR2=V/(V0*ZF**.65)
      AZ1=1.035-0.4*EXP(-0.16*2.)
      AZ2=1.035-0.4*EXP(-0.16*ZF)
      GAMA1=1.0-AZ1*EXP(-0.879*VR1)
      GAMA2=1.0-AZ2*EXP(-0.879*VR2)
      GAMA1=(GAMA1*ZALF)**2
      GAMA2=(GAMA2*ZF)**2
      S=S1*GAMA2/GAMA1
      EL=S*TU
      EF=ERES+EL
      IF(IND.EQ.1)GOTO 74
      IF(IND.EQ.3)GOTO 74
72    ERES=EF
      TU=.01/ABS(COS(THETA))
      IND=IND+1
75    EBM=ERES/AMF
      I=EBM/0.1
      S1=SC(I)-(SC(I)-SC(I+1))*(EBM-.1*I)/0.1
      GOTO 63
74    RETURN
      END
      SUBROUTINE NEUT
      COMMON/DD/EX
*****************************************************************
C     THIS PROGRAM CALCULATES THE NUMBER OF NEUTRONS EMITTED FROM   *
C     NASCENT FISSION FRAGMENTS AT LOW EXCITATION ENERGY OF TARGET  *
C     THE DATA USED IS FROM THE PAPER OF BISHOP ETAL.               *
*****************************************************************
```

```
      COMMON/NEUT/ECM1,ECM2,E1N,E2N,RNU1,RNU2,AM1,AM2
      DIMENSION RNU(2)
      AM1 = ECM2*238.0/(ECM1+ECM2)
      AM2 = 238.0-AM1
      IF(AM1.GT.AM2)THEN
           MASS = AM1 + 0.5
           LIND=1
      ELSE
           MASS=AM2
           LIND=2
      ENDIF
      SLOPE1=0.0517865
      SLOPE2=0.0542135
      I=1
1     IF(MASS.LE.120)THEN
           IF(EX.GT.5.7)THEN
                RINT = -3.3459896 + 0.0497349*(EX-5.7)
           ELSEIF(EX.LT.5.7)THEN
                RINT = -3.3459896 - 0.0497349*(EX-5.7)
           ELSE
                RINT = -3.3459896
           ENDIF
           RNU(I) = SLOPE1*MASS + RINT
           ENE = (FLOAT(MASS-50)) * 0.004117647 + 1.1268382
           IF(LIND.EQ.1)E1N=ECM1+ENE*RNU(I)
           IF(LIND.EQ.2)E2N=ECM2+ENE*RNU(I)
           I=I+1
      ENDIF
      IF(MASS.GT.132)THEN
           IF(EX.GT.5.7)THEN
                RINT = -5.350377 + 0.0514494*(EX-5.7)
           ELSEIF(EX.LT.5.7)THEN
                RINT = -5.350377 - 0.0514494*(EX-5.7)
           ELSE
                RINT = -5.350377
           ENDIF
           RNU(I) = SLOPE2*MASS + RINT
           ENE = (FLOAT(MASS-50)) * 0.004117647 + 1.1268382
           IF(LIND.EQ.1)E1N=ECM1+ENE*RNU(I)
           IF(LIND.EQ.2)E2N=ECM2+ENE*RNU(I)
           I=I+1
      ENDIF
      IF(MASS.GT.120.AND.MASS.LE.132)THEN
           IF(EX.GT.5.7)THEN
                RINT1 = -3.3459896 + 0.0475725*(EX-5.7)
           ELSEIF(EX.LT.5.7)THEN
                RINT1 = -3.3459896 - 0.0475725*(EX-5.7)
           ELSE
                RINT1 = -3.3459896
           ENDIF
           IF(EX.GT.5.7)THEN
                RINT2 = -5.350377 + 0.0492125*(EX-5.7)
           ELSEIF(EX.LT.5.7)THEN
                RINT2 = -5.350377 - 0.0492125*(EX-5.7)
```

```
            ELSE
                RINT2 = -5.350377
            ENDIF
            RP1 = SLOPE1 * 120.0 + RINT1
            RP2 = SLOPE2 * 132.0 + RINT2
            RINT3 = ( RP1 *11.0 - RP2 * 10.0)
            RNU(I) = ((RP2-RP1)/12.0)*MASS + RINT3
            ENE = (FLOAT(MASS-50)) * 0.004117647 + 1.1268382
            IF(LIND.EQ.1)E1N=ECM1+ENE*RNU(I)
            IF(LIND.EQ.2)E2N=ECM2+ENE*RNU(I)
            I=I+1
        ENDIF
        IF(I.GT.2)GO TO 2
        IF(LIND.EQ.1)THEN
            MASS = AM2 + 0.5
            LIND=2
        ELSE
            MASS = AM1 + 0.5
            LIND=1
        ENDIF
        GO TO 1
2       IF(LIND.EQ.1)THEN
            RNU1=RNU(2)
            RNU2=RNU(1)
            AM2=238.0*E1N/(E1N+E2N)
            AM1=238.0-AM2
        ELSE
            RNU1=RNU(1)
            RNU2=RNU(2)
            AM1=238.0*E2N/(E1N+E2N)
            AM2=238.0-AM1
        ENDIF
        EPM1=E1N/AM1
        EPM2=E2N/AM2
C        E1N=E1N+RNU1*EPM1
C        E2N=E2N+RNU2*EPM2
        RETURN
        END
```

APPENDIX 3

```
C       THIS PROGRAM CALCULATES THE NUMBER OF NEUTRONS EMITTED FROM
C       COMPOUND NUCLEUS TO THE SADDLE POINT
        PROGRAM PRESADDLE
        DIMENSION EXCN(20),GAMMAF(20),GAMAN(20),GAMAG(20),GAMAT(20),
     -  ICHANC(20),BS(45),BC(45)
        COMMON/PHI/PI,PISQ
        COMMON/MCS/A,Z,S
        COMMON/CONS/DEF(45),ELDM(45),DELS(45),EDEF(45),ALRO(45),RHO(45)
        COMMON/CONS1/AS,CAPA,C1,W,ALDM,ESO,ECO
        COMMON/BS/(45),BC(45)
        COMMON/MOM/XJPAR,XJPER
        COMMON/A/A1,A2,A3
        DATA BC/0.99761D0,0.99849D0,0.99916D0,0.99963D0,0.99991D0,
     -          1.00000D0,0.99991D0,0.99965D0,0.99921D0,0.99862D0,
     -          0.99786D0,0.99695D0,0.99589D0,0.99467D0,0.99330D0,
     -          0.99178D0,0.99011D0,0.98830D0,0.98634D0,0.98423D0,
     -          0.98197D0,0.97956D0,0.97701D0,0.97430D0,0.97144D0,
     -          0.96843D0,0.96526D0,0.96193D0,0.95845D0,0.95480D0,
     -          0.95099D0,0.94702D0,0.94289D0,0.93859D0,0.93412D0,
     -          0.92949D0,0.92469D0,0.91973D0,0.91460D0,0.90932D0,
     -          0.90387D0,0.89826D0,0.89254D0,0.88666D0,0.88065D0/
        DATA BS/1.00497D0,1.00312D0,1.00172D0,1.00075D0,1.00018D0,
     -          1.00000D0,1.00018D0,1.00070D0,1.00154D0,1.00269D0,
     -          1.00415D0,1.00588D0,1.00789D0,1.01017D0,1.01270D0,
     -          1.01549D0,1.01851D0,1.02178D0,1.02528D0,1.02901D0,
     -          1.03296D0,1.03714D0,1.04154D0,1.04616D0,1.05099D0,
     -          1.05604D0,1.06130D0,1.06678D0,1.07247D0,1.07837D0,
     -          1.08448D0,1.09080D0,1.09732D0,1.10406D0,1.11099D0,
     -          1.11813D0,1.12546D0,1.13299D0,1.14071D0,1.14861D0,
     -          1.15670D0,1.16495D0,1.17336D0,1.18193D0,1.19064D0,
        DATA XJPAR/1.11578,1.09086,1.06688,1.04378,1.02151,1.00000,


     -            0.97921,0.95908,0.93958,0.92067,0.90230,0.88445,
     -            0.86708,0.85018,0.83370,0.81763,0.80196,0.78665,
     -            0.77170,0.75709,0.74281,0.72884,0.71519,0.70184,
     -            0.68879,0.67604,0.66359,0.65144,0.65960,0.62806,
     -            0.61685,0.60596,0.59541,0.58523,0.57541,0.56599,
     -            0.55698,0.54842,0.54032,0.53272,0.52564,0.51914,
     -            0.51323,0.50797,0.50341/
        DATA XJPER/0.95952,0.96552,0.97272,0.98083,0.98992,1.00000,
     -            1.01107,1.02312,1.03618,1.05025,1.06535,1.08151,
     -            1.09875,1.11709,1.13658,1.15726,1.17916,1.20233,
     -            1.22683,1.25272,1.28005,1.30890,1.33933,1.37143,
     -            1.40527,1.44095,1.47856,1.51820,1.55997,1.60400,
     -            1.65039,1.69927,1.75078,1.80506,1.86225,1.92251,
     -            1.98599,2.05288,2.12334,2.19757,2.27576,2.35812,
```

```
     -              2.44485,2.53618,2.63235/
           PRINT'(''$PLEASE GIVE THE BINDING ENERGY OF THE NEUTRON:'')'
           READ*,BN
           PI=(ATAN(1.0))*4.0
           PISQ=PI*PI
           PRINT'(''$PLEASE GIVE THE EX. ENERGY OF THE NUCLEUS:'')'
           READ*,EX
           ALD=3.293D0
           HRED=6.588D-22
           IN=1
           PRINT'(''$PLEASE GIVE THE RANDOM NUMBER SEED HERE:'')'
           READ*,IX
           IHIS=1
           DT=1.0D-21
10         T=0.0
           EXCN=EXCN-2.0
           GAMAF=GAMAF(I)
           AS=19.008
           CAPA=2.84
           C1=0.731
           W=0.185*A**(1.0/3.0)
           ALDM=A*0.176*(1.0-A**(1.0/3.0))
           WRITE(2,1000)A,Z,S,EX,ALDM
           ESO=AS*(1.0-CAPA*((A-2.0*Z)/A)**2)*A**(2.0/3.0)
           ECO=C1*Z*Z/A**(1.0/3.0)
           DO 3 I=1,45
           DEF(I)=(I-1)*0.02+0.9
           ELDM(I)=ESO*(BS(I)-1.0)+ECO*(BC(I)-1.0)
           THETA=(DEF(I)-1.0)*A**(1.0/3.0)/0.24
           DELS(I)=S*SIN(THETA)/THETA
           EXDEF(I)=ELDM(I)+DELS(I)
           EX(I)=EXCN-EDEF(I)
           WRITE(2,1010)I,DEF(I),ELDM(I),DELS(I),EDEF(I),EX(I)
3          CONTINUE
           GAMN=CALL TAUN(EXE,GAMAN)
           GAMF=CALL TAUF(EXE,GAMAF)
           GAMG=CALL TAUG(EXE,GAMAG)
           GAMT=GAMN+GAMF+GAMG
           ICH=1
60         PSRAND=RNDM(IX,IN)
           TEMP=(EX/ALD)**0.5
           BRF=GAMF/GAMT
           BRN=GAMN/GAMT
           PROBF=BRF*GAMT*DT/HRED
           PROBN=BRN*GAMT*DT/HRED
           IF(PROBF-PSRAND)150,150,100
100        WRITE*,T,EX,GAMT,PROBF,PROBN,PSRAND
           ICHANC(ICH)=ICHANC(ICH)+1
           PRINT*,IHIS
           GO TO 500
150        IF(PSRAND.GT.PROBF.AND.(PSRAND.LT.(PROBF+PROBN))GO TO 200
           IF(PSRAND.GT.(PROBF+PROBN))GO TO 300
200        WRITE(*,1030)T,EX,GAMT,PROBF,PROBN,PSRAND
1020       FORMAT(10H,FISSION,/,6D11.4)
```

```
1030    FORMAT(10H,NEUTRON,/,6D11.4)
        EX=EX-BN-2.0*TEMP
        IF(EX.LE.10.0D0)GO TO 700
        T=T+DT
        ICH=ICH+1
        GAMF=GAMAF(I+2*(ICH-1))
        GAMN=GAMAN(I+2*(ICH-1))
        GAMG=GAMAG(I+2*(ICH-1))
        GAMT=GAMF+GAMG+GAMN
        GO TO 60
300     T=T+DT
        GO TO 60
500     IHIS=IHIS+1
        IF(IHIS-100)10,600,600
600     PRINT 1040,(ICHANC(I),I=1,10)
        IF(IHIS.EQ.100)HIS=IHIS
1040    FORMAT(10I8)
        NEUTR=0
        DO 680 I=1,10
680     NEUTR=NEUTR+ICHANC(I)*I
        ANEUTR=NEUTR
        RNEUTR=ANEUTR/HIS
        WRITE(*,1050)RNEUTR
1050    FORMAT(26H,AVERAGE CHANCE NEUTRON IS =,F10.2)
        STOP
700     ICHANC(10)=ICHANC(10)+1
        GO TO 10
        END
        FUNCTION RNDM(IX,IN)
        INTEGER*4 JM,MM,IX,IC
        IF(IN)30,40,30
30      IN=0
        JM=2**10+3
        MM=2**(20)
        FM=MM
40      IC=IX*JM/MM
        IX=IX*JM-IC*MM
        FX=IX
        XD=FX/FM
        RNDM=ABS(XD)
        RETURN
        END
        SUBROUTINE TAUF(EXE,GAMAF,GAMAT)
        IMPLICIT DOUBLE PRESCISION (A-H,O-Z)
        COMMON/PHI/PI,PISQ
        COMMON/MCS/A,Z,S
        COMMON/CONS/DEF(45),ELDM(45),DELS(45),EDEF(45),ALRO(45),RHO(45)
        COMMON/CONS1/AS,CAPA,C1,W,ALDM,ESO,ECO
        COMMON/BS/(45),BC(45)
        COMMON/A/A1,A2,A3
        DIMENSION EX(45)
        DO 10 I=1,45
        SPIN=0
        DLS=DELS(I)
```

```
      EX1=EX(I)
      CALL LEVDEN(A,ALDM,DLS,W,EX1,SPIN,WE,SIGSQ,RHOE,RHO1,ALRO1)
      ALRO(I)=ALRO1
      WRITE(2,1000)I,RHO(I),ALRO(I)
1000  FORMAT(I3,E13.5,E13.5)
10    CONTINUE
      IIMAX=43
      IGS=6
      ISP=6
      DO 20 II=2,IIMAX
      IF(RHO(II+1).LT.RHO(II).AND.RHO(II-1).LT.RHO(II))GO TO 21
      GO TO 22
21    IF(RHO(II).GT.RHO(IGS))IGS=II
22    CONTINUE
      IF(RHO(II+1).GT.RHO(II).AND.RHO(II-1).GT.RHO(II))GO TO 23
      GO TO 20
23    IF(ISP-6)24,24,25
24    ISP=II
      GO TO 20
25    IF(RHO(II).LT.RHO(ISP))ISP=II
20    CONTINUE
      WRITE(2,*)'IGS=',IGS
      WRITE(2,*)'ISP=',ISP
      DLS=DELS(ISP)
      EX1=EX(ISP)
      EX2=EX1-1.0
      EX3=EX2-1.0
      EX4=EX3-1.0
      EX5=EX4-1.0
      EX6=EX5-1.0
      CALL LEVDEN(A,ALDM,DLS,W,EX1,SPIN,WE,SIGSQ,RHOE,RHO1,ALRO1)
      CALL LEVDEN(A,ALDM,DLS,W,EX2,SPIN,WE,SIGSQ,RHOE,RHO2,ALRO2)
      CALL LEVDEN(A,ALDM,DLS,W,EX3,SPIN,WE,SIGSQ,RHOE,RHO3,ALRO3)
      CALL LEVDEN(A,ALDM,DLS,W,EX4,SPIN,WE,SIGSQ,RHOE,RHO4,ALRO4)
      CALL LEVDEN(A,ALDM,DLS,W,EX5,SPIN,WE,SIGSQ,RHOE,RHO5,ALRO5)
      CALL LEVDEN(A,ALDM,DLS,W,EX6,SPIN,WE,SIGSQ,RHOE,RHO6,ALRO6)
      ALRO0=ALRO(IGS)
      GAMA=EXP(ALRO1-ALRO0)/2.0
      GAMA=GAMA+EXP(ALRO2-ALRO0)
      GAMA=GAMA+EXP(ALRO3-ALRO0)
      GAMA=GAMA+EXP(ALRO4-ALRO0)
      GAMA=GAMA+EXP(ALRO5-ALRO0)
      GAMA=GAMA+EXP(ALRO6-ALRO0)
      GAMA=GAMA/2./PI
      GAMAF=GAMA
      GAMT=GAMAF*3.2E21
      TAUF=1.0/GAMT
      WRITE(2,1010)TAUF
      WRITE(2,1020)GAMAF,GAMT
1010  FORMAT(7H GAMAF=,E13.5,3HMEV,5X,E13.5,3H/S)
1020  FORMAT(7H TAUF=,E13.5,3H/S)
      RETURN
      END
      SUBROUTINE LEVDEN(A,ALDM,DELS,W,U,SPIN,WE,SIGSQ,RHOE,RHOEI,ALRH)
```

```
      COMMON/PHI/PI,PISQ
      COMMON/A/A1,A2,A3
      IMPLICIT DOUBLE PRESCISON(A-H,O-Z)
      WE=1.O
      SIGSQ=O.O
      RHOE=1.O
      RHOEI=1.O
      ALRH=O.O
      IF(U.LE.O.O)RETURN
      TP=SQRT(U/ALDM)
10    T=TP
      T1=T
      T2=T+O.OO5
      U1=ALDM*T1*T1-DELS
      U2=ALDM*T2*T2-DELS
      XX1=PI*W*T1
      IF(XX1.GT.15.O)GO TO 700
      XX2=PI*W*T2
      U1=U1+DELS*((XX1)**2*COSH(XX1)/(SINH(XX1))**2)
      U2=U2+DELS*((XX2)**2*COSH(XX2)/(SINH(XX2))**2)
700   CONTINUE
      TP=T1+(U-U1)*(T2-T1)/(U2-U1)
      IF(ABS(T-TP).GT.O.OO5)GO TO 10
      T=TP
      S=2.O*ALDM*T
      XXX=PI*W*T
      IF(XXX.GT.15.O)GO TO 99
      S=S+DELS/T*((XXX)**2*COSH(XXX)/(SINH(XXX))**2-XXX/SINH(XXX))
99    AEFF=S/2.O/T
      GEFF=6.O*AEFF/PISQ
      EM2BAR=O.240*A**(2.O/3.O)
      SISSQ=EM2BAR*GEFF*T
      C=SQRT(PI)/12.O/AEFF**O.25/U**(5.O/4.O)
      C1=1.O/(2.O*PI*SIGSQ)**O.5
      ALRH=S+DLOG(C)+DLOG(C1)
      WE=EXP(S)*C
      RHOE=WE*C1
      RHOEI=RHOE*(2.O*SPIN+1)*EXP(-SPIN*(SPIN+1)/2.O/SIGSQ)
      RHOEI=RHOEI/2.O/SIGSQ
      RETURN
      END
      SUBROUTINE TAUN(EXE,GAMAN)
      IMPLICIT DOUBLE PRECISION(A-H,O-Z)
      COMMON/PHI/PI,PISQ
      COMMON/MCS/A,Z,S
      COMMON/CONS/DEF(45),ELDM(45),DELS(45),EDEF(45),ALRO(45),RHO(45)
      COMMON/CONS1/AS,CAPA,C1,W,ALDM,ESO,ECO
      COMMON/BS/(45),BC(45)
      COMMON/MOM/XJPAR,XJPER
      COMMON/A/A1,A2,A3
      B1=31.O5
      B2=-25.91
      B3=342.4
      Bd=21.89
```

```
      B5=0.223
      B6=0.673
      B7=617.4
      AMAS=A
      A1=B1*AMAS**(-1.0/3.0)+B2
      A2=B3*AMAS**(-1.0/3.0)+B4*AMAS**(2.0/3.0)
      A3=B5*AMAS**(-1.0/3.0)+B6*AMAS**(2.0/3.0)+B7
      DO 10 I=1,45
      SPIN=0
      DLS=DELS(I)
      EX1=EX(I)
      CALL LEVDEN(A,ALDM,DLS,W,EX1,SPIN,WE,SIGSQ,RHOE,RHO1,ALRO1)
      ALRO(I)=ALRO1
      WRITE(2,1000)I,RHO(I),ALRO(I)
1000  FORMAT(I3,E13.5,E13.5)
10    CONTINUE
      IIMAX=43
      IGS=6
      ISP=6
      DO 20 II=2,IIMAX
      IF(RHO(II+1).LT.RHO(II).AND.RHO(II-1).LT.RHO(II))GO TO 21
      GO TO 22
21    IF(RHO(II).GT.RHO(IGS))IGS=II
22    CONTINUE
      IF(RHO(II+1).GT.RHO(II).AND.RHO(II-1).GT.RHO(II))GO TO 23
      GO TO 20
23    IF(ISP-6)24,24,25
24    ISP=II
      GO TO 20
25    IF(RHO(II).LT.RHO(ISP))ISP=II
20    CONTINUE
      DO 30 II=1,45
      DLS=DELS(II)
      EX1=EX(II)
      EX2=EX1-BN-0.5
      EX3=EX2-1.0
      EX4=EX3-1.0
      EX5=EX4-1.0
      EX6=EX5-1.0
      CALL LEVDEN(A,ALDM,DLS,W,EX1,SPIN,WE,SIGSQ,RHOE,RHO1,ALRO1)
      CALL LEVDEN(A,ALDM,DLS,W,EX2,SPIN,WE,SIGSQ,RHOE,RHO2,ALRO2)
      CALL LEVDEN(A,ALDM,DLS,W,EX3,SPIN,WE,SIGSQ,RHOE,RHO3,ALRO3)
      CALL LEVDEN(A,ALDM,DLS,W,EX4,SPIN,WE,SIGSQ,RHOE,RHO4,ALRO4)
      CALL LEVDEN(A,ALDM,DLS,W,EX5,SPIN,WE,SIGSQ,RHOE,RHO5,ALRO5)
      CALL LEVDEN(A,ALDM,DLS,W,EX6,SPIN,WE,SIGSQ,RHOE,RHO6,ALRO6)
      SIG1=SIGR(0.5D0)
      GAMA=DEXP(ALRO2-ALRO1)*0.5*931.0*SIG1/10.0
      GAMA=GAMA+DEXP(ALRO3-ALRO1)*1.5*931.0*SIGR(1.5D0)/10.0
      GAMA=GAMA+DEXP(ALRO4-ALRO1)*2.5*931.0*SIGR(2.5D0)/10.0
      GAMA=GAMA+DEXP(ALRO5-ALRO1)*3.5*931.0*SIGR(3.5D0)/10.0
      GAMA=GAMA+DEXP(ALRO6-ALRO1)*4.5*931.0*SIGR(4.5D0)/10.0
      GAM(II)=GAMA/(PI+197.0)**2
30    CONTINUE
      GAMAN=0.0
```

```
      PROB=0.0
      DO 31 II=1,ISP
      GAMAN=GAMAN+GAM(II)*RHO(II)
      PROB=PROB+RHO(II)
31    CONTINUE
      GAMAN=GAMAN/PROB
      GAMT=GAMAN*3.2E21
      TAUN=1.0/GAMT
      RETURN
      END
      FUNCTION SIGR
CC********NEUTRON CROSS SECTIONS- CHATTERJEE ETAL***********
CC**************PRAMANA 16(1981)391*****************
      COMMON/A/A1,A2,A3
      IMPLICIT DOUBLE PRECISION(A-H,O-Z)
      SIGR=A1*EN+A2+A3/EN
      RETURN
      END
      SUBROUTINE TAUG(EXE,GAMAG)
      IMPLICIT DOUBLE PRECISION(A-H,O-Z)
      COMMON/PHI/PI,PISQ
      COMMON/MCS/A,Z,S
      COMMON/CONS/DEF(45),ELDM(45),DELS(45),EDEF(45),ALRO(45),RHO(45)
      COMMON/CONS1/AS,CAPA,C1,W,ALDM,ESQ,ECO
      COMMON/BS/(45),BC(45)
      COMMON/MOM/XJPAR,XJPER
      COMMON/A/A1,A2,A3
CC*********PARAMETERS FOR GAMMA INVERSE CROSS SECTION CALCULATIONS*****
CC**********************PRAKASH ETAL. PRL 60(1988)1630*************
      GAM1=6.0
      ER=34.0/A**(1.0/6.0)
      DO 10 I=1,45
      SPIN=0
      DLS=DELS(I)
      EX1=EX(I)
      CALL LEVDEN(A,ALDM,DLS,W,EX1,SPIN,WE,SIGSQ,RHOE,RHO1,ALRO1)
      ALRO(I)=ALRO1
      RHO(I)=RHO1
      WRITE(2,1000)I,RHO(I),ALRO(I)
1000  FORMAT(I3,E13.5,E13.5)
10    CONTINUE
      IIMAX=43
      IGS=6
      ISP=6
      DO 20 II=2,IIMAX
      IF(RHO(II+1).LT.RHO(II).AND.RHO(II-1).LT.RHO(II))GO TO 21
      GO TO 22
21    IF(RHO(II).GT.RHO(IGS))IGS=II
22    CONTINUE
      IF(RHO(II+1).GT.RHO(II).AND.RHO(II-1).GT.RHO(II))GO TO 23
      GO TO 20
23    IF(ISP-6)24,24,25
24    ISP=II
      GO TO 20
```

```
5       IF(RHO(II).LT.RHO(ISP))ISP=II
)       CONTINUE
        DO 30 II=1,45
        DLS=DELS(II)
        EX1=EX(II)
        EX2=EX1-0.5
        EX3=EX2-1.0
        EX4=EX3-1.0
        EX5=EX4-1.0
        EX6=EX5-1.0
        CALL LEVDEN(A,ALDM,DLS,W,EX1,SPIN,WE,SIGSQ,RHOE,RHO1,ALRO1)
        CALL LEVDEN(A,ALDM,DLS,W,EX2,SPIN,WE,SIGSQ,RHOE,RHO2,ALRO2)
        CALL LEVDEN(A,ALDM,DLS,W,EX3,SPIN,WE,SIGSQ,RHOE,RHO3,ALRO3)
        CALL LEVDEN(A,ALDM,DLS,W,EX4,SPIN,WE,SIGSQ,RHOE,RHO4,ALRO4)
        CALL LEVDEN(A,ALDM,DLS,W,EX5,SPIN,WE,SIGSQ,RHOE,RHO5,ALRO5)
        CALL LEVDEN(A,ALDM,DLS,W,EX6,SPIN,WE,SIGSQ,RHOE,RHO6,ALRO6)
        SIG1=SIGR(0.5D0)
        GAMA=DEXP(ALRO2-ALRO1)*0.5**2*SIG1/10.0
        GAMA=GAMA+DEXP(ALRO3-ALRO1)*1.5**2*SIGR(1.5D0)/10.0
        GAMA=GAMA+DEXP(ALRO4-ALRO1)*2.5**2*SIGR(2.5D0)/10.0
        GAMA=GAMA+DEXP(ALRO5-ALRO1)*3.5**2*SIGR(3.5D0)/10.0
        GAMA=GAMA+DEXP(ALRO6-ALRO1)*4.5**2*SIGR(4.5D0)/10.0
        GAM(II)=GAMA/(PI+197.0)**2
30      CONTINUE
        GAMAN=0.0
        PROB=0.0
        DO 31 II=1,ISP
        GAMAG=GAMAG+GAM(II)*RHO(II)
        PROB=PROB+RHO(II)
31      CONTINUE
        GAMAG=GAMAG/PROB
        GAMT=GAMAG*3.2E21
        TAUG=1.0/GAMT
        RETURN
        END
```